12-16-2011 12:00 AM

ATPase Regulation in the Maltose Transporter

Alister D. Gould, *The University of Western Ontario*

Supervisor: Dr. Brian Shilton, *The University of Western Ontario*

A thesis submitted in partial fulfillment of the requirements for the Doctor of Philosophy degree in Biochemistry

ATPASE REGULATION IN THE MALTOSE TRANSPORTER

Spine Title: $MalFGK_2$ ATPase Regulation

Thesis format: Integrated-Article

by

Alister D. Gould

Graduate Program in Biochemistry

Thesis submitted in partial fulfillment
of the requirements for the degree of
Doctor of Philosophy

The School of Graduate and Postdoctoral Studies
The University of Western Ontario
London, Ontario, Canada

THE UNIVERSITY OF WESTERN ONTARIO
SCHOOL OF GRADUATE AND POSTDOCTORAL STUDIES

CERTIFICATE OF EXAMINATION

Supervisor	Examiners
_____	_____
Dr. Brian Shilton	Dr. Megan Davey
	_____
Supervisory Committee	Dr. David Heinrichs
_____	_____
Dr. Stan Dunn	Dr. Voula Kanelis
_____	_____
Dr. James Choy	Dr. Gary Shaw

The thesis by

Alister D. Gould

entitled:

ATPase Regulation in the Maltose Transporter

is accepted in partial fulfilment of the
requirements for the degree of
Doctor of Philosophy

Date_____ _____
Chair of the Thesis Examination Board

Abstract

This thesis investigates the mechanism of activity-coupling in the maltose transporter of *Escherichia coli* ($MalFGK_2$); the way ATP hydrolysis is prevented in the absence of maltose, and then enabled to drive maltose transport. Like other ATP binding cassette importers, $MalFGK_2$ requires substrate to be presented by a peripheral substrate-binding protein, in this case the maltose binding protein (MBP). MBP predominantly adopts an 'open' resting state, but undergoes a rotation of its two domains to a 'closed' state after maltose binding. In the closed state MBP is able to activate $MalFGK_2$ to stimulate ATP hydrolysis and maltose transport.

Engineered mutants of MBP have been used to test the responsiveness of the transporter to changes in the conformational state of its binding protein. Careful analysis of ATPase stimulus by wild type MBP indicates that the open state of MBP is able to bind the transporter and promote ATP hydrolysis in the absence of maltose. Another mutant MBP, able to adopt the closed state in the presence of either sucrose or maltose, demonstrates that ATP hydrolysis is activated by interactions between the transporter and binding protein, and not between the transporter and substrate. Further, using MBP mutants incorporating introduced disulfide bonds and inter-domain cross-linkers we show that the closed form of MBP is able to activate substantial, but not maximal, ATPase activity without adopting the open conformation or releasing its bound substrate.

It has been determined that both stable forms of MBP, maltose-bound-closed and unliganded-open, separately stimulate ATP hydrolysis from the transporter. In contrast, the substrate itself does not directly stimulate activity but instead activates hydrolysis by stabilizing the closed state of MBP. Taken together our data indicate that the transporter exists in equilibrium between an inactive resting state and conformations receptive to binding by the closed and open forms of MBP. This suggests that uncoupled ATP hydrolysis is prevented by destabilizing ATPase relevant conformations of the transporter, and that MBP activates hydrolysis by binding these conformations in its closed and open states.

Keywords:

Active Transport, ATP Binding Cassette, ATPase, *Escherichia Coli*, Cell Membrane, Maltose Binding Protein, Maltose Transport, Protein Conformation, Substrate Specificity, X-ray Crystallography

Co-authorship

Chapter 2

Modeling of expected stimulus kinetics was performed by Dr. Brian Shilton. SAXS experiments and analysis were performed by Dr. Brian Shilton and Patrick Telmer. Work with MBP mutants MBP-DM and MBPA96W/I329W was performed by Patrick Telmer. This manuscript was co-written by Dr. Brian Shilton, Patrick Telmer and Alister Gould and appeared in Biochemistry, **2009 August 25; volume 48 (33) 8051-61.** The material is reprinted here in accordance with ACS policies.

Chapter 3:

SAXS data were collected and analyzed by Dr. Brian Shilton. This manuscript was written by Alister Gould and edited with advice from Dr. Brian Shilton. It was published in the Journal of Biological Chemistry. **2010 April 9; volume 285(15) 11290-6.**

Chapter 4:

PCR mutagenesis of MBP-O95/171 and initial BMOE crosslinking was performed by summer student Arjun Chandra. SAXS data was collected with the assistance of Kevin Leung and Dr. Brian Shilton. SAX analysis was performed by Dr. Brian Shilton.

Acknowledgments:

I would like to thank Lee-Ann Briere and Dr. Stanley Nithianantham for assistance and training in protein crystallization, X-ray data collection and structural refinement. I thank Dr. Marc Ostermeier and Dr. Amy Davidson for providing vectors for sMBP and histidine tagged $MalFGK_2$.

I thank Patrick Telmer for passing me the torch of a highly engaging research project, as well as Kevin Leung and Arjun Chandra their companionship and assistance. I would also like to thank my advisory committee, Dr. Stan Dunn and Dr. James Choy, their advice and support, as well as their tolerance of my sometimes opaque presentations of findings.

I thank Dr. Brian Shilton, for offering me a place in his lab, mentoring me through some of the formative challenges of my education, and giving me the tremendous benefit of his experience.

Crystallographic data were collected at the Canadian Light Source, which is supported by Natural Sciences and Engineering Research Council of Canada, National Research Council, Canadian Institutes of Health Research, and the University of Saskatchewan.

SAXS data were collected at the Advanced Photon Source at Argonne national labs. Use of the Advanced Photon Source was supported by the U.S. Department of Energy, Office of Science, Office of Basic Energy Sciences, under Contract No. DE-AC02-06CH11357 and W-31-109-ENG-38. The BioCAT beamline is supported by National Institutes of Health Research Grant RR-08630.

I would also like to thank Frances and Grace Hay, as well as Douglas, Heather, and Megan Gould for the incalculable support they have provided, without which none of this work would have been possible.

Table of Contents

Abstract……iii
Coauthorship……iv
Acknowledgments……v
List of Figures……viii
List of Tables……ix
List of Abbreviations……x

Chapter 1 Introduction……..1
1.1 Background……1
1.2 The Maltose Transporter of *Escherichi Coli*:……6
1.3 Energy Utilization by the ATP Binding Cassette……..10
1.4 Energy and Information Flow Within The Transmembrane Subunits……..11
1.5 Role of the Substrate Binding Protein……16
1.6 Unanswered Questions Concerning Maltose Transporter Activity……...18
1.7 Research Goals and Hypothesis……19
1.8 Experimental Methodology……...22
1.9 Scope of Thesis……26
Bibliography……28

Chapter 2 Stimulation of the Maltose Transporter ATPase by Unliganded Maltose Binding Protein……..32
2.1 Introduction……32
2.2 Materials and Methods……36
2.3 Results……45
2.4 Discussion……72
Bibliography……76

Chapter 3 Studies of the Maltose Transport System Reveal a Mechanism for Coupling ATP Hydrolysis to Substrate Translocation Without Direct Recognition of Substrate……79
3.1 Introduction……79
3.2 Materials and Methods……81
3.3 Results……84
3.4 Discussion……104
Bibliography……109

Chapter 4 Activation of the Maltose Transporter by Cysteine Stabilized MBP Mutants ……111
4.1 Introduction……111
4.2 Materials and Methods……115
4.3 Results……123
4.4 Discussion……159
Bibliography……166

Chapter 5 General Discussion and Conclusions……169
Bibliography…….....180
Appendix 1……182
Appendix 2……183
Appendix 3……184
Curriculum Vitae……....185

List of Figures

Figure 1.1 Conserved Domain Architecture of ABC Transporters……5
Figure 1.2 Conformational Changes in ABC Subunits on ATP Binding……...……9
Figure 1.3 Order of Events in Maltose Transport……..……13
Figure 1.4 Proposed Mechanism of Coupling in $MalFGK_2$.....21
Figure 1.5 The Substrate Binding Site and Balancing Interface Balance Conformational Changes in MBP……..25
Figure 2.1 Stimulation of the $MalFGK_2$ ATPase by Unliganded MBP……48
Figure 2.2 Kinetic Analysis of MBP-$MalFGK_2$ ATPase Stimulation in the Presence of Maltose……50
Figure 2.3 Kinetic Analysis of MBP-$MalFGK_2$ ATPase Stimulation in the Absence of Maltose……53
Figure 2.4 Kinetic Models for Stimulation of $MalFGK_2$ ATPase by Open and Closed MBP.58
Figure 2.5 Expected Rate Curves for $MalFGK_2$ Stimulation by MBP……61
Figure 2.6 Unliganded MBP-A96W/I329W is in a Closed Conformation……..65
Figure 2.7 Stability of Conformationally Engineered MBP Molecules……..…..67
Figure 2.8 Destabilization of the Open Conformation Decreases $MalFGK_2$ ATPase…….…70
Figure 3.1 Open to Closed Conformational Change in sMBP…….86
Figure 3.2 Effect of Ligand on Stimulation of the $MalFGK_2$ ATPase……..…89
Figure 3.3 Sucrose Binding by sMBP……..93
Figure 3.4 Main Chain Disorder in the Open Unliganded sMBP Structure…….96
Figure 3.5 Effect of Mutations on the Surface Properties of Open and Closed sMBP…….98
Figure 3.6 Mutation D14L of sMBP……100
Figure 3.7 Interactions Between the $MalFGK_2$ P3 Loop and the sMBP Ligand Binding Site.103
Figure 3.8 Structural Basis for Communication Between the MalG P3 Loop and ATP Binding Cassettes……108
Figure 4.1 MBP-C Cysteine Mutations……125
Figure 4.2 ATPase Stimulus by MBP-C in Proteoliposomes……..129
Figure 4.3 ATPase Stimulus by MBP-C of Detergent Stabilized $MalFGK_2$……132
Figure 4.4 Maltose Binding Measured by Intrinsic Fluorescence Quenching ……135
Figure 4.5 Changes in SAXS Profile of MBP-C with Maltose……138
Figure 4.6 MBP-O Cysteine Mutations……142
Figure 4.7 Fluorescene Labeling of BMOE Cross-Linked MBP-O……145
Figure 4.8 MALDI-TOF Profile of Cross-Linked MBP-O and MBP-O95/171……..148
Figure 4.9 ATPase Stimulus by MBP-O in Proteoliposomes……..151
Figure 4.10 ATPase Stimulus by MBP-O of Detergent Stabilized $MalFGK_2$……153
Figure 4.11 Changes in SAXS Profile of MBP-O and MBP-O95/171 with Maltose……158

List of Tables

Table 2.1 Kinetic Parameters for Activation of MalFGK2 by Liganded and Unliganded MBP……54
Table 2.2 Rate Constants for Kinetic Models……59
Table 3.1 Crystallographic Statistics……..91
Table 4.1 Mutagenic Primers for MBP Mutants……..116
Table 4.2 Radii of Gyration of MBP-C from GNOM Analysis ……..139
Table 4.3 MALDI-TOF Analysis of Prepared Binding Proteins……146
Table 4.4 Radii of Gyration of MBP-O and MBP-O95/171 from GNOM Analysis ……..155

List of Abbreviations

Å	Angstrom
ABC	ATP Binding Cassette
ATP	Adenosine Tri-Phosphate
BMOE	1,2Bis-maleimido-ethane
Da	Daltons
DMSO	Dimethyl Sulfoxide
DTT	Dithiothreitol
EDTA	Ethylene-diamine-tetra-acetic acid
E. coli	*Escherichia Coli*
FM	Fluorescein Maleimide
IPTG	Isopropyl β-D-1-thiogalactopyranoside
K_D	Substrate concentration at half maximal binding
K_m	Substrate concentration at half maximal activity
MalE	Gene Encoding *E. coli* MBP
$MalFGK_2$	Maltose Transporter of *E. coli*
MalFG	Transmembrane subunits of *E. coli* maltose transporter
MalK	ABC subunits of *E. coli* maltose transorter
MALDI-TOF	Matrix Assisted Time of Flight mass spectrometry
MBP	Maltose Binding Protein
wtMBP	Wild Type MBP
MBP-DM	MBP with a balancing interface deletion
MBP-A96W/I329W	MBP with bulky residues inserted in balancing interface
MBP-C	Closed-Stabilized MBP Mutant
MBP-O	Open-Stabilized MBP Mutant, BMOE Modified
MBP-O95/171	Open-Stabilized MBP Mutant, BMOE Modified
NEM	N-Ethyl Maleimide
PBP	Peripheral Substrate Binding Protein
PDB	Protein Data Bank
PgP	P-glycoprotein
PLS	Proteoliposome
SAXS	Small Angle X-ray Scattering
SBP	Substrate Binding Protein
SDS-PAGE	Sodium Dodecyl Sulfate Polyacrylamide Gel Electrophoresis
sMBP	Sucrose Binding MBP Mutant
TEV	Tobacco Etch Virus
TM	Transmembrane
Tris	Tris-hydroxymethyl-aminomethane
V_{max}	Maximal activity rate with excess substrate

Chapter 1 Thesis Introduction

1.1 Background

Living cells are bounded by semi-permeable membranes composed of lipids, proteins and sugars. Through this membrane the cell is able to restrict, and to a degree control, its communications with the outside world. Biological membranes of this sort fulfill their purpose by restricting the passage of bulky or strongly hydrophilic molecules across their oily interior layer. This creates a problem for the cell because the need to retain and protect desirable compounds within it is in conflict with the need to take in nutrients and expel waste. To meet this need cells have developed a variety of transport systems, macromolecular structures embedded within their cell membranes, which allow them to modify their permeability to specific solutes.

The most conceptually simple of these are 'passive' transporters; pores and channels which perforate the barrier of the membrane to allow a freer exchange of materials. Examples can range in complexity from simple pores like some aquaporins [1,2], which allow the flow of water as well as a diversity of larger molecules, to exquisitely sophisticated ion channels able to distinguish and select among atoms based on their size and charge state [3]. These transporters can be selective of what molecules they permit to pass and can permit or prevent passage in response to varying conditions, but all passive transporters are limited by entropy. Without the expenditure of energy it is not possible to concentrate a compound against its tendency to diffuse from areas of high concentration to areas of relative scarcity.

Unlike passive systems, 'active' transporters are able to accumulate compounds at relatively high concentrations by coupling the movement of their targeted substrate to the expenditure of some form of energy. These transporters harness an existing energy reserve to drive a process that would otherwise be disfavored by entropy. Structurally, this is typically

accomplished by a small occluded space within the transporter, harboring a substrate binding site, that is driven by conformational changes to alternatively access either face of the membrane [4,5,6]. An active transporter can generate a substrate gradient by exposing a high-affinity site on one membrane facing for binding and a low-affinity site on the opposite facing for dissociation. Some active transporters utilize an electrochemical gradient based on existing differences in charge distribution and substrate concentration. Many transporters like the glycerol-3-phosphate transporter GlpT [7], arabinose importer AraE [8], and lactose permease LacY [9] harness a transmembrane proton gradient. The energy stored in this combined pH and charge gradient is referred to as the proton motive force and is used by transporters of the major facilitator superfamily. Other active transporters harness the cell's common energy currency, adenosine tri-phosphate (ATP). ATP stores energy in phosphoanhydride bonds between its three phosphate groups and in its abundance relative to its breakdown products. The hydrolysis of phosphate from ATP is therefore energetically favorable, and can be used to drive unfavorable reactions. This is the energy reserve used by the ATP Binding Cassette (ABC) superfamily of active transporters.

ABC transporters are a family of active transporters with representatives in every species [10,11]. These complexes couple the transmembrane transport of a diverse collection of compounds to the hydrolysis of ATP within the cell. The family was termed in response to the finding that a subset of the human multidrug efflux pump P-glycoprotein (PgP), and later many other eukaryotic exporters, held approximately 30% sequence homology to a collection of binding protein dependent bacterial importers [12]. The family was found to span from human transporters like PgP, which is responsible for drug resistance in many cancers, to bacterial metabolite imports like the molybdate transporter ModBC and maltose transporter $MalFGK_2$

[13,14,15]. The sequence homology of these transporters stems from the conserved cytoplasmic ATP binding cassettes that give the protein family its name. These domains can be sufficiently similar in structure and function that they have been exchanged between differing transporters without abrogating their function [16].

The sequence homology between ABC transporters is limited to the ABC subunits, but the family nonetheless maintains a highly conserved domain structure (Fig. 1.1). Although the various domains of the complex are sometimes fused together in a smaller number of peptide strands, the number and general function of each domain is maintained. Each ABC transporter incorporates a hetero- or homo- dimer of transmembrane (TM) domains, embedded within and spanning the membrane. The TM domains are primarily α-helical and serve to anchor the complex, form the translocation pore itself and account for much or all of the complex's substrate specific function. In addition to the TM regions and anchored to them, by tight binding and/or direct peptide bonds, are the namesake ABC subunits. Each complex incorporates a homo- or hetero-dimer of ABC subunits on the cytoplasmic facing of the membrane, thus allowing access to the cellular pool of ATP.

Prokaryotic importers additionally incorporate a peripheral substrate binding protein (PBP). The PBP is found on the exterior face of the membrane, often floating free in the periplasm of Gram negative bacteria or associated with the membrane exterior. The PBP acts as the initial binding site for substrate before interacting with the TM domains of the transporter. This interaction between binding protein and substrate is necessary for the activation of ATP hydrolysis and substrate transport, as ABC importers do not appear to act on substrate that has not first been bound to a PBP [20,21].

Fig 1.1 Conserved Domain Architecture of ABC Transporters

The X-ray crystal structures of several ABC transporters are shown. Despite acting on different substrates, the structures reveal common architectural features in the ABC subunits (green and cyan), the transmembrane regions (pink, yellow) and the substrate binding protein (magenta). Note that SAV1866 is a substrate exporter and does not have an associated substrate binding protein. PDB reference: 2R6G[17], 2ONK[15], 2QI9[18], 2HYD[19]

MalFGK2
Maltose Transporter

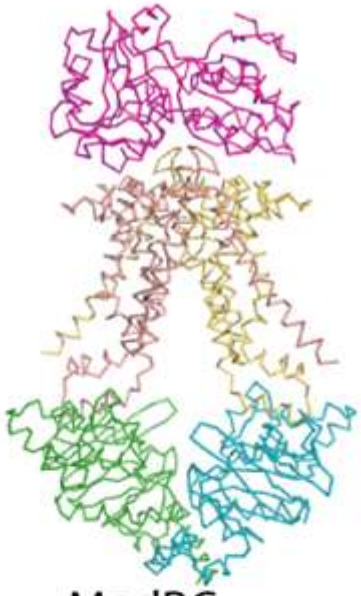

ModBC
Molybdate Importer

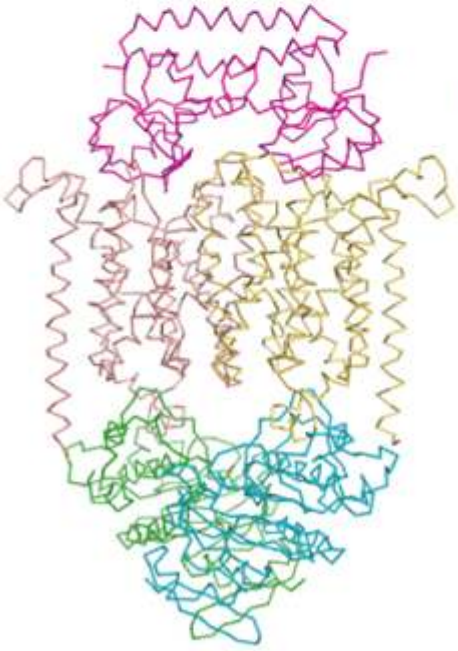

BTUCD
B12 Importer

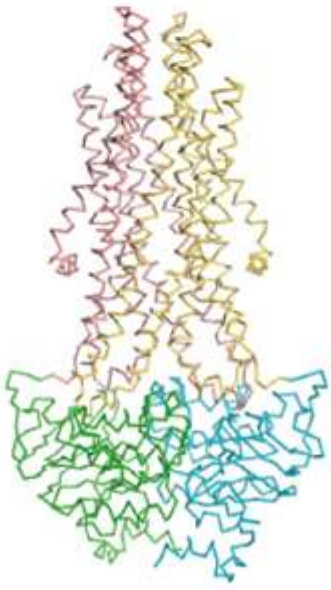

SAV1866
MultiDrug Exporter

Due to this domain arrangement, binding protein dependent ABC importers incorporate a series of features that make them valuable subjects of study to broaden our understanding of protein complex engineering. A signal transduction mechanism is required to communicate the presence of substrate outside the cell to the cell interior, so that ATP hydrolysis can be initiated. Additionally, an energy transduction mechanism is necessary to convert ATP hydrolysis within the cytoplasm into the directed transport of the relatively distant target substrate. The TM domains are required both to form the translocation pathway and also transmit these communications between the ABCs and PBP.

1.2 The Maltose Transporter of *Escherichia coli*:

The mechanisms by which ABC transporters transduce information and energy between their subunits are intriguing subjects of research, both as studies in enzyme engineering and because organisms rely on these systems for the uptake and secretion of vital nutrients and toxins. This thesis seeks to broaden our understanding of these mechanisms by studying the ATPase regulation of the maltose transporter of *Escherichia coli*; $MalFGK_2$. This is one of the most studied ABC transporters and is considered a model system for binding-protein-dependent ABC transport due to the conserved domain architecture of the family [22]. Several features make it an appealing subject of study. These include the transporter's necessary role in maltose metabolism, which enables researchers to assay transport by observing the growth competency of cells on maltose based media, as well as the adoption of its PBP as a research tool in protein secretion and engineering studies [23]. Due to these studies there is a wealth of information on PBP structure, conformational dynamics and substrate binding activity which can be used to inform experiments on $MalFGK_2$.

The maltose transporter shares the common domain architecture of other ABC transporters and each of its domains consists of a separate polypeptide strand (Fig. 1.1). Its TM domains are composed of a heterodimer formed by the MalF and MalG subunits, while its ABCs are a homodimer of 2 MalK subunits. Its cognate PBP is the maltose binding protein (MBP), which floats freely in the periplasm (Fig 1.2).

At the initiation of this thesis a general sequence of events in maltose transport was understood. It was known that maltose enters the periplasm of the cell through the LamB maltose pore by facilitated diffusion [24]. On the periplasmic side of the outer cell membrane maltose is bound and sequestered by MBP. The binding of maltose stabilizes a substantial conformational change in MBP from a resting 'open' state to an alternative 'closed' state (Fig 1.2) [25,26,27]. In the presence of maltose, MBP is able to stimulate rapid ATP hydrolysis and maltose internalization by the transporter (Fig 1.2).

Subsequent to the beginning of this thesis, three X-ray crystal structures of the maltose transporter complex have been resolved adopting different conformations thought to represent stages of the transport cycle [28,13,17]. These structures indicate that transport by the maltose transporter involves a series of rigid body rotations that serve to convert the TM domains from a cytoplasmic facing resting state to a perisplasmic facing state and back (Fig 1.2). This cycle has been termed transport by 'alternating access' [28]. Conversion from the resting state to the periplasmic facing state is linked to closure of the ABC subunits and an opening of the associated MBP, such that maltose can pass into the TM regions through an occluded transport passage [17]. This conformation is additionally thought to be the ATPase catalytic state of the complex because it was observed by arresting ATP hydrolysis through an ATP binding site point mutation. ATP hydrolysis is believed to force the separation of the ABC subunits and return the

Fig 1.2 Order of Events in Maltose Transport

Maltose enters the periplasm through the LamB maltoporin. In the periplasm, maltose is bound by MBP, which shifts from an open to closed conformation. In the closed form, MBP is able to activate $MalFGK_2$, resulting in the conversion of the transporter from the resting state to the ATPase catalytic state. After the passage of maltose into the TM subunits, the hydrolysis of ATP destabilizes the catalytic state and results in a reversion to the resting state, with resulting dissociation of maltose into the cytoplasm.

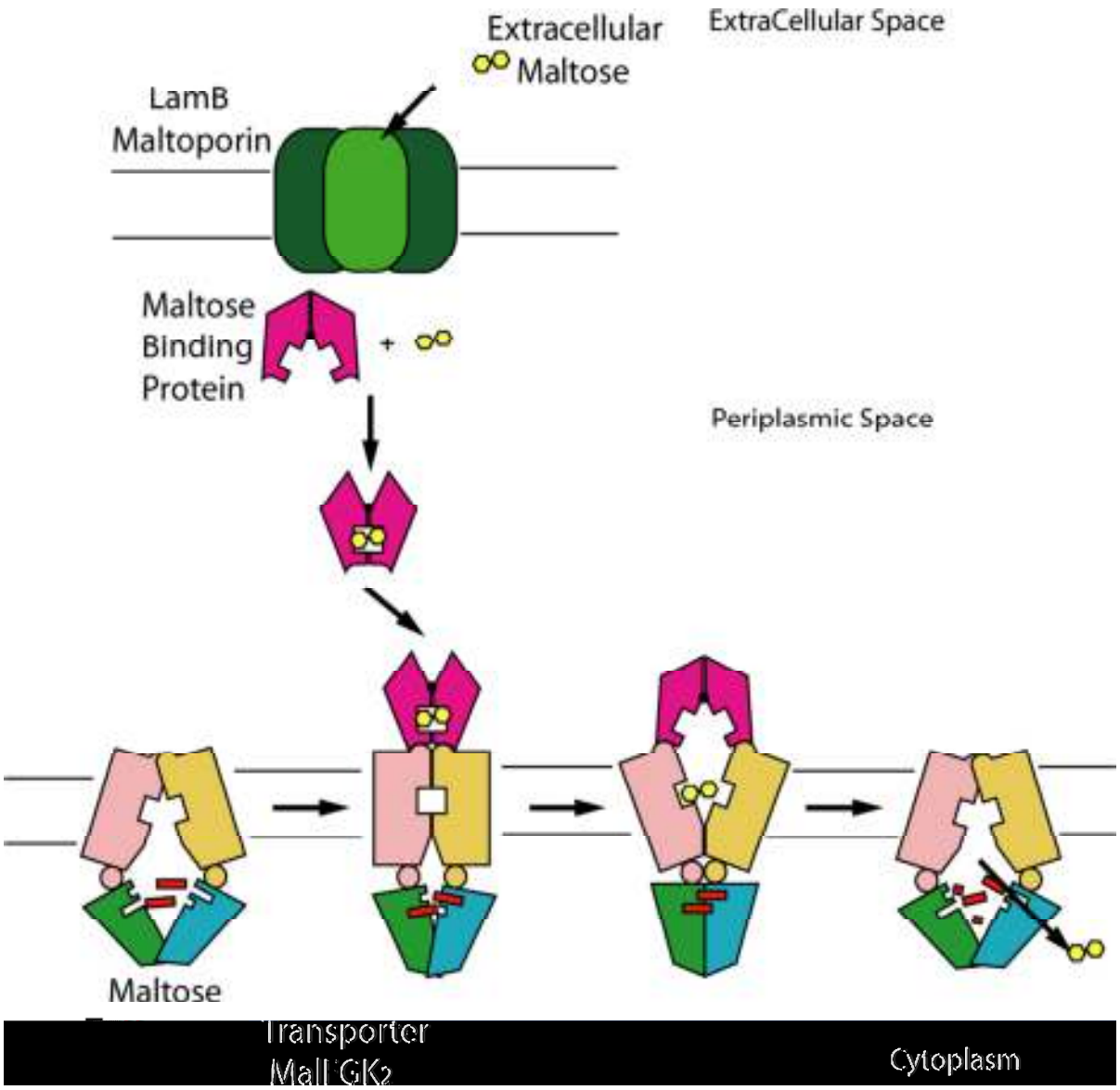
Extracellular
Maltose
ExtraCellular Space
LamB
Maltoporin
Maltose
Binding
Protein
+
Periplasmic Space
Maltose
Transporter
MalFGK2
Cytoplasm

complex to its resting state [29].

1.3 Energy Utilization by the ATP Binding Cassette:

The ATP binding cassettes of ABC transporters are the primary source of energy within these complexes; where ATP is bound and hydrolyzed, causing changes in energy that drive useful conformational changes within the larger complex [30,31]. What is known about conformational changes in the ABCs of the maltose transporter came initially from high-resolution X-ray structures of the isolated MalK subunits in soluble dimers [32,33]. However, these findings have been increasingly validated in X-ray structures of full ABC transporter complexes [17,28,13].

The MalK subunits of the maltose transporter display a structure with broad similarities to other ABCs and additionally incorporate a collection of rigidly conserved ABC sequence features. Among these features are the Walker A and B ATP-binding motifs common to a number of ATP binding enzymes [34]. Each MalK also contains an absolutely conserved 'signature sequence' incorporating the sequence LSGGQ, which is unique to the ABC transporter family and used to define its members [35].

During activity, the Walker A and B motifs of each MalK co-ordinate both the terminal β and γ phosphates of an ATP molecule and a magnesium ion. This arrangement allows for the separate binding of a molecule of ATP to each ABC subunit. When the MalK dimer is isolated in solution or incorporated into an MBP stimulated transporter complex, the binding of ATP causes it to re-organize, with the two subunits more closely associated. A rotation of the two subunits, with respect to each other, allows the LSGGQ motif of each MalK to contact the γ phosphate of the ATP bound to the opposing subunit, forming a 'composite' ATP-binding site

that incorporates residues from each subunit (Figure 1.3). This rotation has been termed a 'tweezers like motion' after the way in which the two subunits are drawn closer together [32]. ATP hydrolysis occurs in this state, with each ATP co-ordinated by both MalK subunits [17]. Note that one of the more energetic contacts in this dimer conformation is a 1.9Å hydrogen bond between Serine 135 of the signature sequence and an oxygen atom of the opposing ATP γ phosphate [36,32]. Following cleavage of ATP to ADP during hydrolysis, and release of the γ phosphate, this bond is no longer possible and likely accounts for a significant portion of the energetic differences between ABC conformations, explaining why ATP and not ADP supports ABC dimer closure [37,38].

This composite binding-site causes substantial, and energetic, conformational changes in the ABC domains to be made contingent on the binding and hydrolysis of ATP (Fig 1.3). These conformational changes take place in the context of a tight association between the ABC dimer and the TM subunits, necessitating an influence of each on the other. ATP binding and hydrolysis must communicate energy, in the form of conformational changes, into the attached TM domains. Additionally, the relative rigidity or flexibility of the TM regions likely plays a role in controlling the ABCs ability to close around and hydrolyze ATP.

1.4 Energy and Information Flow Within The Transmembrane Subunits

The transmembrane (TM) subunits of ABC transporters constitute the bulk of the actual transport machinery of the complex. In ABC exporters, which contain no other substrate-binding site, the TMs are responsible for substrate recognition and selectivity. In binding protein-dependent importers, like the maltose transporter, the TM subunits must still recognize the cognate PBP and respond to the movement of substrate into the translocation pathway. The

Fig 1.3 Conformational Changes in ABC Subunits on ATP Binding

Three X-ray crystal structures are shown of the maltose transporter of *E. coli* with the transmembrane domains (pink,yellow) in-complex with its substrate binding protein (magenta) and ABC subunits (green, cyan). Black lines denote the cell membrane and the substrate maltose is shown within the complex. As the catalytic cycle of the transporter progresses, and with the binding of ATP, the ABC subunits undergo conformational changes from an open state to a semi-open and ultimately closed state (red wedge). This closure enables the formation of a composite binding site for each ATP molecule (red rectangles) and is communicated through the coupling loops (circles) to drive conformational changes in the rest of the complex. PDB reference: 3FH6 [28], 3PVO[13],2R6G [17]

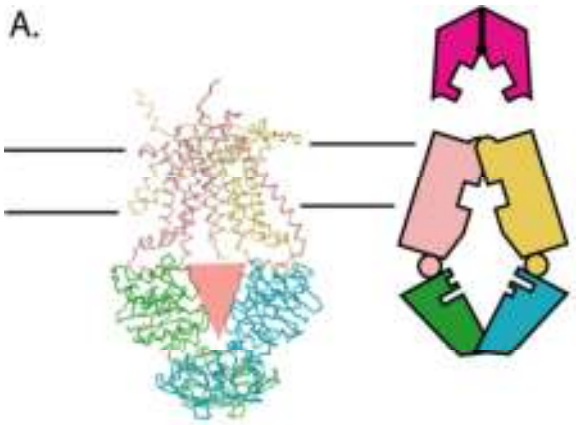

Open Resting State

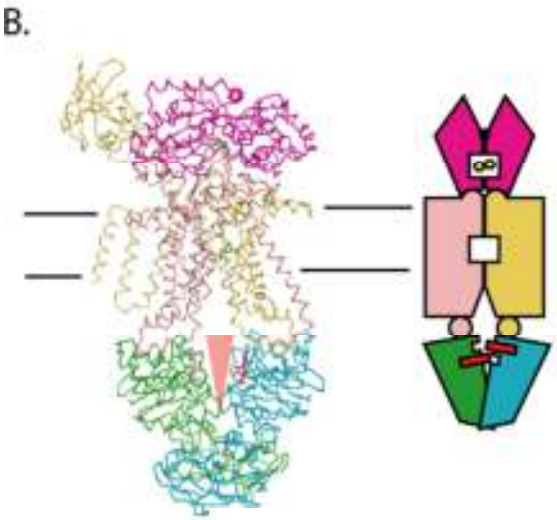

Partially Closed
Pre-catalytic State

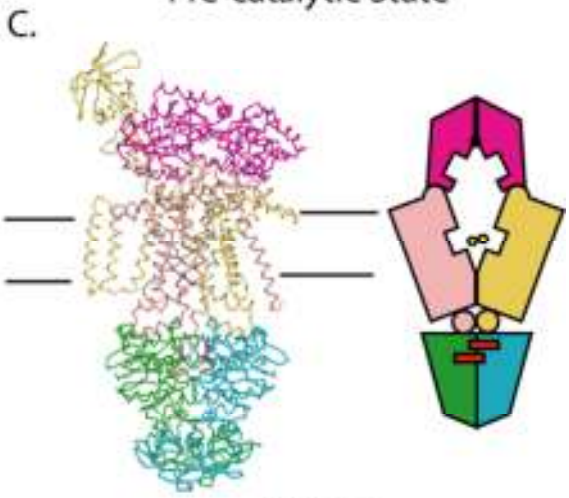

Closed
ATPase Catalytic State

sequences of TM regions within the ABC superfamily have diverged so broadly because of the need to act on substrates of diverse structure. Note that despite this diversity of sequence, phylogenetic analysis indicates a consistent pattern of descent among PBPs, TMs and ABCs [39,40]. This indicates that the transporters have been adapted whole from an ancestral complex and are thus much more likely to share common mechanisms than if they had been built from novel components.

Consistent with this finding, the TM subunits maintain broadly similar α-helical structures and a highly conserved interface with the ABC subunits, despite their varied sequence. Each TM subunit is tightly bound to its associated ABC by means of a conserved feature known as a 'coupling loop' [15]. This short α–helix runs parallel to the surface of the membrane, extends into the cytoplasm and rests within a structurally conserved groove of the ABC. The coupling loops mimic the appearance and function of a pair of handles onto which the ABCs are attached. The arrangement conveys the impression that the ABC subunits act as a power source optimized to drive many systems in a similar fashion. They are affixed to a device that is shaped by the needs of its specific function but maintains features necessary to efficiently draw power.

That the ABC subunits vary so little in structure means that the TM regions must exercise considerable control over their activity in order for each complex to couple ATP hydrolysis to the transport of differently composed substrates. Indeed, in isolation the MalK subunits of the maltose transporter are able to dimerize and close on the binding of ATP as previously discussed, resulting in a small degree of constitutive ATPase activity. However when MalK is bound to the MalF and MalG TM domains, via the coupling loops, this activity is abrogated and ATP hydrolysis is rendered contingent on activation by MBP [41,42]. The TM domains inhibit the

ABC subunits by imposing conformational or energetic restraints that must be relieved to enable activity [29]. This auto-inhibition is particularly striking given that ATP concentrations in the cell are far in excess of the K_m of most ABC subunits, likely causing the ABCs to become saturated with ATP even while in a relaxed open state.

When transport coupled ATPase is activated by maltose bound MBP, the TM domains have the reverse effect and instead stabilize or activate the ABCs to a higher rate of hydrolysis than seen in isolation. A major motivator of the work in this thesis is to investigate how the TM segments of the transporter inhibit the ABC subunits, which are capable of constitutive activity, and then reverse that inhibition so as to support an even higher level of activity when substrate is available.

In $MalFGK_2$ the communication between substrate and ABC subunits is complicated by periplasmic MBP. The system requires substrate to be presented by MBP before transport and ATP hydrolysis are triggered. This requires that the TM domains mediate communications between MBP on the external facing of the membrane and ABCs on the internal face [29,43]. However, a number of mutant complexes have been isolated that incorporate point mutations within the TM regions. These transporters are gain-of-function mutants that have been freed from dependence on MBP and are able to carry out transport in its absence. Known as 'MBP-independent' mutants, these transporters confirm the role of the TM regions in mediating information flow by activating the ATPase of a wild type ABC dimer exclusively through mutation of the TM domains.

An additional informative feature of these mutants is that they are able to overcome MBP dependence only by adopting an uncoupled phenotype. Mutants of this type are able to transport maltose, but do so at a rate that is in direct correlation to the rate of uncoupled ATP hydrolysis

[44]. These complexes are very likely cycling through transport relevant conformations in an uncontrolled manner, 'uncoupling' ATP hydrolysis from maltose transport. ATP is hydrolyzed constitutively, and maltose is transported by chance. It therefore appears that MBP plays an integral role in substrate recognition, as MBP dependence can be overcome only by a loss of ATPase regulation.

1.5 Role of the Substrate Binding Protein

As previously stated, ABC importers like the maltose transporter require substrate to be presented by a periplasmic substrate binding protein. This dependency may be linked to phylogeny, as indicated by the exclusive appearance of ABC importers in prokaryotes, while exporters are common to all domains of life. Like the TM domains, the peripheral substrate binding proteins (PBPs) of ABC transporters exhibit little or no sequence homology, yet most share a broadly conserved structure. Many binding proteins share a common folding motif, based around two domains connected by a flexible hinge region. The substrate binding site is located within a cleft at the domain interface [45,46,47,48]. This is an indication that the way in which these proteins interact with their cognate transporters may also be broadly similar.

Although it is well recognized that the maltose binding protein is necessary for the activation of the maltose transporter, its adaptive role in transport is a matter of some speculation. It has been suggested that MBP allows the substrate to be de-solvated prior to interaction with the transporter and hence greatly accelerates the act of transport as compared to a transporter that must overcome hydration energies during transport [45]. A high-affinity substrate binding site on the PBP may free the TM regions to develop a lower affinity site which will more readily expel substrate into the cytoplasm and allow the maintenance of a larger

substrate gradient than in the absence of a PBP [49]. Indeed, when exposed, the substrate binding site within the TM regions of ABC transporters does have a lower affinity for substrate compared to that of their cognate PBPs [50]. MBP independent maltose transporter mutants appear to have affinities in the low mM range, as compared to the 4 μM affinity of MBP for maltose [51]. Additionally, MBP acts as a substrate sensor for both the maltose transporter and another signaling complex, suggesting that PBPs may sometimes economize gene expression [52]. Finally, high expression of MBP, which is present at 1 mM within the periplasm of *Escherichia coli* can generate an excess of substrate binding sites, enabling the cell to rapidly capture and retain maltose from a nutrient poor environment [22].

All of these factors are likely at play in PBP selection, but several of these explanations hinge on a common feature; that moving the initial substrate-binding site out of the transporter and into a soluble protein enables it to be expressed in far greater copy number. Packing constrains limit the ability of a cell to express proteins within their membrane, as excessive crowding impacts the function of both proteins and membrane [53,22]. Expression of PBPs is over an order of magnitude higher than of their associated binding partners in the membrane, up to 4.6×10^4 MBP molecules are typically present kjfin the periplasm of *E. coli*, while only about 1000 maltose transporter complexes are embedded in the inner membrane [52,54,55,56]. This economizes the use of membrane space without limiting the ability to bind substrate, suggesting that this may be a driving concern in the evolution of PBP dependent transporters.

These features may explain the adaptive advantage of incorporating MBP into the maltose transport system, however its mechanism of action remains more elusive. The ability of MBP to influence the activity of cytosolic ABCs is a complex study in signal transduction.

1.6 Unanswered Questions Concerning Maltose Transporter Activity:

Study of the maltose transporter has been focused largely on the closed form of MBP as the likely effector of transporter activation. This is because high levels of transporter activation are only seen in the presence of maltose, which induces MBP to adopt the closed state [57]. Additionally, ligands that bind to MBP without inducing domain closure are not transported by the maltose transporter [58]. The closed conformation of MBP therefore appears to play a significant role in transporter activation and it was presumed that the open form of MBP represented an inactive state.

However, a long standing observation challenges this understanding. While high levels of ATPase activation are only observed in the presence of MBP and maltose, unliganded MBP stimulates a low level of ATPase activity from the transporter. This is an unusual result as structure determination by both crystallographic and small-angle X-ray scattering analysis indicates that unliganded MBP adopts a primarily open conformation [26]. Activation by unliganded MBP has been explained as arising from a small fraction of unliganded MBP that transiently adopts a closed-like conformation without the stabilizing influence of bound maltose [26]. Such a conformation would be highly unstable [59]. However, a number of studies do indicate that the unliganded protein can adopt closed or partially closed states [60,61].

This explanation has been dubbed the 'lock and key' hypothesis because of the implicit assumption that surface complementarity between the transporter and closed MBP is sufficient to activate ATPase. The lock and key hypothesis is indicative of the general view of the transporter at the initiation of this thesis, as it is grounded in a belief that the closed form of MBP is the sole activator of ATPase.

1.7 Research Goals and Hypothesis

The prevalent theories of $MalFGK_2$ function suggest that the closed ligand-bound conformation of MBP is the primary effecter of ATPase initiation. However the association of MBP with the transporter at multiple stages in transport suggests that the role of MBP may be more sophisticated; with both conformations of MBP and the relative stability of those forms playing integral roles in regulating ATPase coupled transport.

Based on inference from previous studies [44,57,62,63] and an examination of the available structural information [28,13,17], a hypothetical model of maltose transporter activity has been developed by which the transporter is regulated through a series of competing conformations [22]. Under this model, uncoupled ATP hydrolysis is inhibited by a destabilization of those transporter conformations adopted during the catalytic cycle. This effectively limits access to ATPase competent conformations of the transporter (Fig 1.4). The role of MBP is then to modulate the relative stability of these conformations so as to mediate inter-conversion between them (Fig 1.4). The two stable forms of MBP, liganded-closed and unliganded-open, would each bind and stabilize a distinct transporter conformation. First the binding of closed MBP allows conversion of the transporter resting state into the ATPase catalytic conformation. The catalytic state is then stabilized by open conformation MBP to initiate ATP hydrolysis in response to the movement of maltose. The binding protein would thus favor otherwise high-energy intermediate steps in transport as a way to accelerate activity, in a manner that shares broad similarity with enzyme catalysis by transition state stabilization [22].

This thesis describes efforts to test this model of ATPase coupling. The conserved domain structure of the ABC transporter superfamily makes the maltose transporter an ideal

Fig 1.4 Proposed Mechanism of Coupling in $MalFGK_2$

The maltose transporter undergoes a series of conformational changes during the catalytic cycle. Differences in the relative stability of these conformations could 'gate' ATP hydrolysis by barring access to the ATPase catalytic state when maltose is not available for transport. Under this regulatory scheme the transporter conformations normally bound by MBP would exist as high-energy intermediates that required stabilization by MBP. First the binding of closed MBP enables rapid conversion of the transporter resting state into the ATPase catalytic conformation. The catalytic state is then stabilized by open conformation MBP to initiate ATP hydrolysis in response to the movement of maltose.

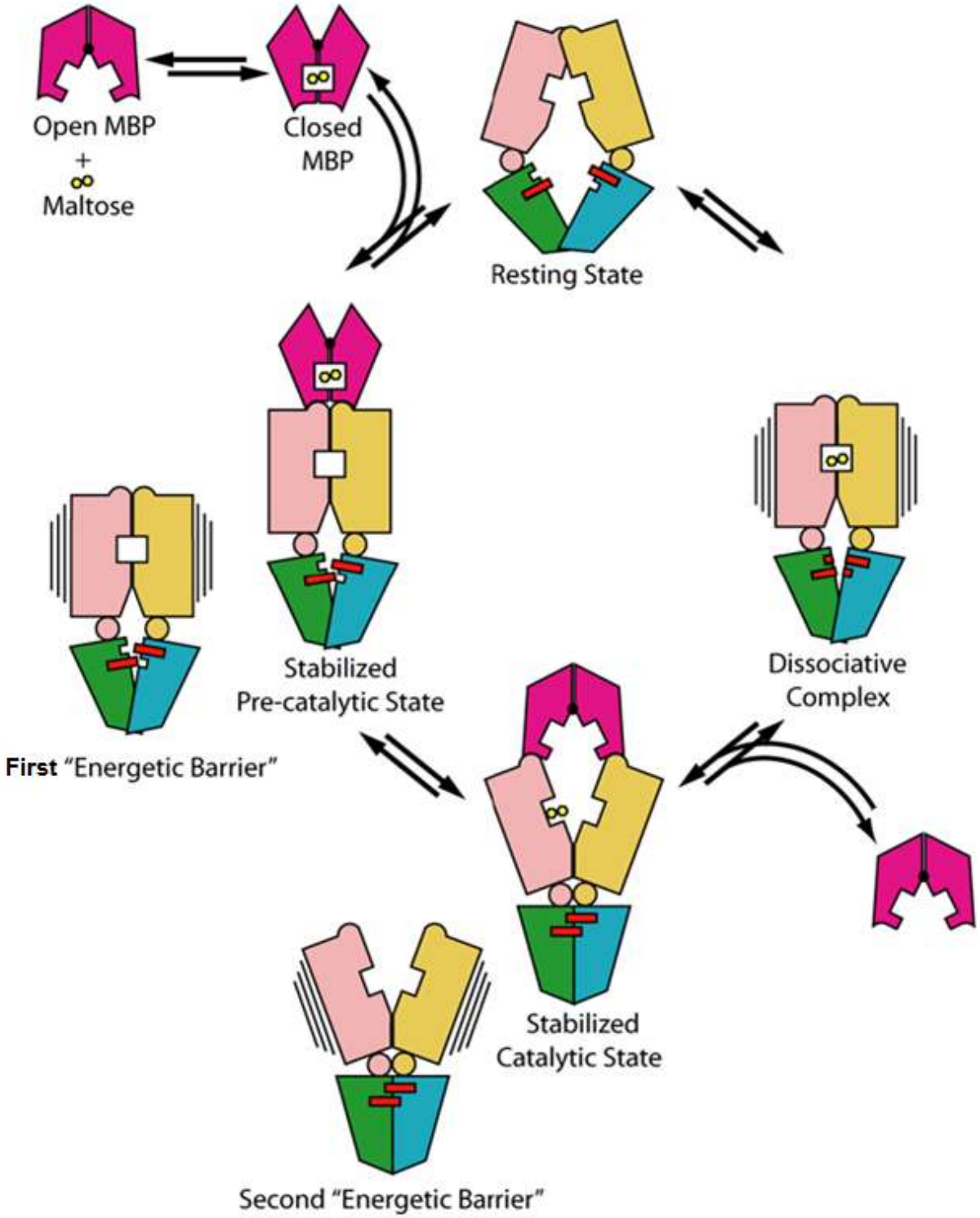
Open MBP
+
Maltose
Closed MBP
Resting State
Stabilized Pre-catalytic State
First "Energetic Barrier"
Dissociative Complex
Stabilized Catalytic State
Second "Energetic Barrier"

model system to investigate transport mechanics with relevance to a staggering diversity of substrates. The ultimate goal of this line of research is to develop an understanding of ABC coupled transport mechanics that will enable the re-engineering of these systems with mutagenic and small molecule interventions that could optimize industrially desirable transport processes and treat transporter based diseases.

1.8 Experimental Methodology

The full maltose transporter complex, with bound MBP, is a relatively large complex of 211 kDa [17]. This size, as well as its membrane embedded environment, makes it difficult to predict the effect of targeted mutations within the complex. However as a subset of the complex, MBP has been much better characterized in terms of its structure, conformational changes and inter-domain interactions. MBP is also relatively small, fully soluble in the aqueous phase and well known for its highly stable low-energy fold. For these reasons MBP is widely used in fusion proteins to augment the solubility of other proteins. These properties make MBP an appealing experimental tool, and greatly simplify the engineering of mutants. The experimental approach taken in each chapter of this thesis was to engineer targeted mutations within MBP, characterize their effect, and then determine what influence these modifications have had on the ability of MBP to activate the transporter ATPase. Predicting and observing the effects of MBP mutations on transporter activity is a means to test models of transporter coupling.

MBP is a classical type II binding protein, in that it consists of two largely independent domains connected by a flexible 'hinge' region (Fig 1.5) [26,27]. Each domain contains a portion of the substrate-binding site. After initial binding of substrate to one of these domains a series of increasingly favorable interactions between the substrate and protein draws the two

domains closed, completing the full binding site and partially occluding the substrate within the protein [64]. This is often referred to as the 'Venus Flytrap' mechanism for the way in which the two domains appear to close around and 'grasp' the bound substrate [65].

This conformational change is normally inhibited by a structure known as the balancing interface. Located opposite the substrate-binding site, across the hinge region, the balancing interface is a cleft-like interface between the two domains consisting of hydrophobic residues. These resides pack together and exclude water when MBP is in the open conformation (Fig 1.5A) but must undergo separation and hydration, disfavored by entropy, when MBP realigns its domains during closure of the maltose-binding site (Fig 1.5B)[25,66]. When maltose is present this energetic cost is countered by favorable interactions between MBP and maltose. It should be noted that the balancing interface does not hold the protein rigidly in a single 'open' conformation, but rather stabilizes an ensemble of closely related open conformations with rare and stochastic forays into less stable closed states. The significance and degree of this oscillation is debated [60,61,59] and is addressed in chapters 2 and 4.

The well-studied nature of these conformational changes and the intrinsic stability of the protein make MBP an appealing target for the engineering of informative mutants. Disruption of the MBP balancing interface, either by removal of favorable interactions or disruption of side-chain packing, pushes the protein towards the closed conformation, increasing the affinity for maltose [25,66]. Similarly, greater stabilization of one competing conformation or alteration of the substrate-binding site can cause predicable shifts in the equilibrium between open and closed conformations. These factors combine with the significant control MBP exerts over ATP hydrolysis to make the binding protein an ideal experimental probe for the study of the maltose transporter.

Fig 1.5 The Substrate Binding Site and Balancing Interface Balance Conformational Changes in MBP.

X-ray crystal structures of the maltose binding protein are shown in the: (A) Unliganded open conformation and (B) the maltose bound closed conformation. The two domains of MBP (Red and Magenta) rotate with respect to each other following the binding of maltose (green). This domain rotation causes an opening of the hydrophobic balancing interface (blue) while inducing the closure of the substrate binding cleft (yellow). Pdb reference: 1OMP [26],1ANF [27]

A.

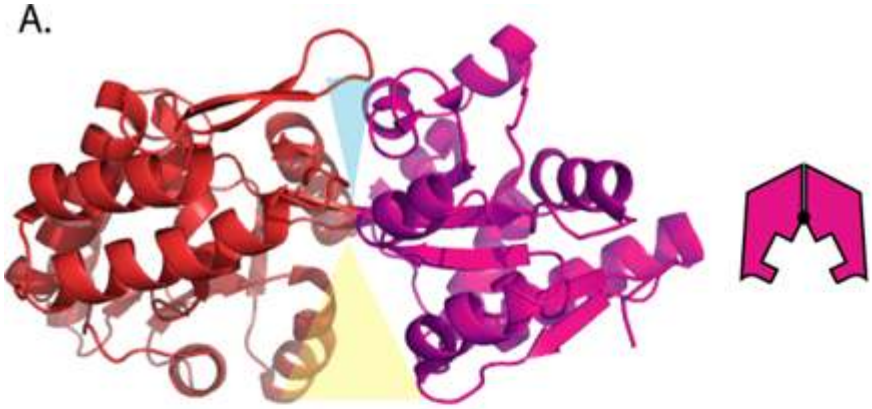

Unliganded Open Conformation

B.

Maltose-Bound Closed Conformation

1.9 Scope of Thesis

The second chapter of this thesis details a careful examination of the kinetics of ATPase activation by maltose saturated and depleted MBP. The purpose of this investigation was to test the previously discussed 'lock and key' hypothesis, that surface complementarity with closed MBP triggers the transporter ATPase. A novel denaturation and dialysis approach has been undertaken to remove all contaminating maltose from prepared MBP. This has enabled observation of the previously unexamined kinetics of ATPase stimulation by unliganded MBP. Our findings indicate that the MBP concentration dependence of this activation is not consistent with current thinking on the subject. It instead suggests that the open conformation of MBP can directly bind and activate a rare conformation of $MalFGK_2$. This suggests that multiple forms of MBP may be responsible for transporter activation.

The third chapter presents findings utilizing a novel substrate-binding mutant of MBP. This mutant undergoes conformational changes from open to closed similar to wild type MBP, but is capable of doing so in response to the binding of sucrose as well was maltose. Point mutations in the substrate-binding site create favorable interactions that enable sucrose binding to counter the opening of the balancing interface. We find in this study that these mutations are sufficient to adapt ATPase activation in the wild-type transporter to a novel substrate. These findings demonstrate that the TM domains do not directly recognize their target substrate as a necessary step in activating ATP hydrolysis. Based on X-ray structure determination a mechanism is proposed by which the transporter can indirectly track the passage of substrate from MBP into the translocation pathway.

In the fourth chapter additional MBP conformational mutants have been prepared. Cysteine mutations were introduced with the intent to stabilize the open and closed

conformations in different mutants. Cross links between these residues create conformational constraints that alter the ability to interconvert between closed and open states. This has enabled the influence of these conformations on the transporter to be separately investigated. The effect of these mutants on wild-type transporter has been additionally examined after extraction of the complex from the membrane by a mild detergent. This treatment is known to cause substantial uncoupling of ATPase activity; disrupting the transporter's normal regulation. The susceptibility of the transporter to activation by the constrained mutant binding proteins is found to differ informatively, suggesting an 'energetic barrier' against uncoupled activation that has its origins in packing interactions between the TM subunits and the membrane.

Bibliography

1. Agre P, Bonhivers M, Borgnia MJ. (1998) The aquaporins, blueprints for cellular plumbing systems. *J Biol Chem*. **273**: 1459-62, 1998.
2. Knepper MA, Nielsen S. (2004) Peter Agre, 2003 Nobel Prize winner in chemistry. *J Am Soc Nephrol*. **15**: 1093-1095, 2004.
3. Nimigean, C.M., and Allen, T.W., (2011) Origins of ion selectivity in potassium channels from the perspective of channel block. *J Gen Physiol*. **137**: 405-13.
4. Yan, R.T., and Maloney, P.C., (1993) Identification of a residue in the translocation pathway of a membrane carrier. *Cell*. **75**: 37-44.
5. Jardetzky, O., (1966) Simple allosteric model for membrane pumps. *Nature* **211**: 969-970.
6. Mitchel, P. (1957) A general theory of membrane transport from studies of bacteria. *Nature*. **180**: 134-136.
7. Lemieux, M.J., Huang, Y., Wang, D.N., (2004) Glycerol-3-phosphate transporter of Escherichia coli: structure, function and regulation. *Res Microbiol*. **155**: 623-9.
8. Maiden, M.C., Jones-Morimer, M.C., Henderson, P.J., (1988) The cloning, DNA sequence, and overexpression of the gene area coding for arabinose-proton symport in Escherichia coli K12. *J Biol Chem.* **263**: 8003-10
9. Abramson, J., Smirnova, I., Kasho, V., Verner, G., Kaback, H.R., Iwata, S., (2003) Structure and Mechanism of the Lactose Permease of Escherichia coli. *Science*. **301**:610-5
10. Ames, G.F., Mimura, C.S., Shyamala, V., (1990) Bacterial periplasmic permeases belong to a family of transport proteins operating from Escherichia coli to human: Traffic ATPases. *FEMS Microbiol Rev*. **6**: 429-46.
11. Saier M.H., Jr., (1998) Molecular Phylogeny as a Basis for the Classification of Transport Proteins from Bacteria, Archaea and Eukarya. *Adv Microb Physiol*. **40**:81-136.
12. Chen C.J., Chin J.E., Ueda, K., Clark, D.P., Pastan, I., Gottesman, M.M., Roninson, I.B., (1986) Internal duplication and homology with bacterial transport proteins in the mdr1 (P-glycoprotein) gene from multidrug-resistant human cells. *Cell* **47**:381-9
13. Oldham, M.L., Chen, J., (2011) Crystal stucture of the maltose transporter in a pretranslocation intermediate state. *Science*. **332**:1202-5
14. Aller, S.G., Yu, J., Ward, A., Weng, Y., Chittaboina, S., Zhuo, R., Harrell, P.M., Trinh, Y.T., Zhang, Q., Urbatsch, I.L., Chang, G., (2009) Structure of P-glycoprotein reveals a molecular basis for poly-specific drug binding. *Science*. **323**:1718-22
15. Hollenstein, K., Frei, D.C., Locher, K.P., (2007) Structure of an ABC transporter in complex with its binding protein. *Nature*. **446**: 213-6.
16. Hekstra, D., Tommassen, J., (1993) Functional exchangeability of the ABC proteins of the periplasmic binding protein-dependent transport systems Ugp and Mal of Escherichia coli. *J Bacteriol*. **175**:6546-52
17. Oldham, M.L., Khare, D., Quiocho, F.A., Davidson, A.L., Chen, J., (2007) Crystal structure of a catalytic intermediate of the maltose transporter. *Nature* **450**:515-21
18. Hvorup, R.N., Goetz, B.A., Niederer, M., Hollenstein, K., Perozo, E., Locher, K.P., (2007) Asymetry in the structure of the ABC transporter-binding protein complex BtuCD-BtuF. *Science*. **317**:1387-90.

19. Dawson, R.J., Locher, K.P., (2006) Structure of a bacterial multidrug ABC transporter. *Nature*. **447**:180-5.
20. Prossnitz, E., Nikaido, K., Ulbrich, S.J., Ames, G.F., (1988) Formaldehyde and photoactivatable cross-linking of the periplasmic binding protein to a membrane component of the histidine transport system of Salmonella typhimurium. *J Biol Chem*. **263**: 17917-20.
21. Cadieux, N., Bradbeer, C., Reeger-Schneider, E., Köster, W., Mohanty, A.K., Wiener, M.C., Kadner, R.J., (2002) Identification of the periplasmic cobalamin-binding protein BtuF of Escherichia coli. *J Bacteriol*. **184**:706-17.
22. Shilton, B.H., (2008) Dynamics of the MBP-MalFGK2 interaction: A prototype for binding protein dependent ABC-transporter systems. *Biochimica et Biophysica Acta*. **1778:**1772-80.
23. Medintz, I.L., Deschamps, J.R., (2006) Maltose-binding protein: a versatile platform for prototyping biosensing. *Curr Opin Biotechnol*. **17**:17-27.
24. Bavoil, P., Wandersman, C., Schwartz, M., Nikaido, H., (1983) A mutant form of maltose-binding protein of *Escherichia coli* deficient in its interaction with the bacteriophage lambda receptor protein. *J Bacteriol*. **155**:919-921.
25. Telmer P.G., Shilton, B.H., (2003) Insights into the Conformational Equilibria of Maltose-binding Protein by Analysis of High Affinity Mutants. *J Biol Chem*. **278**:34555-67.
26. Sharff, A.J., Rdseth, L.E., Spurlino, J.C., Quiocho, F.A. (1992) Crystallographic evidence of a large ligand-induced hinge-twist motion between the two domains of the maltodextrin binding protein involved in active transport and chemotaxis. *Biochemistry.* **31**:10657-63.
27. Quiocho, F.A., Spurlino, J.C., Rodseth, L.E., (1997) Extensive features of tight oligosaccharide binding revealed in high-resolution structures of the maltodextrin transport/chemosensory receptor. *Structure*. **5**:997-1015.
28. Khare D., Oldham, M.L., Orelle, C., Davidson, A.L., Chen, J., (2009) Alternating access in maltose transporter mediated by rigid-body rotations. *Mol Cell*. **33**:528-36
29. Orelle, C., Ayvaz, T., Everly, R.M., Klug, C.S., Davidson, A.L., (2008) Both maltose-binding protein and ATP are required for nucleotide-binding domain closure in the intact maltose ABC transporter. *Proc Natl Acad Sci*. **105**:12837-42.
30. Dean, D.A., Davidson, A.L., Nikaido, H., (1989) Maltose transport in membrane vesicles of Escherichia coli is linked to ATP hydrolysis. *Proc. Natl. Acad. Sci.U.S.A*. **86**: 9134-8.
31. Ames, G.F., Nikaido, K., Groarke, J., Petithory, J., (1988) Reconstitution of Periplasmic Transport in Inside-out Membrane Vesicles. Energization by ATP. *J Biol Chem*. **264**:3998-4002
32. Chen, J., Lu, G., Lin, J., Davidson, A.L., Quiocho, F.A., (2003) A tweezers-like motion of the ATP-binding cassette dimer in an ABC transport cycle. *Mol Cell*. **12**:651-61.
33. Smith, P.C., Karpowich, N., Millen, L., Moody, J.E., Rosen, J., Thomas, P.J., Hunt, J.F., (2002) ATP binding to the motor domain from an ABC transporter drives formation of a nucleotide sandwich dimer. *Mol Cell*. **10**:139-49
34. Walker, J.E., Saraste, M., Runswick, M.J., Gay, N.J., (1982) Distantly related sequences in the α– and β–subunits of ATP synthase, myosin, kinases and other ATP requiring enzymes and a common nucleotide binding fold. *EMBO J*. **1**:945-51.

35. Linton, K.J., and Higgins, C.F., (1998) The Escherichia coli ATP-binding cassette (ABC) proteins. *Mol Microbiol*. 28;5-13.
36. Oloo, E.O., Fung, E.Y., and Tieleman, D.P., (2006) The Dynamics of the MgATP-driven Closure of MalK, the Energy-transducing Subunit of the Maltose ABC Transporter. *J Biol Chem*. **281**:28397-407.
37. Moody, J.E., Millen, L., Binns, D., Hunt, J.F., Thomas, P.J. (2002) Cooperative, ATP-dependent Association of the Nucleotide Binding Cassettes during the Catalytic Cycle of ATP-binding Cassette Transporters. *J Biol Chem*. **277**:21111-4.
38. Lu, G., Westbrooks, J.M., Davidson, A.L., Chen, J., (2005) ATP hydrolysis is required to reset the ATP-binding cassette dimer into the resting-state conformation. *PNAS* **102**:17969-74.
39. Saurin, W., Dassa, E., (1994) Sequence relationships between integral inner membrane proteins of binding protein-dependent transport systems: evolution by recurrent gene duplications. *Protein Sci*. **3**:325-44.
40. Saurin, W., Hofnung, M., Dassa, E., (1999) Getting in or out: early segregation between importers and exporters in the evolution of ATP-bindin cassette (ABC) transporters. *J Mol Evol*. **48**:22-41.
41. Morbach, S., Tebbe, S., Schneider E., (1993) The ATP-binding cassette (ABC) transporter for maltose/maltodextrins of Salmonella typhimurium. Characterization of the ATPase activity associated with the purified MalK subunit. *J Biol Chem*. **268**:18617-21.
42. Sneider, E., Linde, M., Tebbe, S., (1995) Functional purification of a bacterial ATP-binding cassette transporter protein (MalK) from the cytoplasmic fraction of an overproducing strain. *Prot Expr Purif*. **6**:10-14.
43. Borths, E.L., Poolman, B., Hvorup, R.N., Locher, K.P., Rees, D.C., (2005) In vitro functional characterization of BtuCD-F, the Escherichia coli ABC transporter for vitamin B12 uptake. *Biochemistry*. **44**:16301-9.
44. Covitz, K.M., Panagiotidis, C.H., Hor, L., Reyes, M., Treptow, N.A., Shuman, H.A., (1994) Mutations that alter the transmembrane signaling pathway in an ATP binding cassette (ABC) transporter. *EMBO J*. **13**:1752-9.
45. Quiocho, F.A., Vyas, N.K., (1984) Novel stereospecificity of the L-arabinose-binding protein. *Nature* **310**:381-6.
46. Vyas, N.K., Vyas, M.N., Quiocho, F.A., (1988) Sugar- and signal-transducer binding sites of the *Escherichia coli* galactose chemoreceptor protein. *Science* **242**:1290-5.
47. Sack, J.S., Saper, M.A., Quiocho, F.A., (1989) Periplasmic binding protein structure, and function: refined structures of the leucine/isoleucine/valine-binding protein and its complex with leucine. *J Mol Biol* **206:171-91.**
48. Pflugrath, J.W., Quiocho, F.A. (1985) Sulphate sequestered in the sulphate-binding protein of *Salmonella typhimurium* is bound solely by hydrogen bonds. *Nature* **314**:257-260.
49. Davidson, A.L., Maloney, P.C., (2007) ABC transporters: how small machines do a big job. *Trends Microbiol*. **15**:448-55.
50. Petronilli, V., Ames, GF.L., (1991) Binding Protein-independent histidine permease mutants. Uncoupling of ATP hydrolysis from transmembrane signaling. *J Biol Chem*. **266**:16293-6.

51. Treptow, N.A., Shuman, H.A., (1985) Genetic evidence for substrate and periplasmic-binding-protein recognition by the MalF and MalG proteins, cytoplasmic membrane components of the *Escherichia coli* maltose transport sytem. *J Bacteriol*. **163**:654-60.
52. Manson, M.D., Boos, W., Bassford, P.J., Rasmussen, B.A. (1985) Dependence of Maltose Transport and Chemotaxis on the Amount of Maltose-binding Protein. *J Biol Chem*. **260**:9727-33.
53. Lenaz, G., (1987) Lipid Fluidity and Membrane Protein Dynamics. *Biosci Rep*. **7**:823-37.
54. Koman, A., Harayama, S., Hazelbauer, G.L., (1979) Relation of chemotactic response to the amount of receptor: evidence for different efficiencies of signal transduction. *J Bacteriol*. **148**:739-47.
55. Shuman, H.A., Silhavy, T.J., (1981) Identification of the malK Gene Product. *J Biol Chem*. **256**:560-62
56. Richarme G. (1982) Interaction of the maltose-binding protein with membrane vesicles of Escherichia coli. *J Bacteriol*. **149**:662-7.
57. Davidson, A., Shuman, H., and Nikaido, H. (1992) Mechanism of maltose transport in Escherichia coli : Transmembrane signaling by periplasmic binding proteins, *Proc. Natl. Acad. Sci. USA* **89**: 2360-2364.
58. Hall, J.A., Ganesan, A.K., Chen, J., Nikaido, H., (1997) Two modes of ligand binding in maltose-binding protein of Escherichia coli. Functional significance in active transport. *J Biol Chem*. **272**:17615-22.
59. Millet, O., Hudson, R.P., Kay, L.E., (2003) The energetic cost of domain reorientation in maltose-binding protein as studies by NMR and fluorescence spectroscopy. *Proc Natl Sci U S A*. **100**:12700-5.
60. Bucher, D., Grant, B.J., Markwick, P.R., McCammon, J.A., (2011) Accessing a Hidden Conformation of the Maltose Binding Protein Using Accelerated Molecular Dynamics. *PLoS Comput Biol*. **7**:e1002034.
61. Tang C., Schwieters, C.D., Clore, G.M., (2007) Open-to-closed transition in apo maltose-binding protein observed by paramagnetic NMR. *Nature*. **449**:1078-82.
62. Dean, D.A., Hor, L.I., Shuman, H.A., Nikaido, H., (1992) Interaction between maltose-binding protein and the membrane-associated maltose transporter complex in *Escherichia coli*. *Mol Microbiol* **6**: 2033-40.
63. Austermuhle, M. I., Hall, J. A., Klug, C. S., and Davidson, A. L. (2004) Maltose-binding protein is open in the catalytic transition state for ATP hydrolysis during maltose transport*, J Biol Chem* **279**: 28243-50. Epub 2004 Apr 26..
64. Stockner, T., Vogel, H.J., Tieleman, D.P., (2005) A salt-bridge motif involved in ligand binding and large scale domain motions of the maltose binding protein. *Biophys J.* **89**:3362-71.
65. Mao, B., Pear, M.R., McCammon, J.A., Quiocho, F.A., (1982) Hinge-bending in L-arabinose-binding protein: the 'Venus' flytrap' model. *J Biol Chem*. **257**:1131-33.
66. Marvin, J.S., Hellinga, H.W., (2001) Manipulation of ligand binding affinity by exploitation of conformational coupling. *Nat Struct Biol*. **8**:795-8.

Chapter 2 Stimulation of the Maltose Transporter ATPase by Unliganded Maltose Binding Protein

2.1 Introduction

ATP Binding Cassette (ABC) transporters use the chemical energy of ATP hydrolysis to transport solutes across a membrane. ABC transporters can be divided into export systems and import systems, and a key question in both cases is the mechanism by which ATP binding and hydrolysis are regulated and coupled to substrate translocation. For ABC export systems, the substrate itself regulates the ATPase [1,2,3]. ABC import systems, on the other hand, include a peripheral substrate binding protein, and the ATPase activity is regulated by interactions between the binding protein and the transmembrane components [4,5,6].

The *E. coli* maltose transporter ($MalFGK_2$) is a tractable and well-studied ABC import system consisting of the membrane associated complex $MalFGK_2$ and peripheral extracellular maltose binding protein (MBP). MalF and MalG are integral membrane proteins; $MalK_2$ is a dimer of ABC subunits bound to MalFG on the cytoplasmic side of the membrane. Structures of isolated $MalK_2$ have been solved and from these it is known that ATP binds in the dimer interface and promotes a tight association of the subunits, bringing each ATP molecule in contact with catalytic residues from the opposite subunit [7]. Once ATP hydrolysis takes place, the subunits dissociate, allowing release of ADP and inorganic phosphate [8]. In the intact $MalFGK_2$ complex, these conformational changes are coupled to changes in MalFG [9,10,11,12] so that the maltose binding site in MalFG opens alternately to the periplasm or cytoplasm [12].

Stimulation of ATP hydrolysis by the binding protein must involve conformational changes that are transmitted from the extracellular surface through the transmembrane domains to the ATP binding cassettes on the cytoplasmic side. MBP and other class I or II binding

proteins consist of two domains connected by a flexible hinge, and ligand binding brings about a large structural change of the protein [13]. This conformational change, from the "open" unliganded structure, to the "closed" liganded form, is critical for transport since only the ligand-bound conformation can fully stimulate the membrane ATPase [4,14]. On this basis, the ligand-induced conformational change serves to ensure that futile cycles of ATP hydrolysis are avoided.

This picture is complicated by the enigmatic observation, in both the maltose and histidine transport systems, that ATP hydrolysis is stimulated, to a limited degree, by the *unliganded* binding protein [4,5]. While there is no obvious physiological function for the ability of the unliganded binding protein to stimulate the membrane ATPase, it does raise questions about the mechanism of the stimulation. Specifically, it is not clear what conformation of MBP is responsible for the activation of the $MalFGK_2$ ATPase in the absence of maltose. On the one hand, unliganded MBP exists predominantly in an open conformation in solution [15,16], and therefore the open conformation represents a logical candidate for the activation. In support of this idea, during maltose transport and at the point where ATP is poised for hydrolysis, the open unliganded form is found tightly bound to $MalFGK_2$ [11,17]. On the other hand, maltose transport requires an initial interaction with closed, maltose-bound MBP prior to opening and progression to the transition state for ATP hydrolysis. Therefore, the activation of the $MalFGK_2$ ATPase by unliganded MBP could be due to a small amount of a closed, unliganded form of MBP which exists in solution [18]; the presence of such a solution conformation is supported by the crystallization of two other binding proteins in a closed, unliganded state [19,20]. On this basis, a closed unliganded conformation might affect the same changes brought about by the closed *liganded* conformation. This model for stimulation of the ATPase by the binding protein

could be termed "lock-and-key" since it is solely the conformation and the surface complementarity of the binding protein that is important for the interaction.

However, substrate binding affects not only the conformation, but also the stability and molecular dynamics of the binding protein. In the case of MBP, intrinsic tryptophan fluorescence and molecular dynamics simulations indicate that unliganded MBP has a somewhat dynamic structure, with the two domains moving relative to each other, in contrast to the ligand-bound form in which the relative positions of the domains appears to be fixed [21,22]. Furthermore, the closed *unliganded* conformation has a much higher energy and lower stability than the closed, liganded form due to the absence of stabilizing non-covalent bonds between maltose and MBP [23]. Thus, although a closed, unliganded conformation of MBP could, in principle, resemble the closed liganded form, it will be more dynamic and much less stable. On this basis, stimulation of the $MalFGK_2$ ATPase by a closed, unliganded conformation of MBP implies that the conformational stability of the binding protein is not critical for a productive interaction, and this has significant mechanistic implications for how conformational changes are brought about by the interaction between MBP and $MalFGK_2$.

To address the question of whether the closed, unliganded form of the binding protein can stimulate ATP hydrolysis by the transporter, we engineered maltose binding protein so that the open conformation is destabilized relative to the closed conformation, and assayed the ability of these forms of the protein to activate the membrane-bound ATPase. In addition, we have carried out a careful analysis of the ability of unliganded MBP to stimulate the membrane ATPase, and demonstrate that the characteristics of this stimulation are completely different from what is observed for ligand-bound MBP. The results we have obtained make it highly unlikely that, in

the absence of maltose, a closed conformation of MBP is responsible for stimulation of $MalFGK_2$, and we suggest instead that it is the more stable and abundant open conformation.

2.2 Materials and Methods

Bacterial strains and plasmids

The bacterial strain HS3399 was used for expression for all transport complexes, and was originally derived from the parental strain of *Escherichia coli* K12 [24]. This strain contains the Δ*malB*101 allele, a deletion of the entire *mal* operon, and the Δ*atp* allele, a deletion of the gene for F_1-ATPase. *E. coli* strain HS3309 [25] was used for expression of periplasmic MBP and MBP-DM from pLH1 [26] and pLH1-DM [27]. These plasmids code for MBP and MBP-DM with a periplasmic export tag, under a MalT inducible promoter. HS3309 does not produce chromosomally encoded MBP and has constitutive expression of the maltose operon activator, MalT to drive expression from pLH1. In the MBP-DM mutant, residues 172, 173, 175, and 176 are deleted, resulting in a truncated surface loop, and M321 and Q325 are both mutated to alanine. The plasmid pNTSK+ contains *malF* and *malG* genes preceded by the IPTG-inducible pTac promoter. pNTSK+ was produced by digesting the plasmid pCP8 [24] with EcoR1 to remove the tethered MBP expression cassette. Since this cassette also contained the ampicillin resistance marker, pBluescript II SK+ (Fermentas) was cloned into the EcoR1 site to restore ampicillin resistance. pMR11, which is replicative-compatible with pNTSK+, harbors the *malK* gene preceded by the pTac promoter sequence, and contains a chloramphenicol resistance marker. pMal-96W329W contains the coding sequence for cytoplasmic MBP with the balancing interface mutations A96W and I329W [23].

Construction of hexahistidine-tagged MBP. To increase the efficiency of purification and the yield of MBP, the MBP coding sequence was cloned into pProEX-HTa (Invitrogen) for intracellular expression of a hexahistidine-tagged version of MBP connected by a TEV protease cleavable linker. Restriction sites for cutting and inserting Ehe1 and HindIII were introduced into the pLH1 vectors by mutagenic PCR, with primers:

5’CGCCTCGGCTGGCGCCAAAATCGAAG-3’ (forward) and

5’CGCCGCATCCGGCATTTAAGCTTATTACTTGGTGATACGAG-3’ (reverse).

The entire MBP coding sequence was verified.

Expression and purification of MBP

Wild-Type MBP and MBP-DM. All chromatographic media were purchased from GE Healthcare. Plasmids containing wild-type (pLH1) or mutant (pLH1-DM) *malE* coding regions were transformed into *E. coli* strain HS3309. Cultures were grown with vigorous shaking at 30°C in LB broth containing 100 μg/mL ampicillin for 16 to 18 h. Periplasmic proteins were extracted by osmotic shock and dialyzed against 50 mM Tris-HCl, pH 8.5 in preparation for anion exchange chromatography. The extract was applied onto a 2.6 x 15 cm column packed with Q-Sepharose Fast Flow and eluted with a linear gradient from 0 to 1 M NaCl, with a base buffer of 50 mM Tris-HCl, pH 8.5. Fractions containing MBP were pooled and dialyzed against 50 mM Tris-HCl, pH 8.5. Depending on the purity of MBP containing fractions at this step, a further ion-exchange step using a Mono-Q column was sometimes necessary before moving on to the next step.

To effect further purification and remove contaminating maltose from preparations of MBP, protein from the ion exchange column(s) was diluted in 50 mM Tris-HCl, and dialyzed against two changes of a 100-fold excess 2 M guanidine hydrochloride. Guanidine hydrochloride was then slowly removed by dialysis against a four changes of a 100-fold excess of 50 mM Tris-HCl pH 8.5. The refolded MBP was concentrated by ion-exchange chromatography using a 1-mL HiTrap Q column. Concentrated protein was loaded onto a 2.6 x 60 cm column of Superdex 200 Prep Grade gel filtration resin, which had been equilibrated with 20 mM Hepes, 100 mM KCl, pH 7.4. The column was developed with this same buffer at a flow rate of 0.5 mL/min. Fractions containing pure MBP were pooled and dialysed against 2 changes of a 100-fold excess of 50 mM

Tris pH 8.0. MBP was concentrated on a 1 mL HiTrap Q column, and then dialyzed against a 100-fold excess of 50 mM Tris-HCl pH 7.0, 100 mM KCl, 10 mM $MgCl_2$.

MBP-A96W/I329W. To express and purify the cytoplasmic MBP-A96W/I329W, HS3309 cells were transformed with pMal-A96W/I329W, and a single colony was used to inoculate 100 mL LB-Amp. This culture was grown with vigorous shaking to an optical density of 0.1 and 100 µL was added to 1 L of LB-Amp. The culture was grown to an OD_{600} of 0.4 and expression of MBPA96W/I329W was induced by addition of 100 µg/mL IPTG and the culture grown for a further 6 hours at 37°C. Cells were ruptured by passage through a French Pressure cell at 20,000 p.s.i, and pure MBP was obtained by anion-exchange and gel filtration chromatography as described above.

Histidine-Tagged MBP. For later experiments involving stimulation of $MalFGK_2$ with high concentrations of MBP, wtMBP was expressed intracellularly in a BL21(DE3) background, as a fusion protein with a TEV protease cleavable hexahistidine tag. After growth, induction, and harvesting (as described for MBP-A96W/I329W, above) the cell pellet was resuspended in 50 mL of Ni^{2+}-NTA buffer (20mM Hepes, 500 mM KCl, 10 mM imidazole, 10% glycerol, pH 8.0) and supplemented with 1 mM PMSF before lysis by 3 passes through a French pressure cell at 20,000 psi. Cell debris was pelleted at 100,000 *g* and the supernatant applied to Ni^{2+}-loaded Chelating Sepharose FF and proteins eluted using an imidazole gradient from 10 to 250 mM. High purity fractions containing MBP were pooled and a 1:20 mass ratio of TEV protease was added; the solution was dialyzed overnight at 4°C against 4L of Ni^{2+}-NTA buffer to remove excess imidazole. The TEV protease treated protein was loaded onto clean Ni^{2+}-NTA resin and MBP, with the histidine tag removed, was collected from the flow through. The cleaved MBP was dialyzed overnight against 4L of 50 mM Tris-HCl, pH 8.5, in preparation for anion exchange chromatography.

Denaturation and refolding of MBP.

Fractions from the anion exchange column containing pure MBP were pooled and denatured by overnight dialysis against a 5-fold excess of 6 M guanidine-HCl. The denatured protein was subsequently dialyzed against 5 changes of a 10-fold excess of 6 M guanidine-HCl at 4ºC, resulting in a ligand dilution of 500,000-fold; 5 mM EDTA was included in the final 2 dialysis buffers. Protein was refolded by dialysis against 1 M guanidine-HCl, 5mM EDTA, and then dialyzed twice against a 50-fold excess of 50 mM Tris-HCl pH 8.5.

Note that the proper refolding and function of all MBP preparations was tested by fluorescence titrations with maltose and/or maltotriose: the refolded MBP preparations typically yielded a higher degree of fluorescence quenching due to complete removal of ligand. To maintain consistency between ATPase assays in both the absence and presence of maltose, all MBP preparations were subjected to the same unfolding and refolding procedure.

Preparation of Proteoliposomes

Over-expression of $MalFGK_2$. HS3399 cells were co-transformed with plasmids carrying the malF and malG genes (pNTSK+), and the malK gene (pMR11). A single colony was inoculated into 100 mL of LB (containing 100 µg/mL ampicillin, and 50 µg/mL chloramphenicol), and grown to a OD_{600} of 0.1; 100 µL of this culture was added to each liter of the same media, and cells were grown with vigorous shaking at 37°C, to an OD_{600} of 0.4; expression of $MalFGK_2$ was induced by the addition of 100 µg/mL IPTG and grown for 8 hours at 37°C. The cell pellet from each liter was washed twice with 50 mL of 20 mM Hepes pH 7.0, and crude membranes were prepared as follows: each gram of washed cells was re-suspended in 10 mL of 20 mM Hepes 7.0, 5 mM $MgCl_2$, with 10 % glycerol, and passed twice through a French pressure cell at 15,000 psi. Cell debris was removed by centrifugation at 7,000 *g* for 10

minutes. The supernatant was then subjected to ultracentrifugation at 100,000 *g* to recover membranes. Membranes were washed twice in 10 mM MOPS pH 7.5, 5 mM $MgCl_2$, 200 mM sucrose, and resuspended in 10 mM MOPS pH 7.5, 5 mM $MgCl_2$, 200 mM sucrose, with 10% methanol.

Solubilization of membrane protein. Washed membrane vesicles were recovered by centrifugation at 100,000 *g* and re-suspended at a protein concentration of 5 mg/mL in 50 mM Tris-HCl, pH 7.0, 1.2% β-octylglucoside, and 10 mM $MgCl_2$. This solution was kept on ice with occasional agitation for 60 minutes, and was subsequently subjected to ultracentrifugation at 100,000 *g* for 45 minutes to pellet the insoluble material. The remaining supernatant containing the solubilized protein fraction was kept at 4°C until use.

Preparation of Proteoliposomes (PLS). Crude *E. coli* phospholipids (Avanti Polar Lipids) were dissolved at a concentration of 50 mg/mL in chloroform. The chloroform was removed using a rotary evaporator, leaving a lipid film on the round bottom flask, and the lipids were re-hydrated with 50 mM Tris-HCl, pH 7.0, and 1 mM DTT at a concentration of 50 mg/mL. Lipid aliquots of 200 µL were quick-frozen, and stored under argon at –80°C until use. Lipid suspensions were thawed and sonicated to clarity using a microtip sonicator before the next step. To reconstitute the intact transporter into PLS, 450 µL of solubilized transporter (5 mg/mL) was mixed with 100 µL (50 mg/mL) of sonicated lipids, and kept on ice 30 minutes. PLS were then formed using the detergent dilution procedure [28] as follows: the protein/lipid solution was diluted slowly using a peristaltic pump with 50 mM Tris-HCl, pH 7.0, and 1 mM DTT to a volume of 20 mL. PLS were recovered by ultracentrifugation at 100,000 *g* for 45 minutes. PLS were then washed once using this same buffer and re-suspended in 500 µL. Total protein determination was done using the Lowry method. Typically PLS solutions were at a final protein concentration of approximately 2 mg/mL.

Assay of ATPase activity

PLS were added to yield a final concentration of 0.1 mg/mL in 50 mM Tris-HCl pH 8.0, 100 mM KCl, 10 mM $MgCl_2$ in a total volume of 750 µL. Purified MBP was added with and without 5 mM maltose. The reaction was started by the addition of 750 µL of 50 mM Tris-HCl, 8 mM ATP, 10 mM $MgCl_2$, pH 8.0. Aliqouts of 300 µL were removed at 0, 5, 10, 20 and 30 minute time intervals and added to 150 µL of 10% SDS to stop the reaction and disrupt the PLS. The amount of free phosphate liberated during the reaction was then monitored by adding 250 µL color reagent (10 mM ammonium molybdate and 1 mM $FeSO_4$ in 1 N H_2SO_4) and measuring the absorbance at 740 nm. Standard solutions of potassium phosphate were measured using the same reagents to produce a standard phosphate curve. To conserve binding proteins and liposomes, we also used a 5-fold scaled-down version of the assay with a final volume of 360 µL rather than the 1.5 mL described above. In this case, PLS and MBP were mixed in a volume of 342 µL, and the reaction was initiated with 18 µL of 80 mM ATP, 50 mM Tris-HCl, 100 mM KCl, pH 8.0. Aliquots of 60 µL were removed at 0, 5, 10, 20, and 30 minutes and mixed with 30 µL 10% SDS, followed by 50 µL of color reagent.

CD Spectroscopy

Thermal denaturation of wild-type and mutant MBP molecules was monitored using a JASCO J715A spectropolarimeter. Proteins were dialyzed against 10 mM sodium phosphate, pH 7.4, with or without 500 µM maltose. Buffer scans were acquired under similar conditions. A thermal melt was carried out with the refolded proteins in a 0.1 cm path length quartz cuvette by monitoring the CD signal at 222 nm. The sample was heated from 20 to 95°C with a heating rate of 75°C/h using a JASCO PTC-348WI Peltier device. A bandwidth of 0.2 nm and a response

time of 4 s were used. Transition points were determined by linear extrapolation of the plateau regions using the following equation [29]:

$$y = \frac{(y_n + m_n x) + (y_u + m_u x)\exp\left[\frac{\Delta H_m}{R}\left(\frac{1}{T_m} - \frac{1}{x}\right)\right]}{1 + \exp\left[\frac{\Delta H_m}{R}\left(\frac{1}{T_m} - \frac{1}{x}\right)\right]} \quad (1)$$

In this expression x is the temperature in degrees Kelvin; y_n and y_u refer to the molar ellipticity of the folded and unfolded plateaus, respectively; m_n and m_u are the slopes of the plateaus; R is the universal gas constant in units of kcal•mol^{-1}•K^{-1}; T_m is the melting temperature in degrees Kelvin; and ΔH_m is the enthalpy of unfolding at T_m in kcal•mol^{-1}. Thermal denaturation of MBP is largely irreversible and therefore the fitted T_m and ΔH_m values lack quantitative thermodynamic significance, but are useful for a semi-quantitative comparison of thermal denaturation in the presence and absence of maltose.

Small Angle X-ray Scattering

SAXS experiments were carried out at BioCAT beamline ID18 at the Advanced Photon Source (Argonne Illinois, U.S.A.) essentially as described previously [30]. Radii of gyration were calculated with the program *GNOM* [31] and *CRYSOL* [32] was used for matching crystal structures to SAXS data.

Modelling of MBP-Dependent ATPase Kinetics

Steady state and mass balance equations were created based on the kinetic models illustrated in Figure 2.4. In these schemes, BPo and BPc represent open and closed MBP, respectively, and M represents the membrane complex such that BPoM and BPcM are the corresponding complexes between MBP and MalFGK$_2$. For each of the kinetic models, the

equations were solved analytically, providing the steady state concentration of the "active" complex in terms of the total amount of binding protein and membrane complex, plus the rate constants. The rate constants are only relative values: they were initially set at 1 and then adjusted to reflect the observed properties of the system.

For the case where only the closed form of MBP stimulates ATP hydrolysis (Figure 4A), equations 2 to 6 were used:

$$[\mathrm{M}_T] = [\mathrm{M}] + [\mathrm{BPoM}] + [\mathrm{BPcM}] \quad (2)$$

$$\mathrm{d}[\mathrm{BP}_T] = [\mathrm{BPo}] + [\mathrm{BPc}] \quad (3)$$

$$k_3[\mathrm{BPo}] = k_{-3}[\mathrm{BPc}] \quad (4)$$

$$\frac{d[\mathrm{BPoM}]}{dt} = 0 = k_1[\mathrm{BPo}][\mathrm{M}] + [\mathrm{BPcM}](k_{-4} + k_{cat}) - [\mathrm{BPoM}](k_{-1} + k_4) \quad (5)$$

$$\frac{d[\mathrm{BPcM}]}{dt} = 0 = k_2[\mathrm{BPc}][\mathrm{M}] + k_4[\mathrm{BPoM}] - [\mathrm{BPcM}](k_{-2} + k_{-4} + k_{cat}) \quad (6)$$

For simplicity, the equations incorporate the following assumptions: first, the membrane-bound binding protein represents a relatively small proportion of the total, and therefore membrane-bound forms are not included in the mass balance equation for total binding protein (equation 3); second, the open and closed forms of the free binding protein are assumed to be in equilibrium (equation 4).

For the case that includes the presence of an alternate conformation of the membrane complex (denoted by M*) and activation by open MBP (Figure 4B), equations 6 to 10 were used. Here we assumed that the proportion of the activated form of the membrane complex (M* and BPoM*) was relatively small, and was therefore not included in the mass balance equation for the membrane complex (equation 7). Furthermore, all of the binding protein is assumed to be in the open, free form (equation 8).

$$[\mathrm{M}_T] = [\mathrm{M}] + [\mathrm{BPoM}] \quad (7)$$

$$[\mathrm{BP}_T] = [\mathrm{BPo}] \quad (8)$$

$$\frac{d[\mathrm{M}^*]}{dt} = 0 = k_3[\mathrm{M}] + k_{-2}[\mathrm{BPoM}^*] - k_{-3}[\mathrm{M}^*] - k_2[\mathrm{M}^*][\mathrm{BPo}] \quad (9)$$

$$\frac{d[\mathrm{BPoM}]}{dt} = 0 = k_1[\mathrm{BPo}][\mathrm{M}] + [\mathrm{BPoM}^*](k_{-4} + k_{cat}) - [\mathrm{BPoM}](k_{-1} + k_4) \quad (10)$$

$$\frac{d[\mathrm{BPoM}^*]}{dt} = 0 = k_2[\mathrm{BPo}][\mathrm{M}^*] + k_4[\mathrm{BPoM}] - [\mathrm{BPoM}^*](k_{-2} + k_{-4} + k_{cat}) \quad (11)$$

2.3 Results

Stimulation of the MalFGK$_2$ ATPase by MBP

I investigated the roles of MBP and maltose in stimulation of the MalFGK$_2$ ATPase using a proteoliposome (PLS) system. MalFGK$_2$ was over-expressed and PLS were formed from cell membranes by a detergent dilution procedure. After detergent dilution, MalFGK$_2$ will be present in both orientations in the PLS bilayer. A high concentration of Mg^{2+} was used to promote membrane fusion and mixing; therefore, fixed, closed vesicles do not exist in this system, allowing for bi-directional maltose transport [33]. Importantly, the same PLS preparation can be reconstituted with varying concentrations of MBP or MBP mutants, thereby controlling for differences in the amount and specific activity of MalFGK$_2$ in the membranes.

The presence of MalF, MalG, and MalK in the PLS was confirmed by Western blotting (not shown). The PLS on their own had a basal ATPase that represents uncoupled activity from MalFGK$_2$ and/or other soluble or membrane-bound ATPases. Regarding the preparation of MBP, we found that when MBP is purified from a periplasmic extract, it co-purifies with a contaminating ATPase; in addition, MBP tends to retain some maltose, even after several purification steps. Contamination of MBP with an ATPase and/or maltose can confound the ATPase measurements and preclude accurate comparisons between the effect of unliganded and maltose-bound MBP on the MalFGK$_2$ ATPase. I addressed these problems by intracellular expression of MBP as a hexa-histidine tagged fusion protein. After initial purification by Ni^{2+}-NTA chromatography and cleavage of the tag, leaving only two extra residues, glycine and alanine, at the N-terminus, MBP was purified by ion-exchange chromatography yielding a single band by SDS-PAGE with no significant contaminating ATPase activity. To ensure that it was totally free of maltodextrins, the MBP was fully denatured, dialyzed exhaustively against 6 M guanidine-HCl, and then refolded. Proper refolding and function of MBP preparations was

confirmed by fluorescence titration with maltose and/or maltotriose. Unliganded MBP prepared in this manner was used for all assays, with or without maltose.

Unliganded MBP (2 μM) stimulated the ATPase activity by approximately 50% at 20°C and 100% at 37°C (Figure 2.1). As discussed, the MBP preparation that was added to the PLS had no significant ATPase activity on its own, and had been fully denatured, dialyzed, and refolded to ensure that absolutely no maltose was present. Therefore the stimulation was due solely to an interaction between unliganded MBP and $MalFGK_2$. These results, including the ability of unliganded MBP to stimulate $MalFGK_2$, are similar to what was observed previously for the maltose transport system [4], and a significant stimulation by the unliganded binding protein has also been documented for the histidine transporter [5].

Concentration dependence of MBP-mediated $MalFGK_2$ stimulation

To further characterize the activation of the $MalFGK_2$ ATPase by both unliganded and liganded MBP, I studied the effect of changing the MBP concentration at both 20°C and 37°C. In the presence of maltose, increases in MBP concentration led to almost proportional increases in ATPase activity that began to reach a plateau at 10 μM, presumably as membrane-bound $MalFGK_2$ became saturated with maltose-MBP. In this respect the system resembles a single substrate enzyme, where $MalFGK_2$ is the enzyme and MBP-maltose is the substrate. The ATPase rate versus MBP concentration data were fit to a simple Michaelis-Menten equation, yielding a K_M of approximately 15 μM (defined as the concentration of MBP-maltose that yields one half V_{MAX}) at both 20°C and 37°C, and V_{MAX} values of 1400 and 5500 $nmol \bullet mg^{-1} \bullet min^{-1}$ at 20°C and 37°C respectively (Table 2.1 and Figure 2.2).

Fig 2.1 Stimulation of the MalFGK$_2$ ATPase by Unliganded MBP

ATP hydrolsis was measured for proteoliposomes on their own (solid grey bars) as well as with 2 μM MBP (stippled bars) at 20°C and 37°C. The addition of MBP resulted in an 50 % increase in ATPase activity at 20°C, and a 100% increase at 37°C. Shown are the mean ± S.D.; a paired t-test was used to calculate the likelihood that the differences arose by chance.

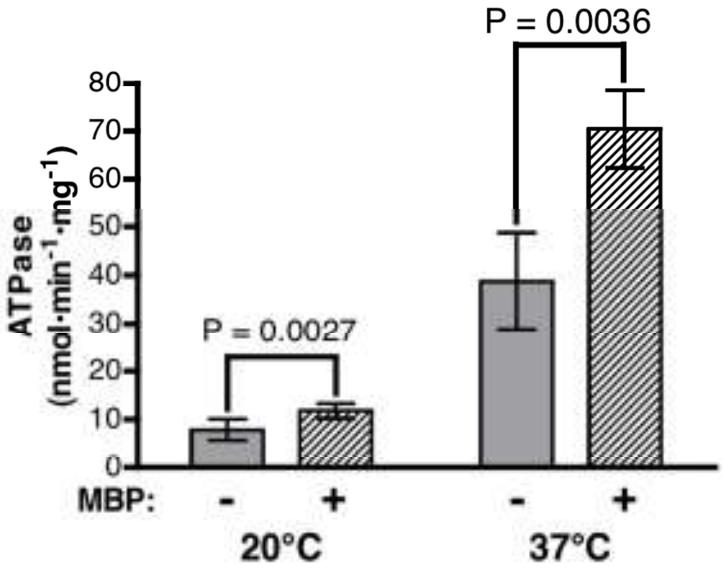
P = 0.0036
P = 0.0027
ATPase
(nmol·min-1·mg-1)
80
70
60
50
40
30
20
10
0
MBP:
-
+
-
+
20°C
37°C

Fig 2.2 Kinetic Analysis of MBP-MalFGK$_2$ ATPase Stimulation in the Presence of Maltose

The ability of wild-type MBP to stimulate the MalFGK$_2$ ATPase, at MBP concentrations from 2 to 100 μM, was measured in the presence of 5 mM maltose at (A) 20°C, filled circles, and (B) 37°C, crosses. The solid curves show the non-linear least-squares fits to the Michaelis-Menten equation, which yielded K_M values (defined as the concentration of MBP that yields half maximal ATPase) of approximately 15 μM and V_{MAX} values of 1400 and 5500 nmol•min^{-1}•mg^{-1} at 20°C and 37°C, respectively (Table 1). The basal rate of activity has been subtracted from these data. Note that all MBP preparations included an unfolding and refolding step, as described in Methods, to completely remove ligand.

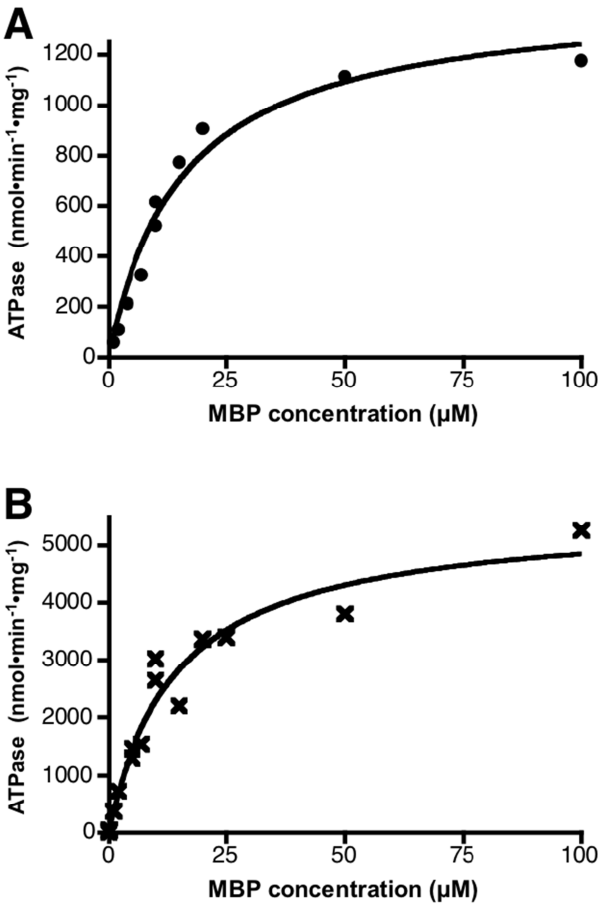
A
ATPase (nmol•min-1•mg-1)
1200
1000
800
600
400
200
0
0
25
50
75
100
MBP concentration (μM)
B
ATPase (nmol•min-1•mg-1)
5000
4000
3000
2000
1000
0
0
25
50
75
100
MBP concentration (μM)

The same experiments were carried out with MBP that was completely free of maltose. At 20°C, addition of unliganded MBP at concentrations of 2 μM and 20 μM produced exactly the same modest increase in ATPase activity (Figure 2.3A). This is in contrast to the situation for maltose-bound MBP, in which a similar 10-fold increase in concentration produced close to a 10-fold increase in activity (Figure 2.2A). Increasing unliganded MBP concentration from 1 to 100 μM produced no significant increase in the stimulation of $MalFGK_2$ ATPase activity (Figure 2.3B). When these data were fit to a Michaelis-Menten equation, the calculated K_M was 0.6 μM, over 20-fold lower than the K_M for liganded MBP. We also carried out the assays at 37°C where the stimulation by unliganded MBP was greater, allowing us to obtain rate data at concentrations of unliganded MBP lower than 1 μM. At 37°C, increasing the unliganded MBP concentration from 0.1 through to 100 μM produced only a modest increase in the activation of $MalFGK_2$, with a calculated K_M of 0.8 μM (Figure 2.2C and Table 2.1), almost 20-fold lower than the K_M obtained for maltose-bound MBP at 37°C.

Kinetic models for stimulation of the $MalFGK_2$ ATPase by unliganded MBP

Unliganded MBP must stimulate the $MalFGK_2$ ATPase through either its closed or open conformation. To investigate in more detail the expected MBP concentration dependence for these two possibilities, we modeled the kinetics of the activation process. A potential complicating factor is the "passive" (i.e. non-activating) interaction between unliganded MBP and $MalFGK_2$ which was first postulated on a theoretical basis and then observed experimentally [34,35]. We incorporated this interaction into two models for the stimulation of the $MalFGK_2$ ATPase by unliganded MBP. The relative affinity of the open conformation of MBP for the transporter is approximately 3-fold less than the closed form (Figure 2.4A and Table 2.2; k_{-1}/k_1 = 50, k_{-2}/k_2 = 15), which is based on mathematical modeling of the system as well as the measured affinities of open and closed MBP for the isolated MalF P2 loop [16,35,36].

Fig 2.3 Kinetic analysis of MBP-MalFGK$_2$ ATPase stimulation in the absence of maltose

(A) In the absence of maltose, MBP produces a small but significant stimulation of the MalFGK$_2$ ATPase that is exactly the same for 2 μM and 20 μM concentrations of MBP at 20°C. The bars show the mean ± S.D. for 6 to 9 determinations in each case. (B) At 20°C and in the absence of maltose, increases in MBP concentration from 1 to 100 μM produced no significant increase in MalFGK$_2$ ATPase activity (filled circles). Note that activities below 1 μM MBP concentration could not be reliably determined at 20°C. (C) At 37°C and in the absence of maltose, the higher activity levels allowed measurement of the MalFGK$_2$ ATPase activity at MBP concentrations below 1 μM (crosses). The data in panels B and C yielded K_M values of less than 1 μM and V_{MAX} values of 5 and 50 nmol•min^{-1}•mg^{-1} at 20°C and 37°C, respectively. For the analysis in panels B and C, the basal ATPase of the proteoliposomes (in the absence of any MBP) was subtracted from all measurements.

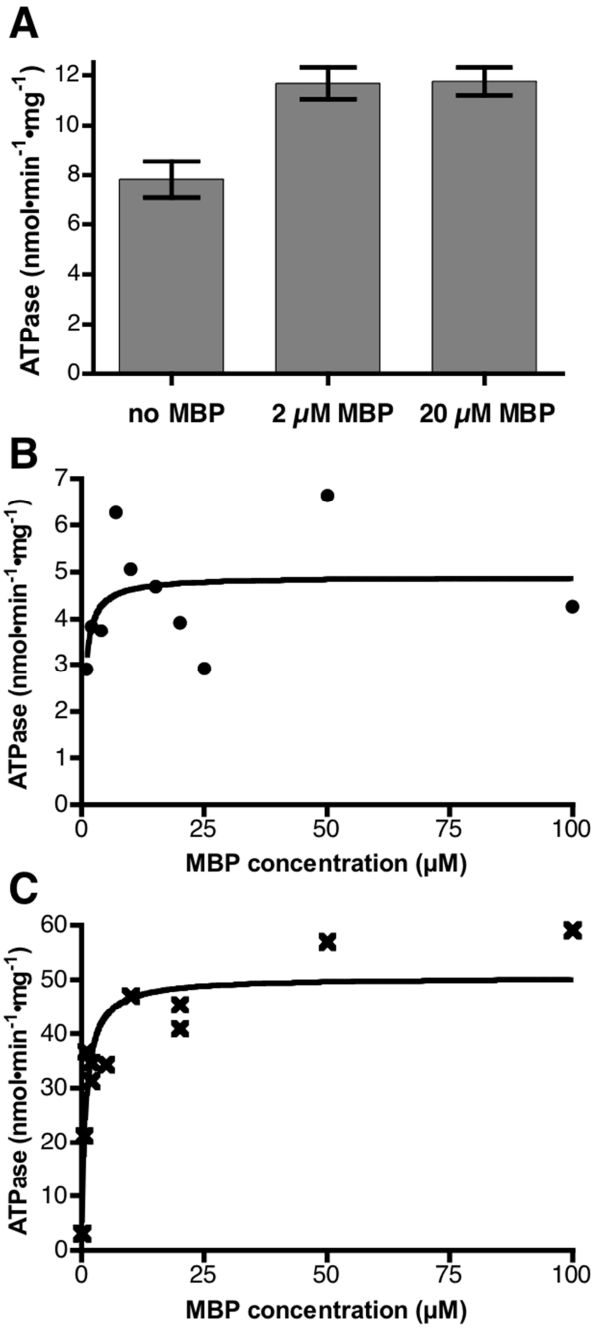
A
ATPase (nmol•min-1•mg-1)
0
2
4
6
8
10
12
no MBP
2 μM MBP
20 μM MBP
B
ATPase (nmol•min-1•mg-1)
0
1
2
3
4
5
6
7
0
25
50
75
100
MBP concentration (μM)
C
ATPase (nmol•min-1•mg-1)
0
10
20
30
40
50
60
0
25
50
75
100
MBP concentration (μM)

Table 2.1: Kinetic Parameters for Activation of $MalFGK_2$ by Liganded and Unliganded MBP

Conditions[a]	K_M **(μM)**	V_{MAX} **(nmol•min^{-1}•mg^{-1})**
Maltose-bound, 20°C	15.7 (9.4 to 22.0)[b]	1400 (1200 to 1700)
Unliganded, 20°C	0.57 (0 to 1.8)	4.9 (3.7 to 6.1)
Maltose-bound, 37°C	14.3 (8.1 to 20.6)	5500 (4600 to 6500)
Unliganded, 37°C	0.81 (0.17 to 1.4)	50 (43 to 58)

[a]The basal ATPase activity measured in the absence of MBP was subtracted from all measurements.
[b]Values in parentheses indicate the 95% confidence interval, as provided by the Prism software.

In the first model (Figure 2.4A), MBP alternates between open and closed conformations with both forms binding to $MalFGK_2$, but only the closed form stimulating ATP hydrolysis. To test the model, we used it to predict what would be observed in the presence of saturating maltose. For this, MBP will be present only in the closed, liganded form, which can be accomplished in the model by making the rate constants for the closed to open transition of MBP (k_{-3} and k_{-4}) very small (Figure 2.4A and Table 2.2). With this set of rate constants, the system produces the observed K_M of 15 μM (Figure 2.5A); from the modeling, we obtain a relative concentration of the "active" species (in this case, liganded MBP bound to $MalFGK_2$), which can vary from 0 to 1. A factor was applied to obtain a V_{max} close to the 5500 nmol•min^{-1}•mg^{-1} that was observed experimentally. The situation in the absence of maltose is similar, except that k_{-3} and k_{-4} are made larger to reflect the shift towards the open conformation of binding protein (Table 2.2); the value of 10 was chosen for both k_{-3} and k_{-4} so that the rate of ATP hydrolysis at 1 or 2 μM unliganded MBP compared well with what was observed experimentally. If the system operated through this mechanism in the absence of maltose, then the apparent K_M for MBP would be just over 40 μM, and there would be a 15-fold increase in the $MalFGK_2$ ATPase activity as the MBP concentration was raised from 1 μM to 25 μM (Figure 2.5B). We attempted to improve the agreement with experimental data by using different parameter sets, but found that the only way to lower the K_M for MBP was to increase the affinity of the interaction between $MalFGK_2$ and open MBP (i.e. decrease k_{-1}) such that it is at least 20-fold higher than the affinity of the interaction between $MalFGK_2$ and closed MBP. Such parameters are at odds with the relatively weak ability of unliganded MBP to inhibit transport by liganded MBP [35] as well as direct binding measurements between MBP and the isolated P2 loop of MalF [36].

The alternative mechanism in which the open conformation of MBP stimulates the $MalFGK_2$ ATPase provides a better fit to the observed data. In this model (Figure 2.4B and Table

2.2 for parameter values), only open unliganded MBP is present and it has the same passive interaction with $MalFGK_2$ as in the previous model. However, there is a second form of $MalFGK_2$, "M*" , which is able to bind open unliganded MBP with high affinity (note the low value of k_{-2} in Table 2.2), producing the transition state complex, leading to ATP hydrolysis and regeneration of $MalFGK_2$ to its "resting" conformation. In addition to the low rate of dissociation of the transition state complex, there is a low rate of formation of M*, which limits the maximum rate of catalysis. The low rate constants for the formation of M* (k_3 and k_4), as well as the low rate constant for dissociation of the transition state complex (k_{-2}) lead to behaviour that is close to what was observed, namely a K_M of ~1 μM and low V_{MAX}. The K_M can be lowered further, to sub-micromolar levels, by slowing the rate of conversion of M* to M (decreasing constants k_{-3} and k_{-4}; Table 2.2 and Figure 2.5B).

In summary, unliganded MBP stimulates the $MalFGK_2$ ATPase with a K_M below 1 μM, and the nature of the stimulation is not consistent with a mechanism in which a minor species adopts a closed, unliganded conformation to mimic the effect of closed, liganded MBP. Instead, the stimulation is consistent with a small amount of $MalFGK_2$ crossing an energetic barrier to adopt an alternate conformation to which open MBP binds with high affinity, leading to ATP hydrolysis in the absence of maltose.

Conformational engineering of MBP

To further address the roles of the open and closed conformations of MBP, we used "conformationally-engineered" MBP molecules in which the open conformation is selectively destabilized relative to the closed conformation. Selective destabilization of the open conformation will shift the open-closed equilibrium of unliganded MBP towards the closed conformation. On this basis, if it is the closed conformation of unliganded MBP that stimulates

Fig 2.4 Kinetic Models for Stimulation of $MalFGK_2$ ATPase by Open and Closed MBP

(A) Stimulation by closed MBP. Both open and closed forms of MBP (BPo and BPc, respectively) interact with $MalFGK_2$ but only the closed form stimulates ATP hydrolysis. In this model, the mechanism of ATPase stimulation is the same for both unliganded and liganded MBP: the closed conformation interacts with $MalFGK_2$ leading to ATP hydrolysis. In the absence of maltose, the relatively low rate of ATP hydrolysis is due to the limiting concentration of closed, unliganded MBP. (B) Stimulation by open MBP. The stimulation is due to a second conformation of $MalFGK_2$ (M*) that is separated from its more predominant "resting" or ground state (M) by an energetic barrier. Open unliganded MBP binds with high affinity to this form of $MalFGK_2$ which leads directly to formation of the transition state for ATP hydrolysis. In this system, the low rate of ATP hydrolysis in the absence of maltose is due to the slow rate of conversion between M and M*. Relative values for the rate constants are provided in Table 2.2.

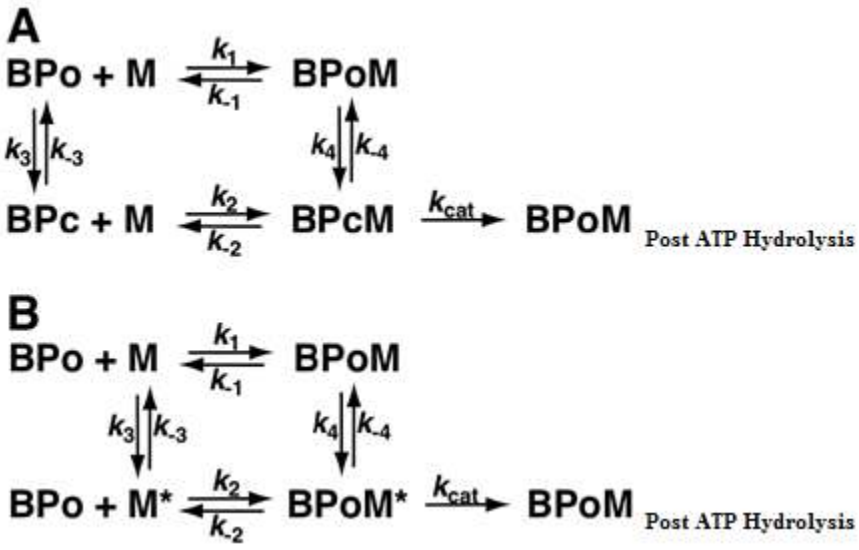
A
BPo + M
BPoM
BPc + M
BPcM
BPoM
Post ATP Hydrolysis
B
BPo + M
BPoM
BPo + M*
BPoM*
BPoM
Post ATP Hydrolysis

Table 2.2: Rate Constants for Kinetic Models

Parameter	Stimulation by Closed MBP		Stimulation by Open Unliganded MBP
	Maltose Saturated	Closed Unliganded	
k_1	1	1	1
k_{-1}	50	50	50
k_2	1	1	1
k_{-2}	15	15	0.015
k_3	1	1	0.01
k_{-3}	0.01	10	0.1
k_4	1	1	0.01
k_{-4}	0.01	10	0.1
k_{cat}	1	1	1

Fig 2.5 Expected rate curves for MalFGK$_2$ stimulation by MBP

The kinetic models in Figure 4 along with rate constants in Table 2 were used to derive curves for the rate of ATP hydrolysis as a function of MBP concentration. Panels A and B represent the same graphs, but with expanded axes in Panel B. In the presence of saturating maltose (solid curve), where all the binding protein is in a closed conformation (accomplished in the model by making the closed to open rate constants very small) the system shows a K_M for MBP of 15 μM, corresponding to what was observed experimentally. In the absence of maltose, the model where the closed, unliganded form is responsible for the stimulation leads to a K_M of just over 40 μM (long dashes) and a significant increase in activity as the concentration of MBP is raised in the region from 1 to 25 μM. Activation by open unliganded MBP (short dashes), as illustrated in Figure 4B and outlined in the text, yields results that are similar to what is observed experimentally.

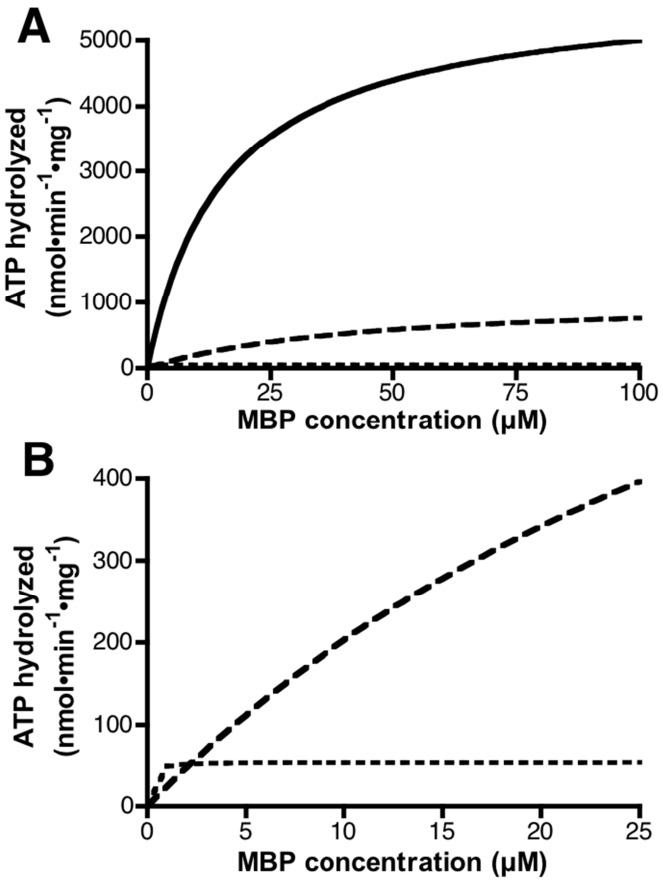
A
5000
4000
3000
2000
1000
0
ATP hydrolyzed
(nmol•min-1•mg-1)
0
25
50
75
100
MBP concentration (μM)
B
400
300
200
100
0
ATP hydrolyzed
(nmol•min-1•mg-1)
0
5
10
15
20
25
MBP concentration (μM)

$MalFGK_2$, then the shift in the open-closed equilibrium should result in a greater stimulation of $MalFGK_2$ in the absence of maltose.

Selective destabilization of the open conformation was accomplished by altering residues in a region we have called the "balancing interface". MBP is composed of two globular domains connected by a flexible hinge: the maltose binding cleft is on one side of the hinge, and the balancing interface is on the opposite side, where it balances or counteracts closing of the maltose-binding cleft. One of the conformationally-engineered MBP molecules, MBP-DM, had been mutated to remove favorable interactions in the balancing interface that stabilize the open conformation [27]. Crystal structures and small angle X-ray scattering (SAXS) of MBP-DM indicated that it adopts exactly the same open and closed conformations as wild-type MBP; however, its maltose affinity is approximately 100 times higher than wild-type due to selective destabilization of the open, unliganded conformation.

Other groups have destabilized the open conformation by replacement of balancing interface residues with bulkier substituents [23,37]. One such mutant, MBP-A96W/I329W, has an average solution conformation corresponding to a domain closure of 28° [23], which is close to the 35° domain closure in maltose-bound MBP. We used SAXS to further verify the perturbed solution conformation of MBP-A96W/I329W. Addition of maltose to ligand-free MBP-A96W/I329W resulted in a barely detectable change in the radius of gyration from 22.2 Å for the unliganded protein, to 22.1 Å for the maltose-bound protein (Figure 2.6A). When compared to wild-type MBP, the solution conformation of MBP-A96W/I329W most closely resembles the closed maltose-bound structure of MBP (Figure 2.6B). As with MBP-DM, the affinity of MBP-A96W/I329W for maltose is much higher than that of wild-type MBP, consistent with selective destabilization of the open conformation. On this basis, and assuming that the wild-type protein

exists to some degree in a closed, unliganded conformation in solution, both of the mutant MBPs are expected to sample a closed unliganded conformation more frequently than wild-type MBP.

The selective destabilization of the open, unliganded conformations of MBP-DM and MBP-A96W/I329W can be seen from thermal denaturation curves (Figure 2.7): in the presence of maltose the T_m values for wild-type MBP, MBP-DM, and MBP-A96W/I329W were similar (65°C for wild-type versus approximately 64°C for the two mutants) whereas in the absence of maltose the T_m values for MBP-DM and MBP-A96W/I329W were both significantly decreased (to 53°C) compared to unliganded wild-type MBP (63°C). The mutations in MBP-DM and MBP-A96W/I329W are not directly involved in ligand binding; furthermore, since they are on the opposite side of the protein from where MBP and $MalFGK_2$ interact, they will not directly interfere with binding to $MalFGK_2$ [11,25,26] and the mutations should not affect the structure of any closed, unliganded conformations that may exist in solution. A productive interaction between these mutants and $MalFGK_2$ is demonstrated by the fact that they both support growth on maltose minimal media in an MBP-deficient strain (not shown). For the purposes of these experiments, therefore, the closed, maltose-bound forms of MBP-DM and MBP-A96W/I329W are identical to wild-type, but the open conformations have been destabilized.

To explore the importance of the open and closed conformations of MBP in maltose transport, we compared the ability of wild-type MBP and MBP-DM to stimulate the $MalFGK_2$ ATPase in both the presence and absence of maltose (Figure 2.8). In the absence of maltose, MBP-DM stimulated ATP hydrolysis to the same degree as wild-type. Therefore, shifting the open-closed equilibrium of MBP towards the closed conformation does not enhance the ability of MBP to stimulate $MalFGK_2$ in the absence of maltose, as would be expected if it were the closed conformation that is responsible for the stimulation. Surprisingly, in the presence of maltose

Fig 2.6 Unliganded MBP-A96W/I329W is in a Closed Conformation

(A) Small-angle X-ray scattering (SAXS) from MBP-A96W/I329W was measured in the absence (thick grey curve) and presence (thin black curve) of maltose. The inset graph shows the difference between the two curves, expressed as a percentage of the total signal. The two curves are almost identical, indicating no observable effect of maltose on the solution conformation of the protein. **(B)** The SAXS data from unliganded MBP-A96W/I329W (thick grey curve) was matched to the open structure of MBP (PDB ID 1OMP [43]; dashed curve) and the closed, ligand-bound structure (PDB ID 1ANF [44]; solid curve). The inset shows the difference between the models and the solution conformation of unliganded MBP-A96W/I329W as a percentage of the total signal. The closed conformation of MBP is a better model for the solution conformation of unliganded MBP-A96W/I329W.

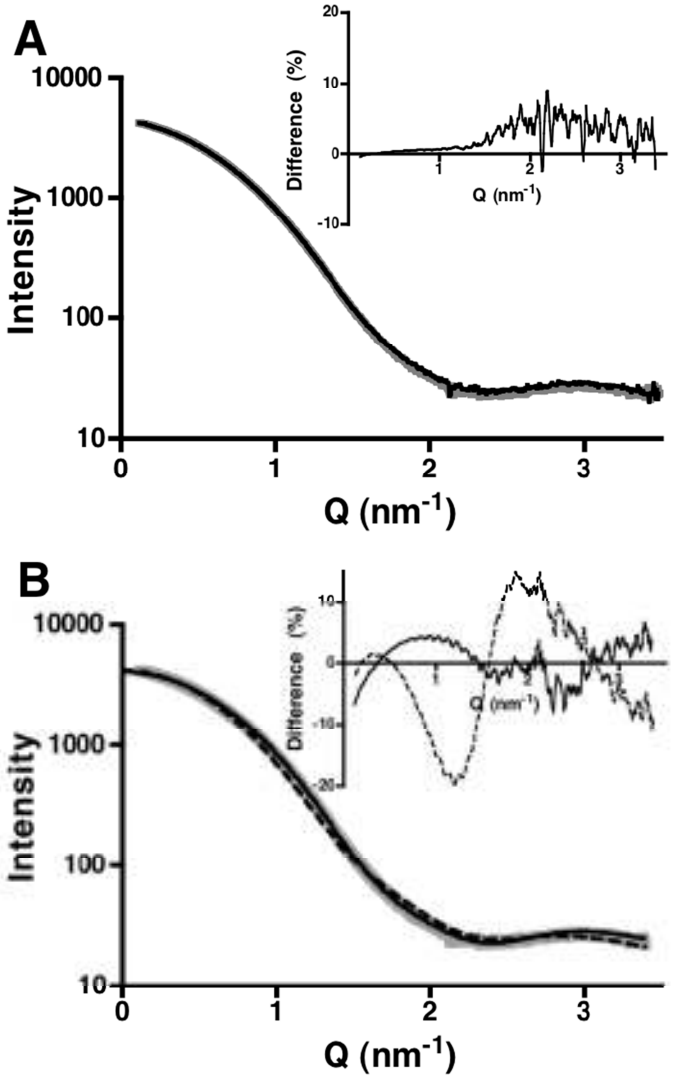
A
10000
1000
100
10
Intensity
0
1
2
3
Q (nm-1)
20
10
0
-10
Difference (%)
1
2
3
Q (nm-1)
B
10000
1000
100
10
Intensity
0
1
2
3
Q (nm-1)
10
0
-10
-20
Difference (%)
Q (nm-1)

Fig 2.7 Stability of Conformationally Engineered MBP Molecules

Conformationally engineered MBP molecules, MBP-DM and MBP-A96W/I329W, were produced by making changes in the "balancing interface" that controls opening and closing of the maltose binding cleft [20,21]. The thermal stabilities of MBP-DM (short dashes) and MBP-A96W/I329W (long/short dashes) were compared to wild-type MBP (solid) in the **(A)** absence of maltose, and **(B)** presence of 500 μM maltose. The samples were heated at 75°K per hour and mean residue ellipticity (θ) at 222 nm was measured every 4 seconds (grey data points; squares for wild-type MBP, circles for MBP-DM, and inverted triangles for MBP-A96W/I329W). The curves are non-linear least-squares fits of the data to an equation describing thermodynamic transitions in terms of the two plateau regions (see Methods). The balancing interface mutations have decreased the stability of the unliganded conformation, but have no significant effect on the stability of the maltose-bound closed conformation.

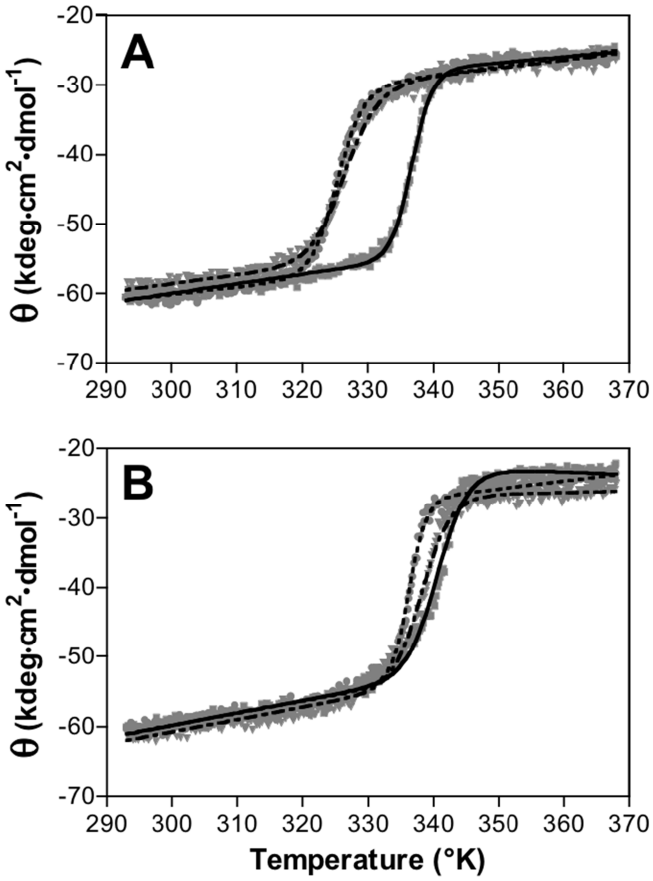
A
B
θ (kdeg·cm²·dmol⁻¹)
-20
-30
-40
-50
-60
-70
290
300
310
320
330
340
350
360
370
Temperature (°K)

MBP-DM was significantly impaired in its ability to stimulate $MalFGK_2$ compared to wild-type MBP. This was an unexpected result because the mutations only affect the stability, and not the structure, of the open conformation. Open MBP forms a tight transition state complex with $MalFGK_2$ [11,17] and these kinetics results show that the balancing interface of MBP contributes to ATP hydrolysis, probably by enhancing the stability of the transition state complex.

The results obtained with MBP-DM were reinforced by experiments with MBP-A96W/I329W (Figure 2.8). In the absence of maltose, stimulation of $MalFGK_2$ by MBP-A96W/I329W was not significant, and in fact the mutations have decreased and possibly abrogated its ability to stimulate $MalFGK_2$ in the absence of maltose. Given that unliganded MBP-A96W/I329W adopts an average conformation that is almost closed, the inability of unliganded MBP-A96W/I329W to stimulate $MalFGK_2$ is not consistent with the idea that the closed conformation alone is responsible for stimulation in the absence of maltose. Addition of maltose to MBP-A96W/I329W brought about a significant stimulation of the $MalFGK_2$ ATPase, although it was much less than stimulation by wild-type MBP. These measurements were made at an MBP concentration of 2 μM, but the same results were obtained at 1 μM and 5 μM MBP concentrations (not shown). In the presence of maltose, increases in the concentration of all three proteins produced increases in stimulation of the $MalFGK_2$ ATPase, but MBP-DM consistently exhibited a modestly compromised ability to stimulate $MalFGK_2$ compared to wild-type MBP, while MBP-A96W/I329W was severely compromised.

Thus, mutations destabilizing the open conformation do not enhance the ability of the proteins to stimulate the $MalFGK_2$ ATPase in the absence of maltose, and in fact reduce the maltose-stimulated $MalFGK_2$ ATPase activity. In this regard, we have considered the possibility that decreases in the ability of the mutants to stabilize the transition state might have offset increased stimulation by higher proportions of the closed conformation. I believe this is highly

Fig 2.8 Destabilization of the Open Conformation Decreases MalFGK$_2$ ATPase

The ability of wild-type MBP (MBP-WT), MBP-DM, and MBP-A96W/I329W to stimulate the MalFGK$_2$ ATPase was measured in either the absence (hollow bars) or presence (filled bars) of 5 mM maltose. An MBP concentration of 2 μM was used in each case, and measurements were made in triplicate; the mean value is shown with error bars representing the standard deviation. The PLS on their own (hollow bar, far left) show a low basal ATPase that is doubled by addition of unliganded MBP and increased over 10-fold by addition of MBP and maltose. In the presence of maltose, MBP-DM does not stimulate the MalFGK$_2$ ATPase to the same degree as wild-type MBP. MBP-A96W/I329W shows a severely impaired ability to stimulate MalFGK$_2$ in both the absence and presence of maltose.

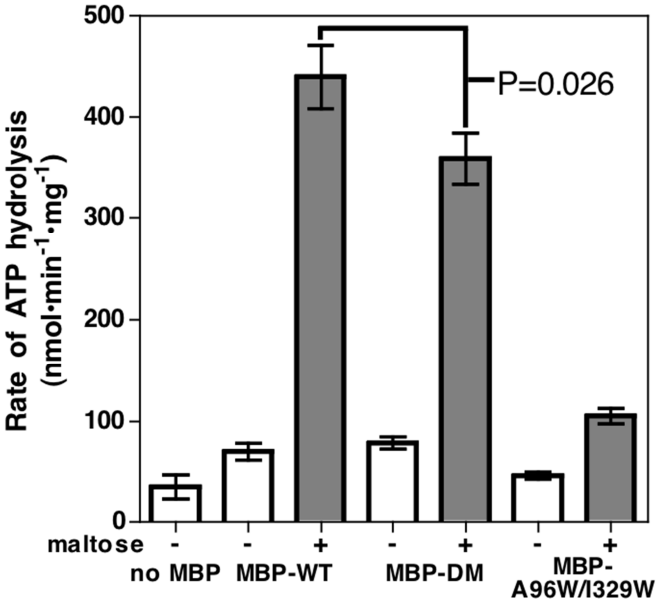
500
400
300
200
100
0
Rate of ATP hydrolysis
(nmol•min-1•mg-1)
P=0.026
maltose - - + - + - +
no MBP
MBP-WT
MBP-DM
MBP-
A96W/I329W

unlikely. Both of the mutants have ligand binding affinities that are at least 2 orders of magnitude higher than wild type, and on this basis the open-closed equilibrium has been severely perturbed. Assuming the destabilizing mutations have the same effect on the unliganded protein as they do on the ligand-bound protein, then one would expect a significant (up to 2 orders of magnitude) increase in the fraction of closed unliganded MBP in solution. In contrast, destabilization of the open conformation produces only a modest 20% decrease in maltose-stimulated ATPase activity for MBP-DM, and a 5-fold decrease for MBP-A96W/I329W. Therefore it is unlikely that increases in the proportion of the closed conformation of these mutants - and associated increases in $MalFGK_2$ stimulation - are being completely masked or offset by their decreased ability to stabilize the transition state.

In summary, the closed conformation is most likely not responsible for stimulation of the ATPase in the absence of maltose. In addition, the results with the conformationally engineered MBP mutants show that the energetics of domain opening, and the stability of the open conformation, are important for ATP hydrolysis.

2.4 Discussion

The mechanism of substrate import by ABC import systems involves binding of ligand to the peripheral binding protein to exert a conformational change that signals to the integral membrane subunits to initiate ATP hydrolysis. The shape complementarity of the interacting surfaces - closed MBP and an undefined conformation of $MalFGK_2$ - is critical, and this has been demonstrated through mutagenic studies [25,26]. Along with many other peripheral binding proteins, unliganded MBP exists in an open conformation in solution [15,38-40], and therefore it has always been difficult to understand how the unliganded binding protein is able to stimulate ATP hydrolysis by the transporter, an effect documented for the two systems that have been tested in this regard - the maltose and histidine transporters [4,5]. One possible explanation is that the unliganded binding protein is able to mimic the closed conformation of the protein. In other words, the system follows a "lock and key" model: as long as the binding protein has the correct shape, it should be able to activate the $MalFGK_2$ ATPase. Evidence for a closed, unliganded conformation includes crystallization of the glucose/galactose binding protein in an unliganded, closed conformation [19], and, more recently, the ChoX protein from *S. meliloti* [20]. In addition, an alternate solution conformation for the maltose binding protein (MBP) has been documented by NMR [18] and in solution the overall conformation of unliganded MBP appears to be slightly more closed than the unliganded crystal structure [15,27] hinting that MBP may exist, to some degree, in closed conformation(s) in solution. Apart from these results, which are consistent with the existence of a small fraction of a closed, unliganded form of the binding protein in solution, there is no experimental evidence for the stimulation of the membrane ATPase by a closed, unliganded conformation of the binding protein. The idea is based solely on the fact that the closed, liganded form is responsible for stimulation in the presence of ligand.

This study was initiated to test whether activation of the $MalFGK_2$ ATPase by unliganded MBP was due to a closed unliganded conformation. Our hope was that this information would help us to understand the molecular mechanics of the system, and, more specifically, to address the role of maltose itself in the transport process. Our results argue against the idea that unliganded MBP stimulates the transporter through a closed conformation. The dependence of the stimulation on MBP concentration does not follow what would be expected if this were the mechanism. Specifically, the unliganded form of the protein stimulates $MalFGK_2$ with a much lower K_M value than maltose-bound MBP, indicating that the species responsible is not mimicking the closed conformation of MBP. Furthermore, destabilization of the open conformation - and consequent increase in the proportion of the closed conformation - had no positive effect on the ability of unliganded MBP to stimulate the $MalFGK_2$ ATPase.

We conclude that a closed, unliganded conformation of MBP is not responsible for MBP-dependent $MalFGK_2$ stimulation in the absence of maltose. One explanation for why this is the case is that ligand is required to stabilize the closed conformation of the binding protein. Much of the experimental work on the maltose transporter is consistent with the existence of energetic barriers to conformational changes in $MalFGK_2$ [41]. These would represent higher energy intermediates of $MalFGK_2$ that prevent futile cycling and ATP hydrolysis in the absence of maltose. MBP may function to stabilize such intermediates, thereby promoting conformational changes in the system. However, to stabilize a high-energy $MalFGK_2$ intermediate, MBP would not only have to be in the correct conformation, but it would also have to be in a low energy state; that is, a high energy form of MBP would not contribute to the stabilization of a high energy form of $MalFGK_2$. While the closed, liganded conformation represents a stable, low energy form of MBP, a closed unliganded conformation is an unstable high energy form [23],

and on this basis, only ligand-bound MBP would be a good candidate for stabilizing a high energy form of $MalFGK_2$.

The activation of the $MalFGK_2$ ATPase by unliganded MBP is most likely due to a high affinity interaction between the open conformation of MBP and a sparsely populated $MalFGK_2$ conformation. The maximum rate of ATP hydrolysis in the absence of maltose would be limited by the population of $MalFGK_2$ that is in the required conformation. $MalFGK_2$ has been crystallized in two conformational states [11,12], and in the membrane there may be other intermediates. At equilibrium the proportion of these different conformations will be determined by their relative energies, and there may also be kinetic barriers to interconversion between conformations. In either case, given finite limits on the energies of the conformations and kinetic barriers, a small proportion of the $MalFGK_2$ population will find itself in higher energy states, and these are the molecules to which open MBP could bind, promoting the ATPase activity by stabilizing the transition state or something close to it. The open, unliganded conformation is the second "low energy" form of MBP (after the closed, liganded conformation), and therefore would be able to stabilize a higher energy conformation of $MalFGK_2$. We have demonstrated that destabilization of the open MBP conformation results in a decreased ability of MBP to stimulate the $MalFGK_2$ ATPase, consistent with the idea that the open conformation of MBP contributes to the stability of the transition state complex [11].

In addition to being consistent with the observations in this study, the idea of direct kinetic stabilization of a high energy form of $MalFGK_2$ by open MBP explains an observation made by Merino and Shuman [42]. In this study, a $MalFGK_2$ mutant was isolated that was able to transport lactose, but only in the presence of MBP, which does not bind lactose. This work confirmed the importance of the interaction between unliganded MBP and the membrane components. Furthermore, given its robust stimulation of lactose transport and the fact that the vast majority of

unliganded MBP is in an open conformation, it is almost certainly the open conformation of MBP that is required for lactose transport in this system.

Bibliography

1. Higgins, C. F., and Linton, K. J. (2004) The ATP switch model for ABC transporters, *Nat. Struct. Mol. Biol*. **11**: 918-926.
2. Sauna, Z. E., and Ambudkar, S. V. (2007) About a switch: how P-glycoprotein (ABCB1) harnesses the energy of ATP binding and hydrolysis to do mechanical work, *Mol Cancer Ther* **6**: 13-23.
3. Tombline, G., and Senior, A. E. (2005) The occluded nucleotide conformation of p-glycoprotein, *J Bioenerg Biomembr* **37**: 497-500.
4. Davidson, A., Shuman, H., and Nikaido, H. (1992) Mechanism of maltose transport in Escherichia coli : Transmembrane signaling by periplasmic binding proteins, *Proc. Natl. Acad. Sci. USA* **89**: 2360-2364.
5. Ames, G. F., Liu, C. E., Joshi, A. K., and Nikaido, K. (1996) Liganded and unliganded receptors interact with equal affinity with the membrane complex of periplasmic permeases, a subfamily of traffic ATPases, *J. Biol. Chem*. **271**: 14264-1470..
6. Borths, E. L., Poolman, B., Hvorup, R. N., Locher, K. P., and Rees, D. C. (2005) In vitro functional characterization of BtuCD-F, the Escherichia coli ABC transporter for vitamin B12 uptake, *Biochemistry* **44**: 16301-16309.
7. Chen, J., Lu, G., Lin, J., Davidson, A. L., and Quiocho, F. A. (2003) A tweezers-like motion of the ATP-binding cassette dimer in an ABC transport cycle, *Mol. Cell* **12:** 651-661.
8. Lu, G., Westbrooks, J. M., Davidson, A. L., and Chen, J. (2005) ATP hydrolysis is required to reset the ATP-binding cassette dimer into the resting-state conformation, *Proc Natl Acad Sci U S A* **102**: 17969-17974.
9. Daus, M. L., Landmesser, H., Schlosser, A., Muller, P., Herrmann, A., and Schneider, E. (2006) ATP induces conformational changes of periplasmic loop regions of the maltose ATP-binding cassette transporter*, J Biol Chem* **281**: 3856-3865.
10. Daus, M. L., Grote, M., Müller, P., Doebber, M., Herrmann, A., Steinhoff, H. J., Dassa, E., and Schneider, E. (2007) ATP-driven MalK dimer closure and reopening and conformational changes of the "EAA" motifs are crucial for function of the maltose ATP-binding cassette transporter ($MalFGK_2$*), J Biol Chem* **282**: 22387-22396.
11. Oldham, M. L., Khare, D., Quiocho, F. A., Davidson, A. L., and Chen, J. (2007) Crystal structure of a catalytic intermediate of the maltose transporter*, Nature* **450**: 515-521.
12. Khare, D., Oldham, M. L., Orelle, C., Davidson, A. L., and Chen, J. (2009) Alternating access in maltose transporter mediated by rigid-body rotations, *Mol Cell* **33**: 528-536.
13. Quiocho, F. A., and Ledvina, P. S. (1996) Atomic structure and specificity of bacterial periplasmic receptors for active transport and chemotaxis: variation of common themes, *Mol. Microbiol*. **20**: 17-25..
14. Bishop, L., Agbayani, R., Ambudkar, S. V., Maloney, P. C., and Ames, G. F. (1989) Reconstitution of a bacterial periplasmic permease in proteoliposomes and demonstration of ATP hydrolysis concomitant with transport, *Proc Natl Acad Sci U S A* **86**: 6953-6957.
15. Evenäs, J., Tugarinov, V., Skrynnikov, N. R., Goto, N. K., Muhandiram, R., and Kay, L. E. (2001) Ligand-induced structural changes to maltodextrin-binding protein as studied by solution NMR spectroscopy, *J. Mol. Biol.* **309**: 961-74..
16. Shilton, B., and Mowbray, S. (1995) Simple Models for the Analysis of Binding Protein-dependent Transport Systems, *Protein Sci.* **4**: 1346-1355.

17. Austermuhle, M. I., Hall, J. A., Klug, C. S., and Davidson, A. L. (2004) Maltose-binding protein is open in the catalytic transition state for ATP hydrolysis during maltose transport, *J Biol Chem* **279**: 28243-50. Epub 2004 Apr 26..
18. Tang, C., Schwieters, C. D., and Clore, G. M. (2007) Open-to-closed transition in apo maltose-binding protein observed by paramagnetic NMR, *Nature* **449**: 1078-1082.
19. Flocco, M., and Mowbray, S. (1994) The 1.9 Å X-ray Structure of a Closed Unliganded Form of the Periplasmic Glucose/Galactose Receptor from Salmonelloa typhimurium*, *J. Biol. Chem.* **269**: 8931-8936.
20. Oswald, C., Smits, S. H. J., Hoing, M., Sohn-Bosser, L., Dupont, L., Le Rudulier, D., Schmitt, L., and Bremer, E. (2008) Crystal Structures of the Choline/Acetylcholine Substrate-binding Protein ChoX from Sinorhizobium meliloti in the Liganded and Unliganded-Closed States, *J Biol Chem* **283**: 32848.
21. Döring, K., Surrey, T., Nollert, P., and Jahnig, F. (1999) Effects of ligand binding on the internal dynamics of maltose-binding protein, *Eur. J. Biochem*. **266**: 477-83..
22. Stockner, T., Vogel, H. J., and Tieleman, D. P. (2005) A salt-bridge motif involved in ligand binding and large-scale domain motions of the maltose-binding protein, *Biophys J* **89**: 3362-3371.
23. Millet, O., Hudson, R. P., and Kay, L. E. (2003) The energetic cost of domain reorientation in maltose-binding protein as studied by NMR and fluorescence spectroscopy, *Proc. Natl. Acad. Sci. U. S. A.* **100**: 12700-12705.
24. Panagiotidis, C. H., Reyes, M., Sievertsen, A., Boos, W., and Shuman, H. A. (1993) Characterization of the structural requirements for assembly and nucleotide binding of an ATP-binding cassette transporter. The maltose transport system of Escherichia coli, *J Biol Chem* **268**: 23685-23696.
25. Treptow, N., and Shuman, H. (1988) Allele-specific malE Mutations that Restore Interactions Between Maltose-binding Protein and the Inner-membrane Components of the Maltose Transport System, *J. Mol. Biol*. **202**: 809-822.
26. Hor, L., and Shuman, H. (1993) Genetic Analysis of Periplasmic Binding Protein Dependent Transport in E. coli: Each lobe of maltose-binding protein interacts with a different subunit of the MalFGK2 membrane transport complex, *J. Mol. Biol*. **233**: 659-670.
27. Telmer, P. G., and Shilton, B. H. (2003) Insights into the conformational equilibria of maltose-binding protein by analysis of high affinity mutants, *J Biol Chem* **278**: 34555-34567.
28. Davidson, A., and Nikaido, H. (1990) Overproduction, Solubilization, and Reconstitution of the Maltose Transport System from Escherichia coli, *J. Biol. Chem*. **265**: 4254-4260.
29. Swint, L., and Robertson, A. D. (1993) Thermodynamics of unfolding for turkey ovomucoid third domain: thermal and chemical denaturation, *Protein Sci* **2**: 2037-2049.
30. Telmer, P. G., and Shilton, B. H. (2005) Structural studies of an engineered zinc biosensor reveal an unanticipated mode of zinc binding, *J Mol Biol* **354**: 829-840.
31. Semenyuk, A., and Svergun, D. (1991) GNOM - a program package for small-angle scattering data processing, *J. Appl. Cryst*. **24**: 537-540.
32. Svergun, D., Barberato, C., and Koch, M. (1995) CRYSOL - a Program to Evaluate X-ray Solution Scattering of Biological Macromolecules from Atomic Coordinates, *J. App. Cryst*. **28**: 768-773.

33. Liu, C. E., Liu, P. Q., and Ames, G. F. (1997) Characterization of the adenosine triphosphatase activity of the periplasmic histidine permease, a traffic ATPase (ABC transporter), *J Biol Chem* **272**: 21883-21891.
34. Bohl, E., Shuman, H., and Boos, W. (1995) Mathematical Treatment of the Kinetics of Binding Protein Dependent Transport Systems Reveals that Both the Substrate Loaded and Unloaded Binding Proteins Interact with the Membrane Components, *J. Theor. Biol*. **172**: 83-94.
35. Merino, G., Boos, W., Shuman, H., and Bohl, E. (1995) The inhibition of maltose transport by the unliganded form of the maltose-binding protein of Escherichia coli: experimental findings and mathematical treatment, *J. Theor. Biol*. **177**: 171-179.
36. Jacso, T., Grote, M., Daus, M., Schmieder, P., Keller, S., Schneider, E., and Reif, B. (2009) The periplasmic loop P2 of the MalF subunit of the maltose ATP binding cassette transporter is sufficient to bind the maltose binding protein MalE, *Biochemistry*. **48**:2216-25
37. Marvin, J. S., and Hellinga, H. W. (2001) Manipulation of ligand binding affinity by exploitation of conformational coupling, *Nat. Struct. Biol*. **8**: 795-78.
38. Newcomer, M. E., Lewis, B. A., and Quiocho, F. A. (1981) The radius of gyration of L-arabinose-binding protein decreases upon binding of ligand, *J. Biol. Chem*. **256**: 13218-13222.
39. Shilton, B., Flocco, M., Nilsson, M., and Mowbray, S. (1996) Conformational changes of three periplasmic receptors for bacterial chemotaxis and transport: the maltose-, glucose/galactose- and ribose-binding proteins, *J. Mol. Biol*. **264**: 350-363.
40. Hall, J. A., Thorgeirsson, T. E., Liu, J., Shin, Y. K., and Nikaido, H. (1997) Two modes of ligand binding in maltose-binding protein of Escherichia coli. Electron paramagnetic resonance study of ligand-induced global conformational changes by site-directed spin labeling, *J Biol Chem* **272**: 17610-17614.
41. Shilton, B. H. (2008) The dynamics of the MBP-MalFGK(2) interaction: a prototype for binding protein dependent ABC-transporter systems, *Biochim Biophys Acta* **1778**: 1772-1780.
42. Merino, G., and Shuman, H. A. (1997) Unliganded maltose-binding protein triggers lactose transport in an Escherichia coli mutant with an alteration in the maltose transport system, *J Bacteriol* **179**, 7687-7694.
43. Sharff, A., Rodseth, L., Spurlino, J., and Quiocho, F. (1992) Crystallographic Evidence of a Large Ligand-Induced Hinge-Twist Motion between the Two Domains of the Maltodextrin Binding Protein Involved in Active Transport and Chemotaxis, *Biochemistry* **31**: 10657-10663.
44. Spurlino, J. C., Lu, G. Y., and Quiocho, F. A. (1991) The 2.3-A resolution structure of the maltose- or maltodextrin-binding protein, a primary receptor of bacterial active transport and chemotaxis, *J. Biol. Chem*. **266**: 5202-5219.

Chapter 3 Studies of the Maltose Transport System Reveal a Mechanism for Coupling ATP Hydrolysis to Substrate Translocation Without Direct Recognition of Substrate.

3.1 Introduction

ATP Binding Cassette (ABC) transporters move various substrates across membranes, with substrate movement coupled to the hydrolysis of ATP. While the ATPase activity of ABC exporters like P-glycoprotein is generally stimulated by substrate binding, the ATPase activity of ABC importers is activated by a peripheral substrate binding protein and not the free substrate [for recent reviews see 1-3]. However, the mechanism of ATPase regulation is still not fully understood. Here, we use one of the most well-studied ABC importers, the *Escherichia coli* maltose transporter ($MalFGK_2$), to investigate the roles of maltose binding protein (MBP) and maltose itself in regulation of ATPase activity

In its resting state $MalFGK_2$ contains a substrate-binding site that is exposed to the cytoplasm [4]. In the periplasm MBP binds maltose, which stabilizes a change from an 'open' to 'closed' conformation, enabling it to stimulate the $MalFGK_2$ ATPase [5,6]. Interactions with closed, maltose-bound MBP lead to exposure of the $MalFGK_2$ maltose-binding site to the periplasmic side where maltose can move from MBP into an occluded translocation pathway [7,8]. After ATP hydrolysis the transporter returns its binding site to the cytoplasmic face to allow the substrate to enter the cytoplasm. This is known as the alternating access model of maltose transport [4] and may be a common mechanism among ABC transporters [2,9,10].

The structure of a transition state complex between MBP and $MalFGK_2$, as well as biochemical data [7,8] indicates that maltose enters the substrate binding site of $MalFGK_2$ prior to ATP hydrolysis, but it is unclear how maltose-bound MBP activates the $MalFGK_2$ ATPase

[11] and how ATP hydrolysis is coupled to the movement of maltose across the membrane. Of particular interest are the roles that maltose itself might play in regulating the ATPase activity of $MalFGK_2$.

There are two ways maltose could regulate ATP hydrolysis: the first is by stabilizing the closed conformation of MBP and the second is through direct interactions with $MalFGK_2$. While it is clear from previous studies that substrate induced domain closure in MBP is critical for robust stimulation of $MalFGK_2$ ATPase activity and substrate transport [6], it is not known whether direct interaction between maltose and $MalFGK_2$ is also required for ATPase activity.

To address this question, we have used an MBP mutant that is able to bind an alternate substrate, sucrose, with high affinity [12]. The sucrose-binding MBP (sMBP) enables us to present the maltose transporter with either maltose or sucrose in equivalent contexts and distinguish whether the substitution influences the ATPase activity of $MalFGK_2$. Sucrose is a good alternate substrate for this purpose because experiments from Shuman's laboratory have shown that it has a very poor ability to compete for the maltose binding site in $MalFGK_2$, indicating that the change in sugar structure is sufficient to disrupt specific binding interactions with $MalFGK_2$ [13,14].

Using sMBP we have determined that ATP hydrolysis by $MalFGK_2$ is not dependent on the exact nature of the substrate, and therefore the coupling of ATPase activity to substrate translocation is due solely to interactions between MBP and $MalFGK_2$. Based on these findings and detailed structural analysis of sMBP, we propose that a productive interaction between MalG and the vacated maltose binding site in MBP is required for ATP hydrolysis. In this manner, substrate translocation from MBP to $MalFGK_2$ is coupled to ATP hydrolysis without requiring a direct interaction between maltose and $MalFGK_2$.

3.2 Materials and Methods

Cloning of MBP mutants

Plasmid pDIM-C8MalE, containing sMBP, was kindly provided by the Ostermeier group [12]. A 923 bp Kpn21/Bcl1 fragment of this vector, containing the W62Y and E111Y substitutions, was ligated into pLH1, which contains the MBP signal sequence for export to the periplasm. The D14L and K15F mutations were substituted by mutagenic PCR using primers: 5'-CTGGATTAACGGCCTTTTCGGCTATAACGGTCTCGC-3' and 5'-GCGAGACCGTTATAGCCAAAAAGGCCGTTAATCCAG-3'.

To produce intracellularly expressed sMBP and wtMBP with a hexa-histidine affinity tag, restriction cut sites for Ehe1 and Hind3 were added to excise the two genes (without localization tag) using primers:
5'CGCCTCGGCTGGCGCCAAAATCGAAG-3' and
5'CGCCGCATCCGGCATTTAAGCTTATTACTTGGTGATACGAG-3'
Digested PCR products were then ligated into the multicloning site of pPROEX-HTa (Invitrogen) to introduce an N-terminal hexa-histidine tag attached by a tobacco etch virus (TEV) protease cleavable linker. Cleavage of this linker left an N-terminal glycine-alanine insertion that was common to both the sMBP and wtMBP used in this study.

Growth on Minimal Media

Bacterial strain HS3309, lacking endogenous wtMBP production, was transformed with no plasmid, pLH1 containing wtMBP, or pLH1-S containing sMBP. These strains were streaked on M9 minimal media augmented with 5% maltose and incubated at 37˚C for up to 7 days. Colony formation was observed and recorded.

Expression and Purification

Hexa-histidine tagged sMBP and wtMBP were expressed and purified from HS3309 ($MalE^{-/-}$) *E. coli* by Ni^{2+}-affinity chromatography. Removal of the affinity tag was accomplished by TEV protease cleavage, and pure sMBP and wtMBP was obtained by ion exchange chromatography, as previously reported [15]. Both proteins were denatured in 6 M guanidine and dialyzed exhaustively to remove trace sugars before being refolded by drop wise dilution in 50 mM Tris-HCl pH 8, concentrated, and stored in the same buffer [15].

Preparation of wt-MalFGK$_2$-containing proteoliposomes

$MalFGK_2$ was over-expressed from plasmids pNT1SK+ and pMR111 in *E. coli* HS3399 cells, which contain deletions for all transporter components. Membrane fractions were prepared and solubilized as previously reported [15].

Liposomes were prepared from Avanti™ crude *E. coli* phospholipids and after homogenization by sonication were combined with $MalFGK_2$-containing membranes by detergent dilution [15]. The proteoliposomes were frozen at -80˚C under N_2 until used.

ATPase Assays

ATPase measurements were made in a solution of 50 mM Tris-HCl pH 8.0, 100 mM KCl, and 10 mM $MgCl_2$, with proteoliposomes added to a final concentration of 0.1 mg/mL protein. Purified sMBP or wtMBP was added at various concentrations and in the presence or absence of 5 mM maltose or sucrose. ATP hydrolysis at 37˚C was measured *in vitro* by assaying the appearance of inorganic phosphate, using ammonium molybdate, as previously described [15].

Crystallization and X-ray Diffraction

Crystals of sucrose-bound sMBP were grown in 21% PEG 3350K, 100 mM sodium acetate pH 6.5, 60 mM $MgCl_2$ and 10 mM $ZnCl_2$ with 100 mM sucrose. Crystals of unliganded sMBP were grown from PEG 5k-MME, sodium acetate pH 6.5, 60 mM $MgCl_2$ and 10 mM $ZnCl_2$. Crystals of sucrose-bound and unliganded sMBP diffracted to 2 Å and 1.5 Å, respectively, at the Canadian Light Source beamline CMCF1 (08ID-1).

Phases were determined by molecular replacement with the wild-type proteins (PDB-ID 1ANF and 1OMP). Rigid body refinement of the two isolated domains was carried out first to capture any domain movements relative to the wild-type structures. Structures were refined using CNS [21] (Table 1) with manual adjustment in COOT [22]. The structures have been deposited in the PDB with IDs 3KJT and 3HPI for the open and closed forms respectively. Molecular figures were made using PyMOL [23].

Small Angle X-ray Scattering

SAXS experiments were carried out at BioCAT beamline ID18 at the Advanced Photon Source (Argonne Illinois, U.S.A.) as previously described [25].

3.3 Results

A sucrose-binding MBP

Sucrose-binding Maltose Binding Protein (sMBP) is a mutant form of MBP developed by Marc Ostermeier's Group [12]. The sMBP molecule has four point mutations, D14L, K15F, W62Y and E111Y, all within the substrate binding cleft. While wild-type MBP (wtMBP) has a dissociation constant (K_D) of 1 μM for maltose and no measurable ability to bind sucrose [6], sMBP has a K_D for maltose of 24 μM and for sucrose of 6.6 μM [12]. These values were confirmed for my sMBP constructs using fluorescence titrations. Furthermore, we measured substrate induced conformational changes in sMBP, in solution, by small angle X-ray scattering. Sucrose-induced changes in the conformation of sMBP were identical to changes seen in wtMBP (Figure 3.1). I also observed that sMBP could partially complement the growth of wtMBP deficient *E. coli* on M9 maltose minimal media, resulting in colony formation on agar plates after 2 days, rather than overnight growth as seen with wtMBP, or no growth, as seen in the absence of binding protein expression. Although growth was slow compared to wild-type, it was clear that sMBP could interact productively with $MalFGK_2$ to promote maltose transport.

sMBP stimulates $MalFGK_2$ with bound sucrose or maltose

$MalFGK_2$ has a binding site that is relatively specific for maltodextrins [13], and binding of the substrate to this site may be important for stimulation of the $MalFGK_2$ ATPase. To determine the importance of specific interactions between maltose and $MalFGK_2$, we used sMBP to present $MalFGK_2$ with either maltose or sucrose as a transport substrate, and measured the resulting stimulation of ATPase activity *in vitro*. Consistent with literature findings, $MalFGK_2$-containing proteoliposomes showed a low level of basal activity (Figure 3.2). This activity was unaltered by the addition of 5 mM maltose or sucrose, confirming that free sugar cannot stimulate

Fig 3.1 Open to Closed Conformational Change in sMBP

Small angle X-ray scattering (SAXS) from purified sMBP was measured in the absence (dashed curve) and presence (solid curve) of 5 mM sucrose. The inset shows the difference between the two curves, expressed as a percentage of the total signal. Sucrose binding brings about a decrease in the radius of gyration from 23.8 to 21.9 Å; the curves for sMBP in the absence and presence of sucrose match those of wtMBP in the absence and presence of maltose.

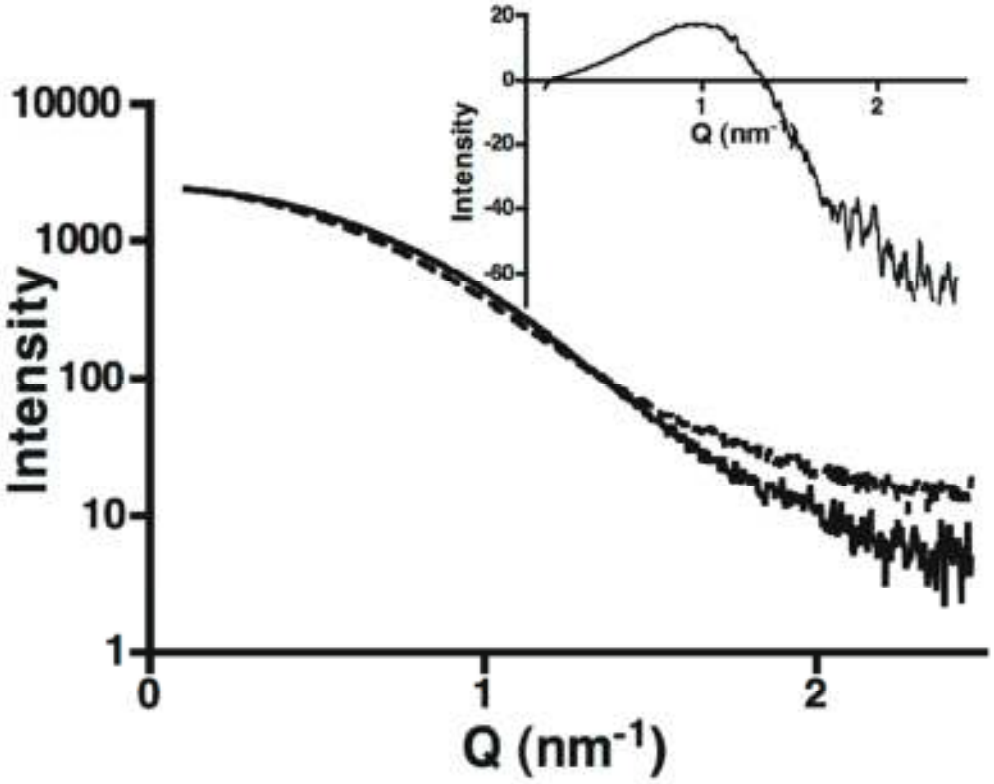
10000
1000
100
10
1
Intensity
0
1
2
Q (nm-1)
20
0
-20
-40
-60
Intensity
1
2
Q (nm-1)

the transporter in the absence of MBP [11]. When 20 μM sMBP was added to wild type $MalFGK_2$, no statistically significant increase in activity was observed. However, in the presence of *either* 5 mM maltose or sucrose, sMBP stimulated a 4-fold increase in ATP hydrolysis over background (Figure 3.2A, diagonal fill). We have therefore observed that, with respect to ATPase activation, $MalFGK_2$ cannot distinguish sucrose from maltose. To demonstrate that the equivalence of maltose- and sucrose-bound sMBP was not limited to 20 μM sMBP concentration, a range of concentrations, from 1 to 100 μM, were tested (Figure 3.2B). Across this concentration range, maltose- and sucrose-bound sMBP stimulate the $MalFGK_2$ ATPase to similar levels; the overall trend - in both cases a proportional increase in $MalFGK_2$ ATPase activity as sMBP concentration is raised - suggests that the mechanism for stimulation is the same, irrespective of which sugar $MalFGK_2$ comes in contact with.

Although maltose- and sucrose-bound sMBP both stimulate the $MalFGK_2$ ATPase to the same extent, the absolute levels of ATPase activity produced by sMBP were much lower than those produced by wtMBP. For example, in the presence of maltose the level of ATPase stimulation by 20 μM wtMBP was 40 fold higher than the stimulation produced by the same concentration of either maltose- or sucrose-bound sMBP. In addition, unliganded sMBP did not produce a significant increase in $MalFGK_2$ ATPase, in contrast to unliganded wtMBP which consistently produces a 2-fold stimulation (Figure 3.2A)[11,15]. Therefore, while the substitution of sucrose for maltose did not influence stimulation of the $MalFGK_2$ ATPase, when compared to wtMBP the mutations in sMBP have drastically compromised its overall ability to stimulate the $MalFGK_2$ ATPase.

Structural analysis of open and closed sMBP

To determine how the mutations in sMBP disrupt its ability to stimulate $MalFGK_2$, I

Fig 3.2 Effect of Ligand on Stimulation of the $MalFGK_2$ ATPase

$MalFGK_2$ was reconstituted into a proteoliposome system (PLS) and the effect of MBP and ligands on the $MalFGK_2$ ATPase were measured. (A) The PLS have a basal ATPase (clear bar) that is not significantly increased by unliganded sMBP. When bound to either sucrose or maltose, sMBP produces a 4-fold stimulation over the basal rate (bars with diagonal fill). The much larger ATPase stimulation by 20 μM wtMBP (bars with horizontal fill) shows that the mutations in sMBP have impaired its ability to stimulate the $MalFGK_2$ ATPase compared to wtMBP. (B) The abilities of sucrose-sMBP (black) and maltose-sMBP (grey) to stimulate $MalFGK_2$ above its basal ATPase were compared over a range of sMBP concentrations; the sugars were present at a concentration of 5 mM.

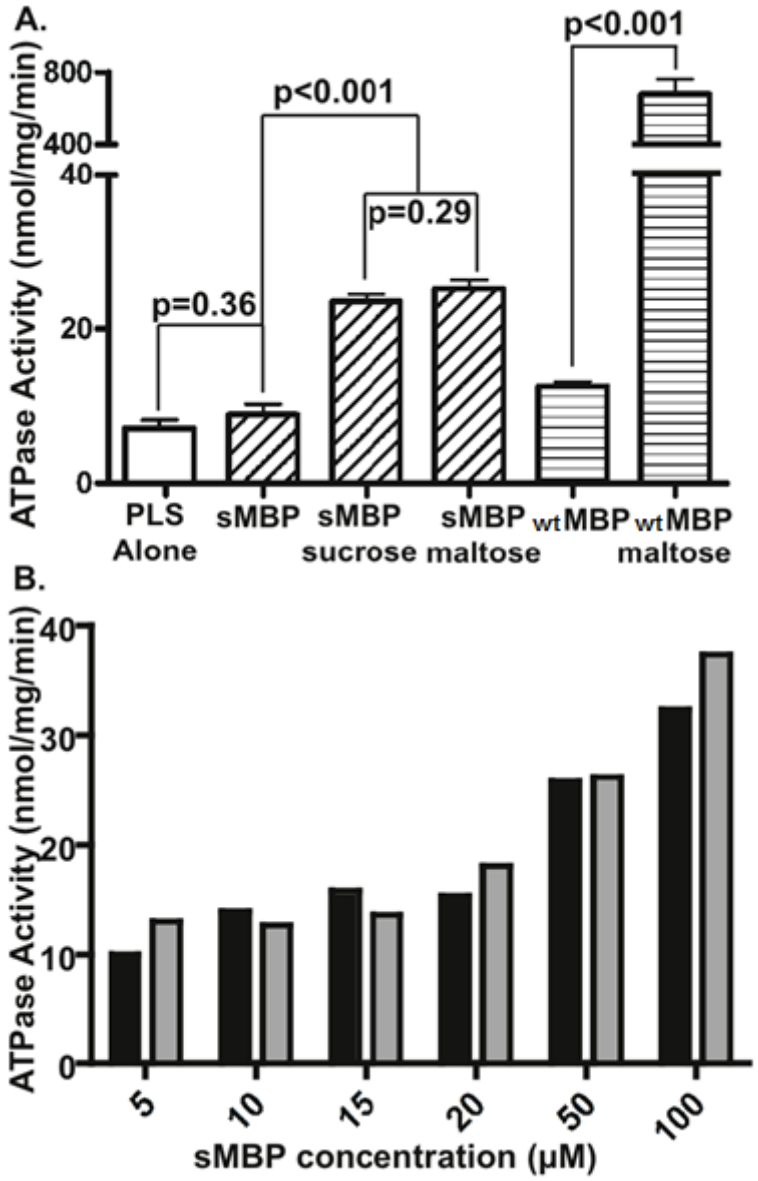
A.
ATPase Activity (nmol/mg/min)
800
400
40
20
0
p<0.001
p<0.001
p=0.29
p=0.36
PLS Alone
sMBP
sMBP sucrose
sMBP maltose
wtMBP maltose
wtMBP
B.
ATPase Activity (nmol/mg/min)
40
30
20
10
0
5
10
15
20
50
100
sMBP concentration (μM)

solved the crystal structures of sMBP in both the sucrose-bound and substrate-free forms to resolutions of 2.0 Å and 1.5 Å respectively (Table 3.1). In both forms sMBP adopts a wild type fold, with main chain atoms differing from wtMBP by an RMSD for CA positions of 0.48 Å in the closed form and 0.55 Å in the open form.

Well-defined electron density for sucrose was seen in the binding site of the sMBP-sucrose structure; the electron density clearly defines each hydroxyl group of sucrose and does not fit maltose (Figure 3.3A). Like maltose-bound wtMBP, sMBP binds sucrose through hydrogen bonds with each of the two sugar rings. The first, non-reducing, glucose unit is common to both maltose and sucrose and occupies an identical binding pocket in wtMBP and sMBP (Figure 3.3B). The second sugar ring differs between maltose and sucrose, being an α-1,4 linked reducing glucose in maltose and an α-1,2 linked fructose in sucrose. As a result, sucrose adopts a 90° bend compared to maltose. This bend allows the C3 hydroxyl to hydrogen bond with residue W62Y, which was likely selected for this purpose (Figure 3.3B). The bend also creates a cavity in the binding site and separates the sugar from residues 14 and 15 (Figure 3.3C). The D14L, K15F and E111Y mutations modify this hydrophobic cavity by removing what would otherwise be unmatched buried charges or polar groups.

We also solved the crystal structure of the open conformation of sMBP to 1.5 Å resolution, and were surprised to find a significant change in the structure of the ligand binding site. The W62Y mutation is able to adopt an alternate conformation that displaces the main chain segment from residues Y62 to G69 (Figure 3.4). This difference was evident from clear electron density for the Y62 side chain in two different places, one of which necessarily displaces F67 and is therefore incompatible with the wild-type main chain conformation (Figure 3.4C). The only way this change can be accommodated is for residues 62-69 to partially extend into the substrate binding cleft. The occupancies of the two conformations of residues 66 to 69 were set such that

Table 3.1 Crystallographic Statistics

	sMBP-Sucrose	Unliganded sMBP
PDB-ID	3HPI	3KJT
Resolution limit (Å)	2.0	1.5
Space Group	$P2_12_12_1$	$P2_1$
Unit cell Parameters		
a,b,c (Å)	60.042, 85.229, 132.864	43.888, 65.544, 57.5
α,β,γ (deg)	90, 90, 90	90, 101.141, 90
Molecules per AU	2	1
Solvent content	0.41	0.4
Unique reflections	44813	48552
[a]Mean I/(σI)	16.1 (2.38)	17.8 (2.03)
[a]Rmerge	0.092 (0.468)	0.048 (0.329)
[a]Completeness (%)	96.2 (86.4)	88.1 (58.5)
[a]Redundancy	5.8 (4.4)	3.3 (2.2)
Number of reflections		
Total	40799	43724
Rfree	2032	2345
Refinement		
Resolution range (Å)	34.8 - 2.0	24.8 - 1.5
Rwork	0.228	0.215
Rfree	0.284	0.243
RMSD bond length (Å)	0.00621	0.00497
RMSD bond angle (deg)	1.22	1.17
B-Factors ($Å^2$)		
Protein	34.2	16.7
Ligand	29.1	N/A
Solvent	33.1	25.2
Ramachandran Analysis		
Most favored	92%	91%
Allowed	8%	9%
Generously Allowed	0	0
Disallowed	0	0

[a]Values in parentheses refer to the highest resolution shell.

Fig 3.3 Sucrose Binding by sMBP.

The structure of sucrose bound sMBP was solved and refined to 2 Å resolution (Table 1); coordinates for wtMBP and maltose were from PDB-ID 1ANF [24]. (A) Bound sucrose (dark green) and the mutated residues (pale green) are show, along with $2F_O$-F_C electron density for the sucrose (blue mesh) contoured at 2σ. The electron density map was calculated using phases from the partially refined structure, prior to the addition of sucrose to the binding site. (B) Hydrogen bonding interactions between sucrose and sMBP (top) are compared to those between maltose and wtMBP (bottom). Hydrogen bonding interactions to the first glucose ring are the same in both proteins. (C) Comparison of the ligand binding sites of sMBP and wtMBP. The molecular surface that sMBP and wtMBP have in common is shown in grey; carbon atoms from maltose and wtMBP are shown in orange and yellow, respectively, while those from sucrose and sMBP are shown in dark green and pale green. The conformation of sucrose creates a cavity that would normally be filled with atoms from the second glucose unit of maltose, to which three charged residues (D14, K15, and E111) would be hydrogen bonded, as illustrated in Panel B. The mutations in sMBP (pale green) convert these three charged residues to neutral residues.

A.

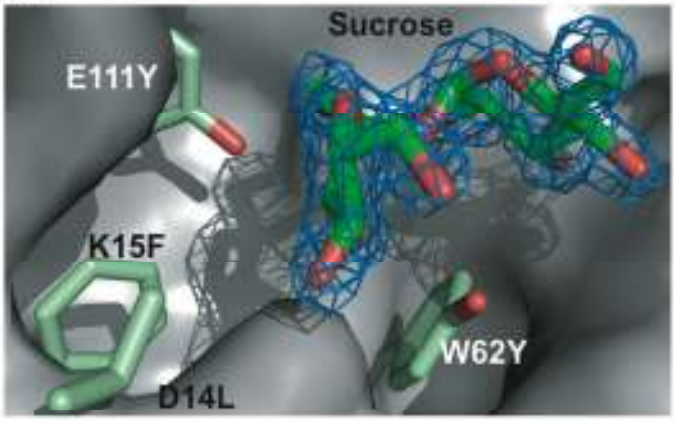

B.

Sucrose-Bound sMBP

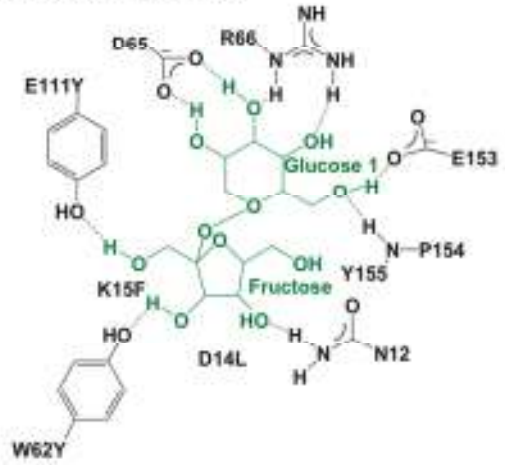

Maltose-Bound wtMBP

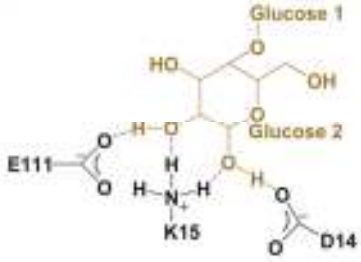

C.

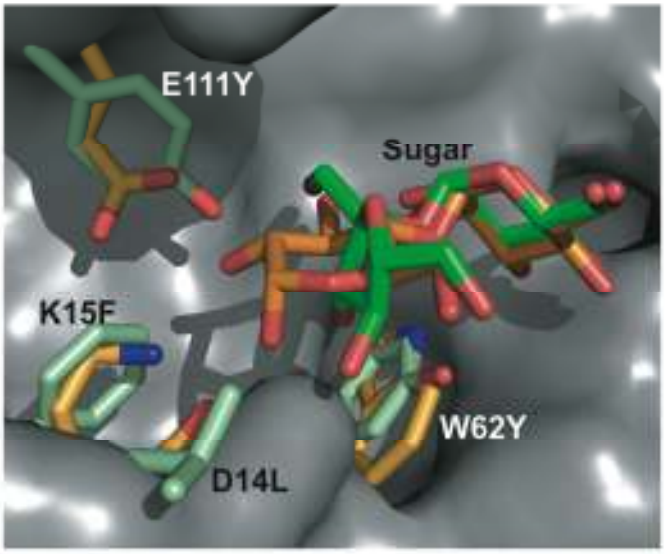

the temperature factors for the wild-type conformation are similar to the main chain average, as is the case with open, wild-type MBP [5]. On this basis, the occupancy of the wild type conformation is estimated at 0.4, and that of the alternate conformation is 0.6.

Both the open and closed conformations of MBP are involved in maltose transport [8,14,15,16]. To understand why sMBP has such a compromised ability to stimulate the $MalFGK_2$ ATPase, we compared its surface in both the open and closed conformations to that of wtMBP. The changes in sMBP necessary to support sucrose binding require only side chain substitutions, most of which are buried in the sugar binding site and not surface accessible in the closed form of the protein. As a result the surface morphology of closed sMBP is virtually unaltered from closed wtMBP (Figure 3.5A), with only a slight perturbation caused by the exposure of a methyl group on D14L (Figure 3.6).

In contrast to the closed state, the open conformation of sMBP fully exposes all 4 binding site mutations to the solvent (Figure 3.5B) as well as the alternate and partially disordered conformations for residues 62 to 69, caused by the W62Y mutation (Figure 3.4). To summarize, our structural analysis found that in the sucrose- bound closed form, sMBP closely mimics the surface morphology of wtMBP, but open unliganded sMBP displays a drastically altered sugar-binding site.

Altered interactions between open sMBP and $MalFGK_2$

To investigate how the mutations in open sMBP could cause such a drastic defect in its ability to stimulate the $MalFGK_2$ ATPase, we replaced wtMBP with sMBP in the crystal structure of MBP-$MalFGK_2$ that corresponds to the transition state for ATP hydrolysis [7,8]. The backbone positions of sMBP fit the MBP component of the trapped transition state to an RMSD of 0.84 Å.

Fig 3.4 Main Chain Disorder in the Open Unliganded sMBP Structure

Residues 62 to 69 adopt two different conformations in the open, unliganded structure of sMBP, which was refined to 1.5 Å resolution (Table 1). The molecular surface of sMBP (excluding residues 62 to 69) is shown with residues 62 to 69 included as stick models in either (A) the conformation resembling that observed in wtMBP, or (B) the alternate conformation observed in sMBP. (C) A superposition of the two conformations observed in sMBP, along with $2F_O$-F_C electron density calculated from phases obtained through a simulated annealing procedure with residues 62 to 69 omitted from the structure. Note the electron density for Y62 in two different positions. The A position for Y62 corresponds to the position of W62 in wtMBP; occupancy of the B position requires an alternate conformation for the main chain residues.

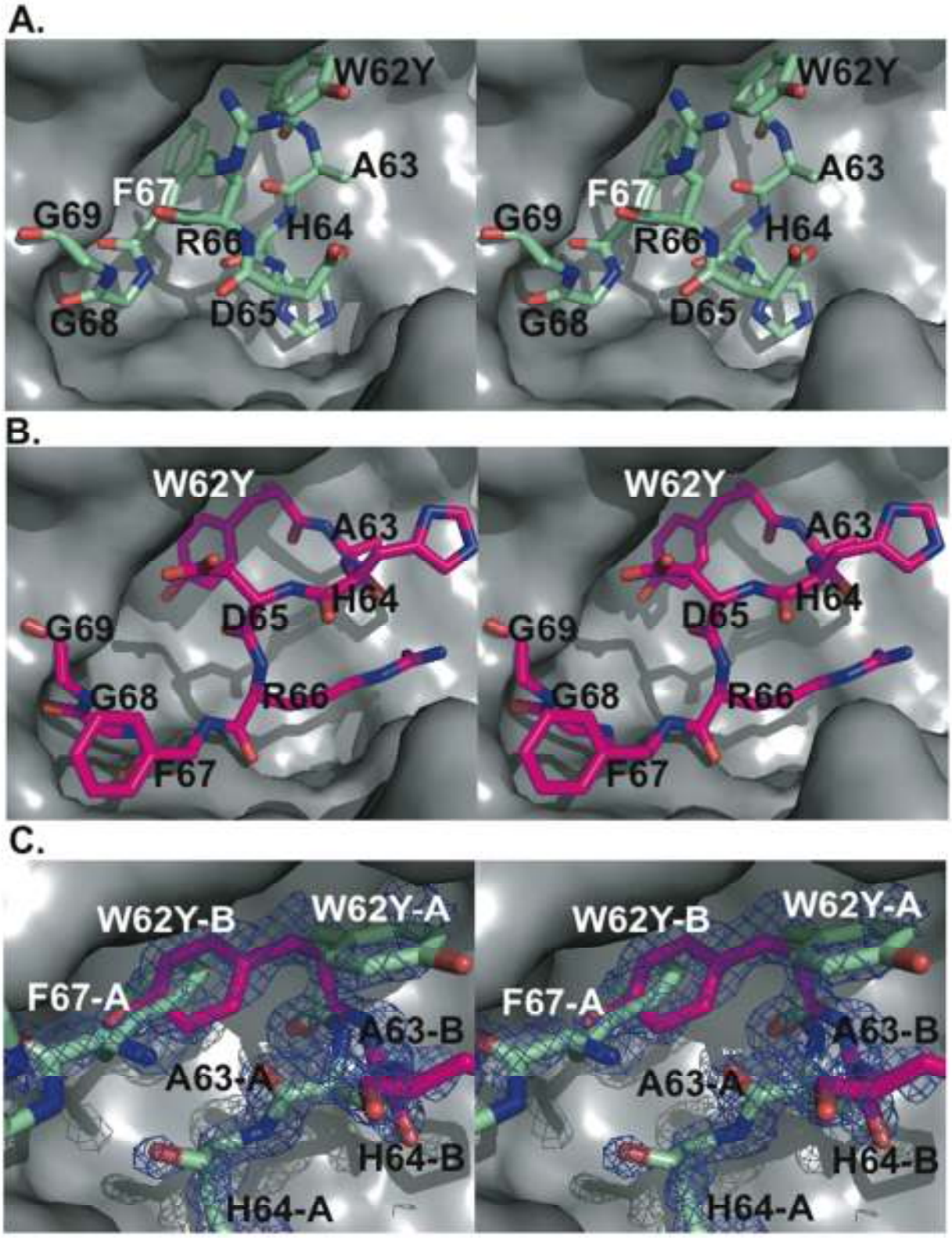
A.
W62Y
A63
F67
G69
R66
H64
G68
D65
W62Y
A63
F67
G69
R66
H64
G68
D65
B.
W62Y
A63
H64
D65
G69
G68
R66
F67
W62Y
A63
H64
D65
G69
G68
R66
F67
C.
W62Y-B
W62Y-A
F67-A
A63-B
A63-A
H64-B
H64-A
W62Y-B
W62Y-A
F67-A
A63-B
A63-A
H64-B
H64-A

Fig 3.5 Effect of Mutations on the Surface Properties of Open and Closed sMBP

The molecular surfaces of wtMBP (tan) and sMBP (pale green) are compared for both the (A) closed and (B) open conformations. In the closed conformation, the surfaces of bound maltose and sucrose are coloured orange and dark green, respectively. The D14L and W62Y mutations are visible (red patches), but have very little effect on the accessible surface of sMBP compared to wtMBP. (B) In the open conformation, all of the mutations are visible (red patches). In addition, the main chain residues 62 to 69 are partially disordered; the alternate conformation for these residues is shown in magenta. Coordinates for open and closed wtMBP correspond to 1OMP [5] and 1ANF [24], respectively.

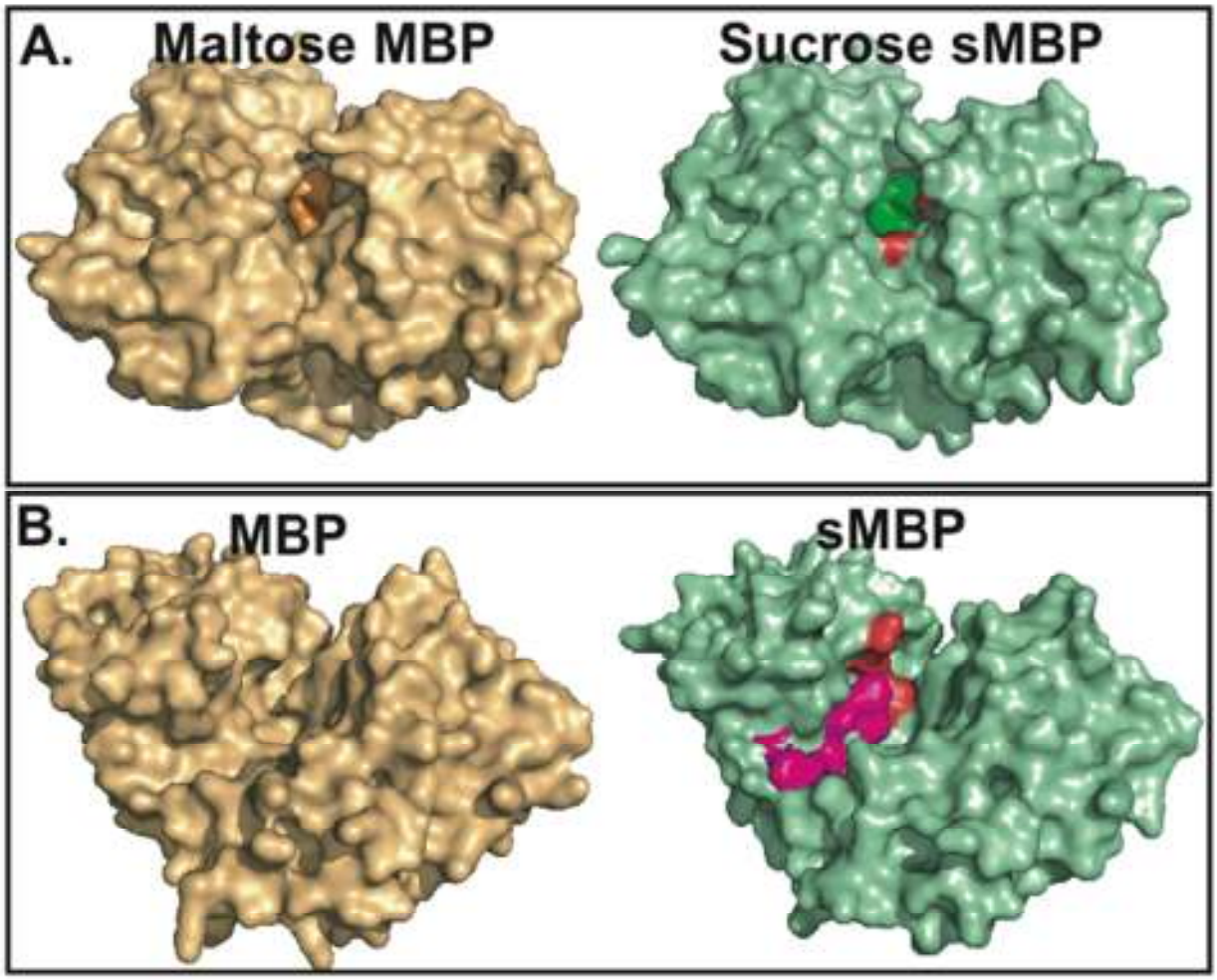
A.
Maltose MBP
Sucrose sMBP
B.
MBP
sMBP

Fig 3.6 Mutation D14L of sMBP

Apart from the sugar ligand (dark green), the only surface accessible change between closed wtMBP and closed sMBP is residue D14L (pale green). This mutant residue extends the hydrophobic surface of sMBP 2 Å further from the CA atom of D14 in MBP (tan).

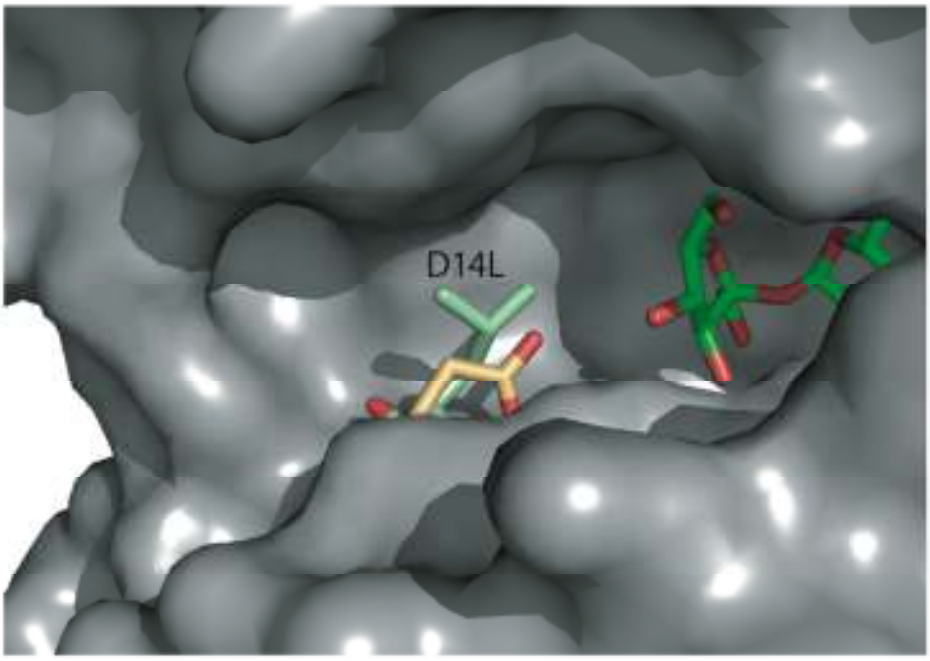
D14L

The binding of sMBP to the transporter transmembrane (MalFG) domains was not obviously compromised across the exterior surface of the binding protein, including contacts between sMBP and the MalF P2 arm [17,18]. However mutations D14L, W62Y and E111Y disrupted interactions of the maltose-binding site with residues 253-258 of MalG, which occupy the maltose binding site in the transporter transition state (Figure 3.7). These residues comprise an invasive structure known as the MalG P3 'scoop loop,' named for its probable role in excluding maltose from the MBP maltose-binding site [8]. D14L clashes with N254 of MalG while W62Y and E111Y remove stabilizing van der Waals and hydrogen bond interactions. In addition, the alternate conformation adopted by residues 62-69 will interfere with MalG interactions. Altogether, the mutations in the open conformation of sMBP would be expected to disrupt interactions with the MalG P3 loop in the transition state for ATP hydrolysis.

In summary, the mutations in sMBP have a drastic effect on its ability to stimulate $MalFGK_2$ ATPase activity. Structural analysis indicates that this effect is due to a disruption of interactions between residues 253-258 of MalG and the empty sugar binding site of MBP as it occurs in the transition state for ATP hydrolysis. The magnitude of this effect shows that these interactions are critical for stimulation of the $MalFGK_2$ ATPase.

Fig 3.7 Interactions Between the MalFGK$_2$ P3 Loop and the sMBP Ligand Binding Site

The open conformation of sMBP was superimposed onto wtMBP in the transition state structure of the MBP-MalFGK$_2$ complex (PDB-ID 2R6G; [8]. The MalG P3 'scoop loop' comprising residues 254 to 258 (cyan) extend into the sugar binding site, making contacts with wtMBP residues 14, 62, and 111 (yellow). The contacts made between MalG and the ligand binding site would be affected by the mutations in sMBP. In addition, interaction with the MalG P3 loop would be disrupted due to disorder in sMBP residues 62 to 69, as outlined in Figure 3.

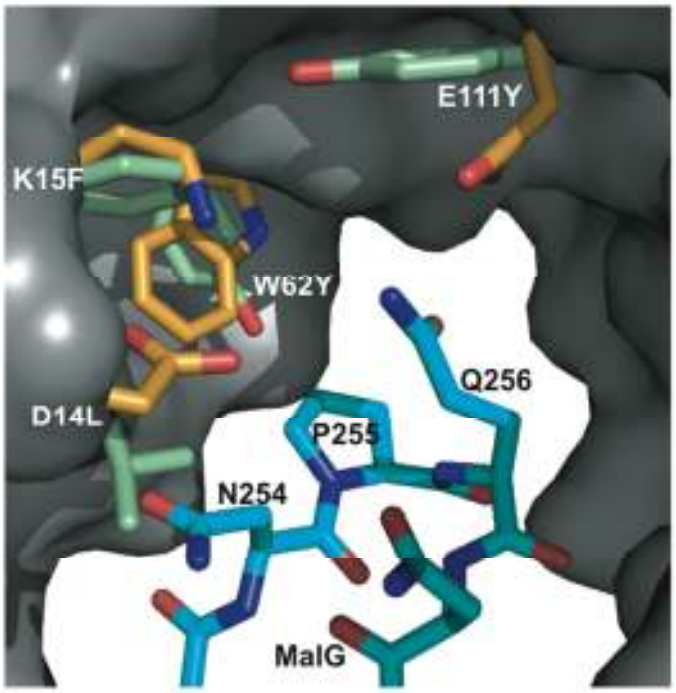
E111Y
K15F
W62Y
Q256
D14L
P255
N254
MalG

3.4 Discussion

We observed that a sucrose-binding mutant of MBP was able to stimulate the ATPase activity of $MalFGK_2$ with either maltose or sucrose present as substrate. The activation was indistinguishable between maltose and the non-physiological substrate, sucrose. The available evidence suggests that sucrose is unable to interact with the maltose binding site in $MalFGK_2$. For example, in transport assays using MBP-independant $MalFGK_2$ mutants, sucrose was incapable of competitively inhibiting the transport of maltose [13] indicating that substrate binding site of $MalFGK_2$ has little, if any, affinity for sucrose. This can be explained using the $MalFGK_2$ structure in complex with maltose [8]: modeling sucrose into the same position as maltose results in clashes with MalF residues 383, 433 and 436, including steric clashes with backbone atoms. Since sucrose is unable to occupy the maltose binding site of $MalFGK_2$, the observation that maltose- and sucrose-bound sMBP have equal abilities to stimulate $MalFGK_2$ demonstrates that specific binding of the carbohydrate by $MalFGK_2$ is not important for activation of its ATPase. Therefore it is the substrate induced conformational change in MBP, but not the identity of the substrate itself, that is critical for stimulation of the $MalFGK_2$ ATPase.

In principle, ATP-dependent transporters should couple ATP hydrolysis to actual movement of substrate. Our results with sMBP show that direct interactions with the substrate are not required for stimulation of the $MalFGK_2$ ATPase, and therefore coupling of ATP hydrolysis to substrate translocation must depend solely on interactions between MBP and $MalFGK_2$. In this regard, the very strong defect in the ability of sMBP to stimulate the $MalFGK_2$ ATPase indicates that a critical interaction between MBP and $MalFGK_2$ has been disrupted by the mutations.

Both the open and closed conformations of MBP interact with $MalFGK_2$ during the catalytic cycle [3,7,8,15]. The surface of closed sMBP is almost identical to that of wtMBP,

suggesting that this conformation is not responsible for the reduced ability of sMBP to stimulate the $MalFGK_2$. In fact, L14 (D14 in wtMBP) is the only mutant residue that causes a change in the exposed surface of closed sMBP and could therefore alter interactions with $MalFGK_2$. Although functional genetic screens have demonstrated that the region around residue 14 is important for the interaction of MBP and $MalFGK_2$ [19,20], the only change found at residue 14 in the genetic screens was a mutation to tyrosine, a much larger residue that cannot be buried in the ligand-bound conformation of MBP, and would therefore produce a large change in the surface of the closed conformation. In contrast, the D14L mutation is mostly buried and almost isosteric, resulting in only a very small change in the surface, namely a 2 Å extension of an existing hydrophobic patch (Figure 3.6). Therefore, the small effect of the D14L mutation on the surface of closed sMBP does not provide a convincing explanation for the profound effect of the mutations on the ability of sMBP to stimulate $MalFGK_2$.

The surface of open sMBP, on the other hand, is drastically altered by the exposure of mutant residues in the sugar-binding site and the creation of an area of conformational instability due to the W62Y mutation. On this basis, the profound defect in sMBP is most likely due to a disruption of interactions between the open, rather than the closed, conformation of MBP. This conclusion is consistent with an important role for open MBP in stabilization of the transition state for ATP hydrolysis [8,15].

In fact, the reduced activation of $MalFGK_2$ ATPase by sMBP coincides with a disruption of interactions between sMBP ligand binding site residues and the invasive MalG P3 loop of $MalFGK_2$ [8]. These interactions are only possible once MBP adopts the open conformation and maltose has vacated the MBP sugar binding site to enter $MalFGK_2$. The interactions between the MalG P3 loop and the ligand binding site of MBP appear to play a critical role in transport coupling by allowing hydrolysis of ATP only once the ligand has translocated from the binding

site in MBP to the $MalFGK_2$ binding site.

A role for the MalG P3 loop in energetic coupling is consistent with its position in $MalFGK_2$ (Figure 3.8). The P3 loop is connected to MalG helices 15 and 16, which extends from the scoop loop to the MalG C-terminus, located in a hydrogen bond network equidistant between the two ATP binding sites of $MalK_2$. Our data indicate that in addition to extracting maltose from the MBP sugar binding cleft [8] interactions between the MalG P3 loop and MBP also play a direct role in promoting ATP hydrolysis. These interactions do not depend on the specific chemical identity of the substrate, and therefore a similar mechanism might be operative in multi-drug exporters and other ABC transporters that couple ATP hydrolysis to the transport of diverse substrates.

Fig 3.8 Structural Basis for Communication Between the MalG P3 Loop and ATP Binding Cassettes

The MBP-MalFGK$_2$ transition state complex (PDB-ID 2R6G)[8] is shown. As detailed in Figure 5, MalG residues 254 to 257 (cyan) make contacts with the sugar binding site of MBP (pale green). These contacts are only possible when maltose is absent, hence the term "scoop loop" was used to assign a function this region of MalG [8]. Residues that are mutated in sMBP are shown in green CPK representation. The loop is connected with the MalK$_2$ ATP binding sites (red) via the MalG C-terminus (violet).

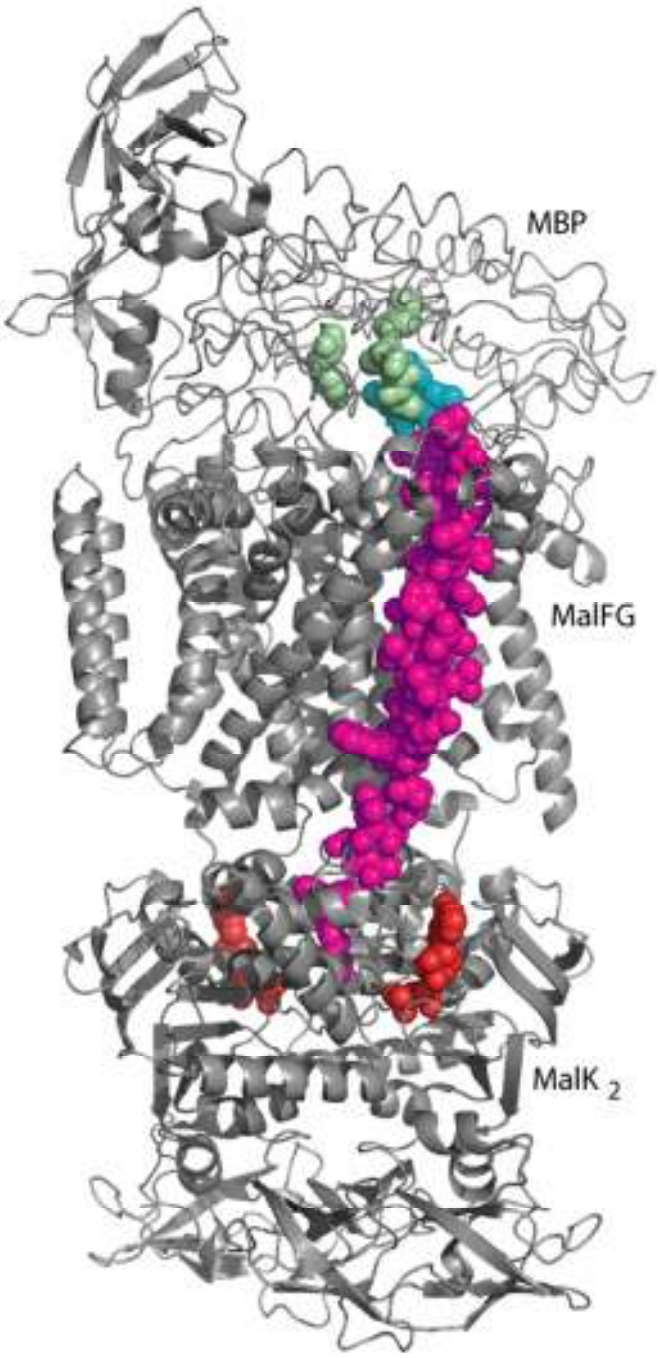
MBP
MalFG
MalK 2

Bibliography

1. Davidson, A. L., Dassa, E., Orelle, C., and Chen, J. (2008) Structure, function and evolution of bacterial ATP-binding cassette systems. *Microbiol Mol Biol Rev* **72**: 317-364
2. Jones, P. M., O'Mara, M. L., and George, A. M. (2009) ABC transporters: a riddle wrapped in an mystery inside an enigma. *Trends Biochem Sci* **34**: 520-531
3. Shilton, B. H. (2008) The dynamics of the MBP-MalFGK(2) interaction: a prototype for binding protein dependent ABC transporter systems. *Biochim Biophys Acta* **1778**: 1772- 1780
4. Khare, D., Oldham, M. L., Orelle, C., Davidson, A. L., and Chen, J. (2009) Alternating access in maltose transporter mediated by rigid-body rotations. *Mol Cell* **33**,528-536
5. Sharff, A., Rodseth, L., Spurlino, J., and Quiocho, F. (1992) Refined 1.8-A structure reveals the mode of binding of beta-cyclodextrin to maltodextrin binding protein. *Biochemistry* **31:**, 10657-10663
6. Hall, J. A., Thorgeirsson, T. E., Liu, J., Shin, Y. K., and Nikaido, H. (1997) Two modes of ligand binding in maltose-binding protein of Escherichia coli. Electron paramagnetic resonance study of ligand-induced global conformational changes by site-directed spin labelling. *J Biol Chem* **272**: 17610-17614
7. Austermuhle, M. I., Hall, J. A., Klug, C. S., and Davidson, A. L. (2004) Maltose-binding protein is open in the catalytic transition state for ATP hydrolysis during maltose transport. *J Biol Chem* **279**: 28243-28250
8. Oldham, M. L., Khare, D., Quiocho, F. A., Davidson, A. L., and Chen, J. (2007) Crystal structure of a catalytic intermediate of the maltose transporter *Nature* **450**: 515-521
9. Dawson, R. J., Hollenstein, K., and Locher, K. P. (2007) Structure and mechanism of ABC transporter proteins. *Mol Microbiol* **65**: 250-257
10. Hollenstein, K., Frei, D. C., and Locher, K. P. (2007) Structure of an ABC transporter in complex with its binding protein *Nature* **446**: 213-216
11. Davidson, A., Shuman, H., and Nikaido, H. (1992) Mechanism of maltose transport in Escherichi coli: transmembrane signalling by periplasmic binding proteins. *Proc. Natl. Acad. Sci. USA* **89**: 2360-2364
12. Guntas, G., Mansell, T. J., Kim, J. R., and Ostermeier, M. (2005) Directed evolution of protein switches and their application to the creation of ligand-binding proteins. *Proc Natl Acad Sci U S A* **102**: 11224-11229
13. Shuman, H. (1982) Activ transport of maltose in Escherichia coli K12. Role of the periplasmic maltose-binding protein and evidence for a substrate recognition site in the cytoplasmic membrane. *J. Biol. Chem.* **257**: 5455-5461
14. Merino, G., and Shuman, H. A. (1997) Unliganded maltose-binding protein triggers lactose transport in an Escherichi coli mutant with an alteration in the maltose transport system. *J Bacteriol* **179**: 7687-7694
15. Gould, A. D., Telmer, P. G., and Shilton, B. H. (2009) Stimulation of the maltose transporter ATPase by unliganded maltose binding protein. *Biochemistry* **48**: 8051-8061 Appears as chapter 2 of this thesis.
16. Bohl, E., Shuman, H., and Boos, W. (1995) Mathematical treatment of the

kinetics of binding protein dependent transport systems reveals that both the substrate loaded and unloaded binding proteins interact with the membrane components. *J. Theor. Biol.* **172**:83-94
17. Daus, M. L., Grote, M., and Schneider, E. (2009) The MalF P2 loop of the ATP-binding cassette transporter MalFGK2 from Escherichia coli and Salmonella enterica serovar typhimurium interacts with maltose binding protein (MalE) throughout the catalytic cycle. *J Bacteriol* **191**:754-761
18. Grote, M., Polyhach, Y., Jeschke, G., Steinhoff, H. J., Schneider, E., and Bordignon, E. (2009) Transmembrane signalling in the maltose ABC transporter MalFGK2-E: periplasmic MalF-P2 loop communicates substrate availability to the ATP-bound MalK dimer. *J Biol Chem* **284**: 17521-17526
19. Hor, L., and Shuman, H. (1993) Two modes of ligand binding in maltose-binding protein of Escherichia coli. Functional significance in active transport. *J. Mol. Biol.* **233:** 659-670
20. Treptow, N., and Shuman, H. (1988) Allele-specific male mutations that restore nteractions between maltose-binding protein and the inner-membrane components of the maltose transport system. *J. Mol. Biol.* **202**: 809-822
21. Brünger, A. T., Adams, P. D., Clore, G. M., DeLano, W. L., Gros, P., Grosse-Kunstleve, R. W., Jiang, J. S., Kuszewski, J., Nilges, M., Pannu, N. S., Read, R. J., Rice, L. M., Simonson, T., and Warren, G. L. (1998) Crystallography & NMR systems: A new software suite for macromolecular structure determination. *Acta Crystallogr. D Biol. Crystallogr.* **54**: 905-921
22. Emsley, P., and Cowtan, K. (2004) Coot: model-building tools for molecular graphics. *Acta Crystallogr D Biol Crystallogr* **60**: 2126-2132
23. DeLano, W. (2002) *The PyMOL User's Manual*
24. Quiocho, F. A., Spurlino, J. C., and Rodseth, L. E. (1997) Extensive features of tight oligosaccharide binding revealed in high-resolution structures of the maltodextrin transport/chemosensory receptor. *Structure* **5**: 997-1015.
25. Telmer, P.G., Shilton, B.H., (2005) Structural studies of an engineered zinc biosensor reveal an unanticipated mode of zinc binding, *J Mol Biol* **354**:829-40.

Chapter 4 Activation of the Maltose Transporter by Cysteine Stabilized MBP Mutants

4.1 Introduction

The maltose transporter ($MalFGK_2$) of *Escherichia coli* efficiently couples the hydrolysis of ATP to the internalization of maltose. This coupling is enforced by the prevention of futile ATP hydrolysis when the transporter is in a resting state and has not been activated by its primary substrate receptor, the maltose binding protein (MBP). Under the influence of maltose liganded MBP this autoinhibition is reversed and rapid ATP hydrolysis is coupled to maltose transport [1,2,3].

MBP binds maltose and other short maltodextrins at the interface between its two domains. On the binding of maltose, interactions within the maltose-binding site cause these domains to rotate about a flexible hinge region and close around the bound ligand. This results in a shift in conformation from a stable 'open' resting state to a 'closed' state that has been likened to the snapping shut of a venus flytrap [4,5]. The closed conformation of MBP is known to play a major role in transporter stimulus as only those MBP ligands that induce domain closure are transported [3]. Additionally, MBP residues identified as significant for stimulus cluster together in the closed, but not open, conformation [6].

The transporter is thought to act by an alternating access model, in which conformational changes during the ATPase catalytic cycle alternately expose an internal binding site to the periplasm, where substrate can be collected, and to the cytoplasm, where it can dissociate [7]. It has been demonstrated that during these conformational changes the transporter interacts with both the closed and open forms of MBP which could suggest that both forms play functional roles [8,9,10].

Previous analysis has supported this theory by showing that the activity of MBP is tied to the stability of both its dominant conformers. Destabilizing the unliganded open form of MBP, and thus shifting the protein towards closed unliganded forms, decreased the ATPase observed with unliganded MBP [11]. This indicates that the stability of the open form, or the ability of the closed form to convert to the open, plays a role in ATPase stimulus. The open conformation is likely responsible for the activation of ATP hydrolysis seen with unliganded MBP, suggesting that the interaction between open MBP and the transporter, seen in the ATPase transition state, promotes ATP hydrolysis [8]. That ATPase stimulus in the absence of maltose was not consistent with causation by transiently closed MBP may further be an indication that the stability of the closed form is a factor in activity [12].

These findings justify a deeper investigation of the separate functional roles of the closed and open forms of MBP, however previous investigations have been complicated by the conformational flexibility of MBP. MBP exists in an equilibrium between its most stable forms, ligand bound closed and unliganded open, and more transient forms such as unliganded semi-closed and ligand-bound open conformations [13,14]. This equilibrium, and an understanding that closed MBP is opened by the transporter during the transport cycle, obscures the role of each MBP conformation.

The intent in this study was to better de-convolute the separate abilities of the closed-liganded and the unliganded-open forms of MBP to support ATP hydrolysis by the transporter. To this end we have exploited the known structures of MBP to introduce cysteine mutations and cross-links predicted to stabilize the

open or closed forms of MBP. These interventions were intended to shift or abolish the equilibrium between open and closed MBP, producing binding proteins that favor a single conformation. The transporter has additionally been extracted from the lipid bilayer and solubilized using a mild detergent. This treatment is known to disrupt the transporters normal auto-inhibiton behavior and result in a much higher constitutive ATPase activity [15]. If both forms of MBP play a role in transport, then this disruption in regulation may differently impact the ability of the open and closed forms to stimulate ATP hydrolysis, enabling their individual contributions to be better determined.

Here we determine that a closed form of MBP is sufficient to activate substantial, although not maximal, ATPase activity *in vitro*. However, when the relative stabilities of differing transporter conformations are altered by detergent solubilization, the ability of the closed conformation of MBP to stimulate the $MalFGK_2$ ATPase is relatively small compared to that of unliganded open MBP. This is the opposite of the result seen from the membrane bound system. This suggests that the role played by the closed form is diminished in importance, while that of the open form is increased for detergent solubilized $MalFGK_2$. This supports our hypothesis that both conformations play functional roles in hydrolysis; with the liganded-closed state mediating a conversion of the transporter to its catalytic conformation and the unliganded-open state stabilizing the catalytic state to promote ATPase.

These results also indicate that the conformational stability, or the availability, of those transporter conformations targeted by the closed and open

forms of MBP is sensitive to packing interactions between the transmembrane regions and lipid bilayer. Freeing the complex from the membrane simultaneously makes the transporter more available to productively interact with open MBP and less available to closed MBP.

We additionally find that a mutant MBP, stabilized in the open conformation by a cysteine coupled cross-linker, stimulates a high degree of ATPase activity from the transporter even in the absence of maltose. This uncoupling phenotype offers insights into the conformational changes of the transporter following hydrolysis, as it leaves the ATPase catalytic state and it reverts to the resting state.

4.2 Materials and Methods

Cloning, Growth and Purification of Binding Protein Mutants

Cloning of MBP-Closed (MBP-C), MBP-Open (MBP-O) and MBP-O95/171

A previously identified mutant of MBP was reproduced, with cysteine mutations introduced at positions G69C and S337C (MBP-C) of the otherwise cysteineless MBP [16]. Two additional mutants were engineered, MBP-O and MBP-O95/171, with cysteines introduced at positions G101C/G174C and D95C/Y171C respectively. These mutations were cloned into plasmid pPROEX-hta [12,17] containing a previously cloned sequence for wtMBP lacking a periplasmic export tag but with a TEV-protease cleavable hexahistidine tag. These mutations were incorporated by two rounds of mutagenic PCR utilizing the stated complementary primer pairs (Table 4.1).

Expression of MBP Mutants

MBP-C was expressed from pPROEX-hta in a BL21 (DE3) background by induction with IPTG as previously performed for other binding protein mutations [12,17]. Cells were lysed by passage through a French Pressure cell and expressed protein extracted by Ni^{2+} affinity, followed by cleavage of the histidine tag and repeat passage across a Ni^{2+}-loaded Chelating Sepharose column as previously described [12,17].

MBP-O, MBP-O95/171 and wtMBP were expressed and extracted as described for MBP-C. wtMBP was additionally unfolded by serial dialysis against 50 mM Tris- Cl pH8.0, 100 mM NaCl, 6 M guanidine-HCl to reduce maltose contamination, then refolded and purified as previously reported [12].

Table 4.1 Mutagenic Primers for MBP Mutants

Mutant	Mutation	Primer Sequence (5'->3')
MBP-C69/337		
	G69C	CGACCGCTTTGGTTGCTACGCTCAATCTGGCC
	S337C	CCCGCAGATGTGCGCTTTCTGGTATGCCG
MBP-O 101/174		
	G101C	CGTACGTTACAACTGCAAGCTGATTGCTTACC
	G174C	CGTTCAAGTATGAAAACTGCAAGTACGACATTAAAGACG
MBP-O95/171		
	D95C	CGTTTACCTGGTGTGCCGTACGTTAC
	Y171C	GGTTATGCGTTCAAGTGTGAAAACGG

Oxidation and Cross-Linking of Binding Protein Mutants

Purified MBP-C and MBP-O mutants were dialyzed in 50 mM NaH_2PO_4 pH 7.0, 100 mM NaCl, 1 mM TCEP to reduce mixed disulfides that may have formed during lysis or TEV digestion. After dialysis in 50 mM NaH_2PO_4 pH 7.0, 100 mM NaCl to remove reducing agent both proteins were left to incubate for 2 days with 10 μM $CuCl_2$; MBP-C with 10 μM of maltose and MBP-O mutants without substrate. Oxidized MBP-C was purified by affinity chromatography on immobilized amylose (New England Biolabs) and collected from the non-binding flow-through fraction. MBP-C was then concentrated and purified by size exclusion chromatography on a 60 x 2.6 cm Superdex 200 (GE Healthcare) column equilibrated with 50 mM Tris-Cl pH 8.0, 100 mM NaCl. MBP-C was concentrated and frozen in aliquots at -80°C for future use.

$CuCl_2$ failed to oxidize MBP-O and instead the protein was cross-linked by reaction with 1,2-Bis(Maleimido)ethane (BMOE). The protein was dialyzed in 20mM Hepes pH 7, 0.1 M NaCl and diluted to 4 mg/mL. BMOE modification was accomplished by incubating the protein at room temperature and adding a ½ molar equivalent of BMOE (dissolved in DMSO) up to 10 times at half hour intervals. The cross-linking reaction was left to complete at 4°C overnight. MBP-O was then concentrated and purified on a 60 x 2.6 cm Superdex 200 (GE Healthcare) column equilibrated with 50 mM Tris-Cl pH 8.0, 100 mM NaCl. MBP-O95/171 was expressed, modified and purified in the same way as MBP-O. Following modification and purification, both proteins were concentrated and flash frozen at -80°C.

Aliquots of these frozen proteins were observed to be >99% pure by SDS-PAGE (appendix 1).

Analysis of Protein oxidation and Cross-linking

Oxidized MBP-C was analyzed by SDS-PAGE with samples prepared in a loading buffer lacking reducing agent. A mobility shift on non-reducing SDS-PAGE was seen, like that observed by Zhang et al., indicating disulfide formation [16]. Samples were additionally analyzed by SDS-PAGE using loading buffer without reducing agent, but containing 15 μM fluorescein maleimide (FM) and visualized by fluorescence on a UV table. This demonstrated the blocking of free sulfhydrils by a total loss of fluorescence labeling.

Analytical samples of MBP-O and MBP-O95/171 were removed at 30 minute intervals during BMOE cross-linking and further reaction in the sample was arrested by the addition of excess FM. An additional sample was collected following over-night incubation of the BMOE reaction. All BMOE reaction samples were analyzed by SDS-PAGE and the degree of FM labeling was visualized by fluorescence on a UV table. The blocking of free sulfhydryls was observed as a reduction in fluoresce in progressing time-point samples.

Mass spectrometry was performed on oxidized and modified proteins using an Applied Biosystems 4700 Proteomics Analyzer MALDI-TOF-TOF in linear mode. Prior to mass spectrometry all proteins were serially dialyzed against deionized water. The mass of the modified proteins was consistent with the covalent attachment of a single BMOE molecule. Note that when MBP-O was modified using

an excess concentration of BMOE, mass analysis indicated dual modification of the protein, with a separate BMOE linked to each cysteine.

Measurement of Maltose Binding by Intrinsic Tryptophan Fluorescence Quenching

Several tryptophan residues in wtMBP undergo significant changes in their local environments on maltose binding and MBP domain closure that, in aggregate, result in a partial quenching of fluorescence. The affinity of MBP mutants for maltose was therefore measured by intrinsic tryptophan fluorescence quenching. Fluorescence measurements of wtMBP, MBP-C and MBP-O were taken with a Horiba-Jobin Yvon Florolog-3 spectrofluorimeter. Proteins were diluted into 50 mM Tris-Cl pH 8.0, 100 mM KCl, 10 mM $MgCl_2$ and excited at 280 nm. Fluorescence emission was measured at 347nm. Maltose was added with rapid stirring at 2-minute intervals and the decrease in fluorescence caused by maltose binding was recorded as a percentage of initial fluorescence [18]. K_D values for wtMBP and MBP-O were derived using GraphPad Prism version 4.0b to fit data by non-linear regression to a Michaelis-Menten curve.

Small Angle X-ray Scattering Analysis of Binding Protein Mutants

Protein samples were thawed and aggregate was removed by size exclusion chromatography on a 60 x 2.6cm Superdex 200 (GE Healthcare) column equilibrated with 20 mM Tris-Cl pH 7, 100 mM NaCl, 4 % glycerol, 1 μM sodium azide. Small angle x-ray scattering (SAXS) was performed at the BioCAT beam line of the Argonne national labs Advanced Photon Source. Data collection and

processing were performed as previously described [12], and the radius of gyration was calculated with the program GNOM [19].

Preparation of Proteoliposomes and Detergent Solubilized Transporter

Expression of $MalFGK_2$

$MalFGK_2$ was expressed in an AD126 background co-transformed with plasmids pFG_{23} and pKJ [20]. The transmembrane subunits MalF and MalG were expressed from plasmid pFG_{23} while MalK, with a C terminal hexahistidine tag, was expressed from plasmid pKJ [20]. A single colony was picked and grown for 6 hours in 5mL LB media as a starter culture under the selection of 100 µg/mL ampicillin (selective for pFG_{23}), 50 µg/mL chloramphenicol (selective for pKJ), and 50 µg/mL kanamycin (selective for a LacIq Tn5 transposon in AD126). The starter culture was used to inoculate fresh 2xYT media at a dilution of 1:1,000,000 with the same antibiotic selection. These cultures were grown to an OD_{600} of 0.4, induced with 10µg/mL IPTG and grown for 8 hours at 27°C. Cells were harvested by centrifugation, re-suspended in 20mM Hepes pH 7, 100mM NaCl, 5% Glycerol and flash frozen in liquid nitrogen for storage at -80°C.

Preparation of Membranes

Frozen cells were thawed, augmented by the addition of 1µM PMSF and lysed by 2 passes through a French pressure cell at 20,000x p.s.i. Cell debris was pelleted by centrifugation at 10,000 g for 30 minutes. Cell membranes were then pelleted by ultracentrifugation at 100,000 g for 1 hour. Membranes were resuspended and washed twice in 20mM Hepes pH 7.0, 5mM $MgCl_2$, 200mM sucrose, then

resuspended a final time in 20mM Tris-Cl, pH 7.5, 5mM $MgCl_2$, 25 mM KCl, flash frozen and stored at -80°C for future use.

Solubilization of Membrane Proteins and Proteoliposome Reconstitution

Thawed membranes were pelleted at 100,000 g for 1 hour and re-suspended at 5 mg/mL in 50 mM Tris-Cl pH 7.0, 10 mM $MgCl_2$, 1.0 % dodecyl-maltoside. This solution was incubated on ice for 30 minutes while protein was solubilized. Insoluble material was removed by another centrifugation step at 100,000 g for 1 hour. Detergent solubilized $MalFGK_2$ was purified by nickel affinity chromatography on a Ni^{2+} charged, 30 mL, chelating Sepharose chromatography column equilibrated with 20mM Tris-Cl pH 7.0, 10mM MgCl2, 10% glycerol, 0.01% dodecyl-maltoside (Buffer A). The protein was washed with Buffer A and eluted in Buffer A with 250mM imidazole. The eluted protein was dialyzed over night against 20mM Tris-Cl pH 7.0, 10mM MgCl2, 10% glycerol, 0.01% dodecyl-maltoside to remove the imidazole. One half of this purified transporter solution was flash frozen as detergent solubilized transporter. The remaining protein was augmented with 1% B-octylglucoside, incubated for 30 minutes, then reconstituted into previously prepared lipsomes by dilution, as previously performed [12]. Liposomes were prepared by the Bangham method as previously described [12,21]. Reconstituted proteoliposomes, with incorporated $MalFGK_2$, were flash frozen and stored at -80°C for future use. The presence of MalF and MalK in the final preparations of proteoliposomes and detergent solubilized transporter was confirmed by SDS-Page and Coomassie stain (appendix 2).

Assay of ATPase Activity

ATPase assays were performed as previously described [12]. Briefly, proteoliposomes were added to a concentration of 0.1mg/mL in 342 µL of 50mM Tris-Cl pH 8.0, 100mM KCl, 10mM $MgCl_2$, in the presence or absence of maltose and purified binding protein. The reaction was started by the addition of 18µL of 80µM ATP in the same buffer. 60µL samples were removed at time 0, 5, 10, 15 and 20-minute time intervals and arrested with 30µL of 10% SDS solution. Once the reaction was complete, all samples were measured by the addition of 50µL of Molybdate color-reagent (1.6% Ammonium Molybdate, 5% Ferrous Sulfate-Heptahydrate, 2M Sulfuric Acid) and measurement at 740nM on a Varian Cary 100Bio UV-Vis spectrophotometer. Absorbance measurements were converted to phosphate concentrations using a Na_2PO_4 standard curve ranging from 0 to 1mM phosphate. Phosphate concentrations for each time point were analyzed by linear regression and normalized against the mass of $MalFGK_2$ used to obtain the rate of ATP hydrolysis.

4.3 Results

Expression of a Locked closed Maltose Binding Protein

MBP undergoes well-characterized domain rotations from 'open' to 'closed' on the binding of maltose, closing the maltose binding site and partially burying the substrate [5]. Previous studies suggest that both open and closed conformations, as well as dynamic domain rotations might play roles in the activation of the transporter by MBP [10,11,12,16]. However, analysis of the respective roles of closed and open MBP can be complicated by the flexibility of the protein and interchange between these two conformations. In principle it is possible to incorporate mutations into MBP to alter substrate binding or domain rotation [11,22]. Here a mutant form of MBP has been used, which is predicted to be perpetually in the closed conformation. This mutant enables study of the role of closed MBP, in transporter activation, in isolation from the open form and competing conformational changes. This protein enables us to observe the ability of the closed form of MBP to activate ATP hydrolysis.

A disulfide containing MBP mutant was reproduced from the studies of Zhang et al. [16]. The mutant was engineered with cysteine substitutions at positions G69 and S337 (Fig. 4.1). Crystal structures of wtMBP indicate that these mutations are near the maltose-binding cleft and are proximal in the maltose-bound closed conformation, with sulfur atoms 4.1 Å apart. However, in the open state the sulfur atoms are separated by 6.5 Å (Fig. 4.1). This separation is only compatible with a disulfide bond in the closed conformation, and should hold the protein in, or strongly favor, the closed conformation. The characterization and phenotype

Fig 4.1 MBP-C Cysteine Mutations.

The positions and spacing of MBP-C cysteines G69C and S337C are shown (yellow) modeled onto X-ray crystal structures of the open and closed conformations. The distances shown correspond to the separation of sulphur atoms in a hypothetical cystine. The maltose-binding site is shown as a yellow wedge, with bound maltose (green and red). PDB Code 2R6G[8], 1ANF[4]

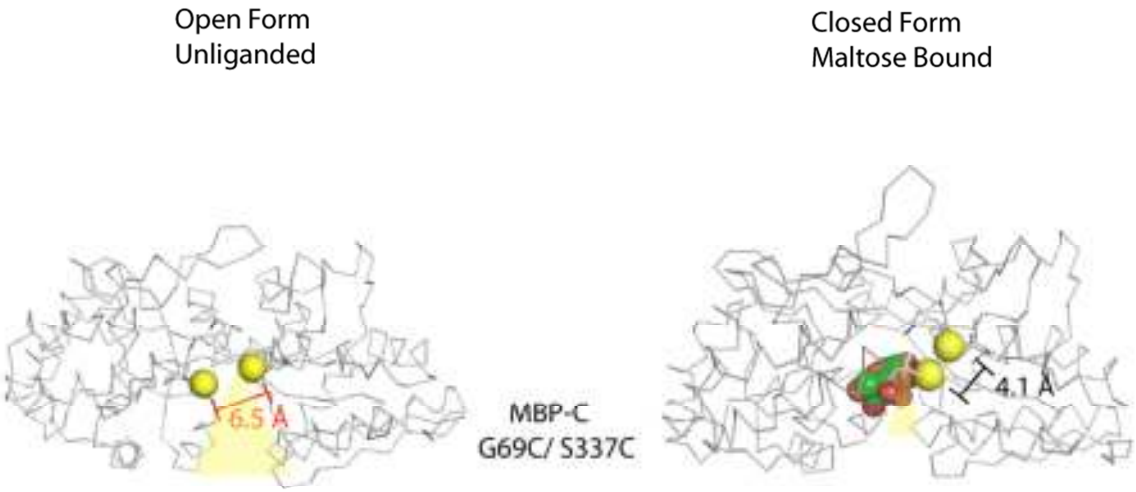
Open Form
Unliganded
Closed Form
Maltose Bound
6.5 Å
MBP-C
G69C/ S337C
4.1 Å

observed by Zhang *et al.* was consistent with this prediction [16]. In this study we refer to the disulfide constraining mutant MBP G69C/S337C as MBP-closed (MBP-C).

At high levels of expression *in-vivo*, MBP-C is known to inhibit maltose transport in a dominant negative manner. This phenotype is reversed by reducing reagent, which indicates that it is caused by the disulfide bond [16]. Inhibition is likely a result of competition between MBP-C and wtMBP for binding sites on the maltose transporter. Although its dominant negative phenotype indicates that MBP-C cannot support maltose transport, the degree to which it can induce or inhibit ATP hydrolysis is not known. For that reason MBP-C was cloned, purified and oxidized in the presence of maltose.

ATPase stimulation by MBP-C in proteoliposomes

Wild-type maltose transporter ($MalFGK_2$) was purified and reconstituted into proteoliposomes (PLS) made from *E. coli* phospholipids. Proteoliposomes form an environment for $MalFGK_2$ similar to the native membrane, but are ideal for *in vitro* experimentation and have been widely used for this reason [23,24]. The successful incorporation of the transporter into finished proteoliposomes was confirmed by SDS-Page and Coomassie stain (appendix 2).

With MBP-C prepared and oxidized we examined its ability to activate the maltose transporter. MBP-C was incubated at 37°C with PLS containing $MalFGK_2$ and the resulting level of ATP hydrolysis was measured. Purified $MalFGK_2$ displays a low level of basal ATPase in liposomes. As previously reported, in the absence of

maltose wtMBP activates a small level of ATPase above this background activity. When wtMBP is added with saturating maltose a large increase in activity is seen, which is dependent on binding protein concentration (Fig 4.2A). MBP-C was observed to activate the transporter to a significantly higher level than wtMBP, but far less than the fully activated system with wtMBP-maltose (Fig. 4.2B). The addition of maltose had no effect on the level of ATPase stimulus by MBP-C, although the rate was increased by the addition of maltose and DTT (data not shown).

Given its dominant negative effects on maltose transport *in vivo*, we were surprised by the ability of MBP-C to stimulate ATPase activity. Further, MBP-C does not support growth on minimal maltose, which indicates that it cannot support significant maltose transport, but we observed that it can activate more than 25% of the maximal ATPase rate [16](Fig. 4.2). Given these unexpected results I explored the ability of MBP-C to stimulate detergent solubilized $MalFGK_2$.

ATPase stimulation of detergent uncoupled $MalFGK_2$ by MBP-C and wtMBP

The maltose transporter is most commonly studied in proteoliposomes because of the similarity of this system to the transporter's cellular environment. When extracted from the membrane and stabilized in solution by a mild detergent the transporter acquires a very high basal rate of ATP hydrolysis, independent of the presence of MBP [15,25]. This unregulated phenotype is reversible if the transporter is reconstituted into a membrane. This suggests that important features

Fig 4.2 ATPase Stimulus by MBP-C in Proteoliposomes.

Purified $MalFGK_2$ was reconstituted into proteoliposomes and incubated at 37°C with (A.) wtMBP, wtMBP with maltose (5mM) and (B.) MBP-C. The production of free phosphate was measured at 5-minute time intervals as described in Materials and Methods. The rate of ATP hydrolysis was calculated from these data using linear regression and a phosphate standard curve before being plotted for each binding protein concentration.

A.

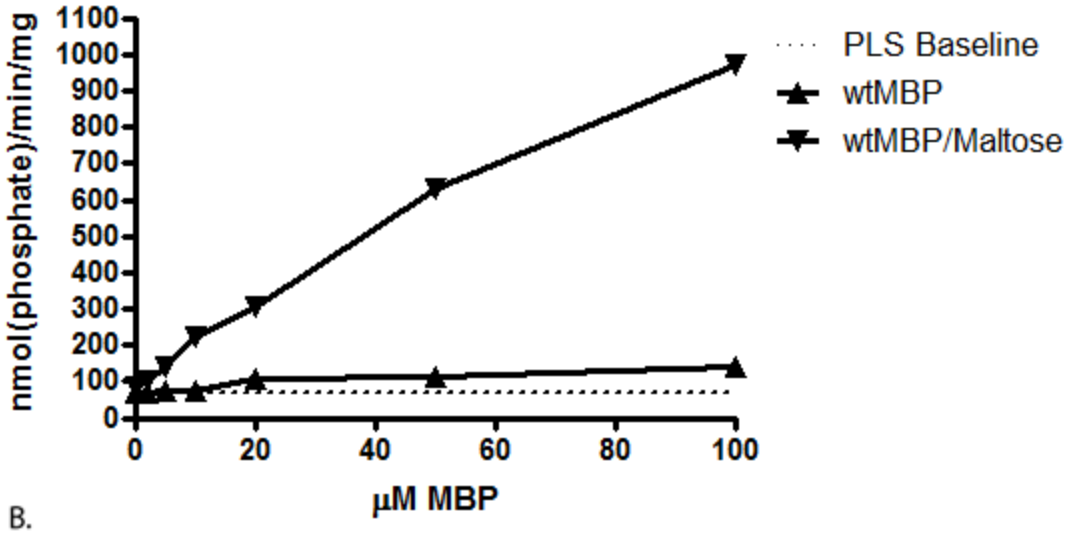
nmol(phosphate)/min/mg
1100
1000
900
800
700
600
500
400
300
200
100
0
0
20
40
60
80
100
µM MBP
PLS Baseline
wtMBP
wtMBP/Maltose

B.

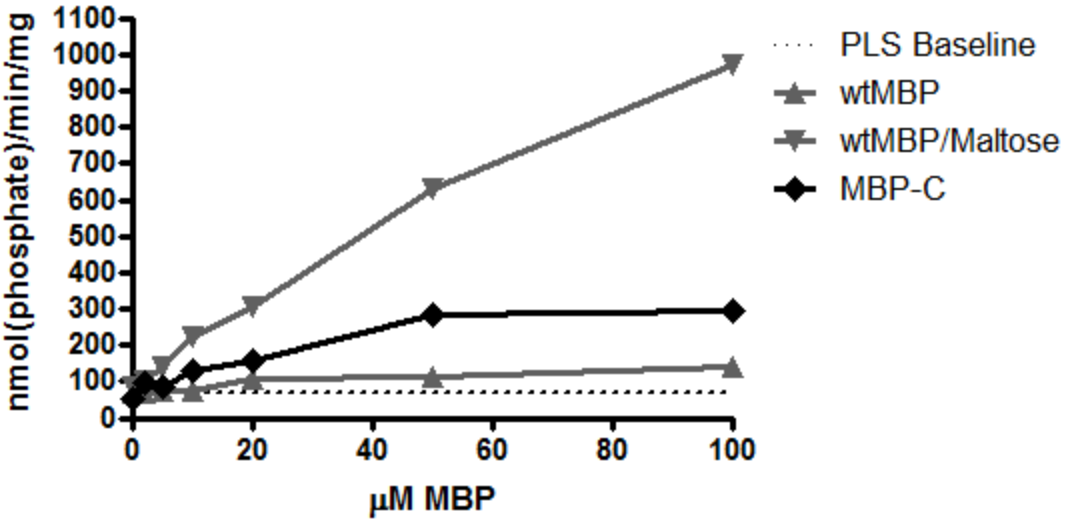
nmol(phosphate)/min/mg
1100
1000
900
800
700
600
500
400
300
200
100
0
0
20
40
60
80
100
µM MBP
PLS Baseline
wtMBP
wtMBP/Maltose
MBP-C

of the transporter catalytic cycle are dependent on membrane interactions, and altered by detergent solubilization. We hypothesized that disruption by detergent might differently impact the transporter conformations targeted by the closed and open forms of MBP. We therefore prepared $MalFGK_2$ as per our previous experiments, but rather than reconstituting the transporter into membranes, left it solubilized by the mild detergent n-dodecyl-β-D-maltoside (DDM).

We incubated purified wtMBP and MBP-C with the detergent stabilized transporter at 37°C and measured ATP hydrolysis as previously described. As reported elsewhere the transporter shows a much higher level of basal unregulated activity in the detergent soluble phase than in PLS and can be further stimulated by the addition of MBP and maltose (Fig. 4.3A) [15,25]. The addition of MBP-C resulted in a much smaller activation of ATP hydrolysis than wtMBP-maltose (Fig. 4.3B). Closed conformation MBP is therefore still relevant to transporter activation in detergent, although MBP-C stimulates a smaller fold-wise increase in activity over the basal rate because of the higher basal activity of the solubilized transporter. This suggests that the transporter conformation normally stabilized or complemented by closed MBP has been rendered less relevant in the detergent uncoupled system, although it is not removed from the catalytic cycle.

This low-level activation in detergent by MBP-C is far more intriguing when contrasted with the surprising activation by unliganded wtMBP. Unlike in PLS, where a low level of ATP hydrolysis is observed, unliganded wtMBP activates a high level of hydrolysis from DDM solubilized transporter; more than MBP-C or wtMBP-

Fig 4.3 ATPase Stimulus by MBP-C of Detergent Solubilized MalFGK$_2$.
Purified MalFGK$_2$ was extracted from the cell membrane and stabilized in 50 mM Tris pH7, 4mM MgCl2, 5% glycerol, 0.01% dodecyl-maltoside [15]. The resulting uncoupled transporter was incubated at 37°C with (A.) wtMBP, wtMBP with maltose(5mM) and (B.) MBP-C. The resulting rate of ATP hydrolysis was calculated as described in Fig. 4.2.

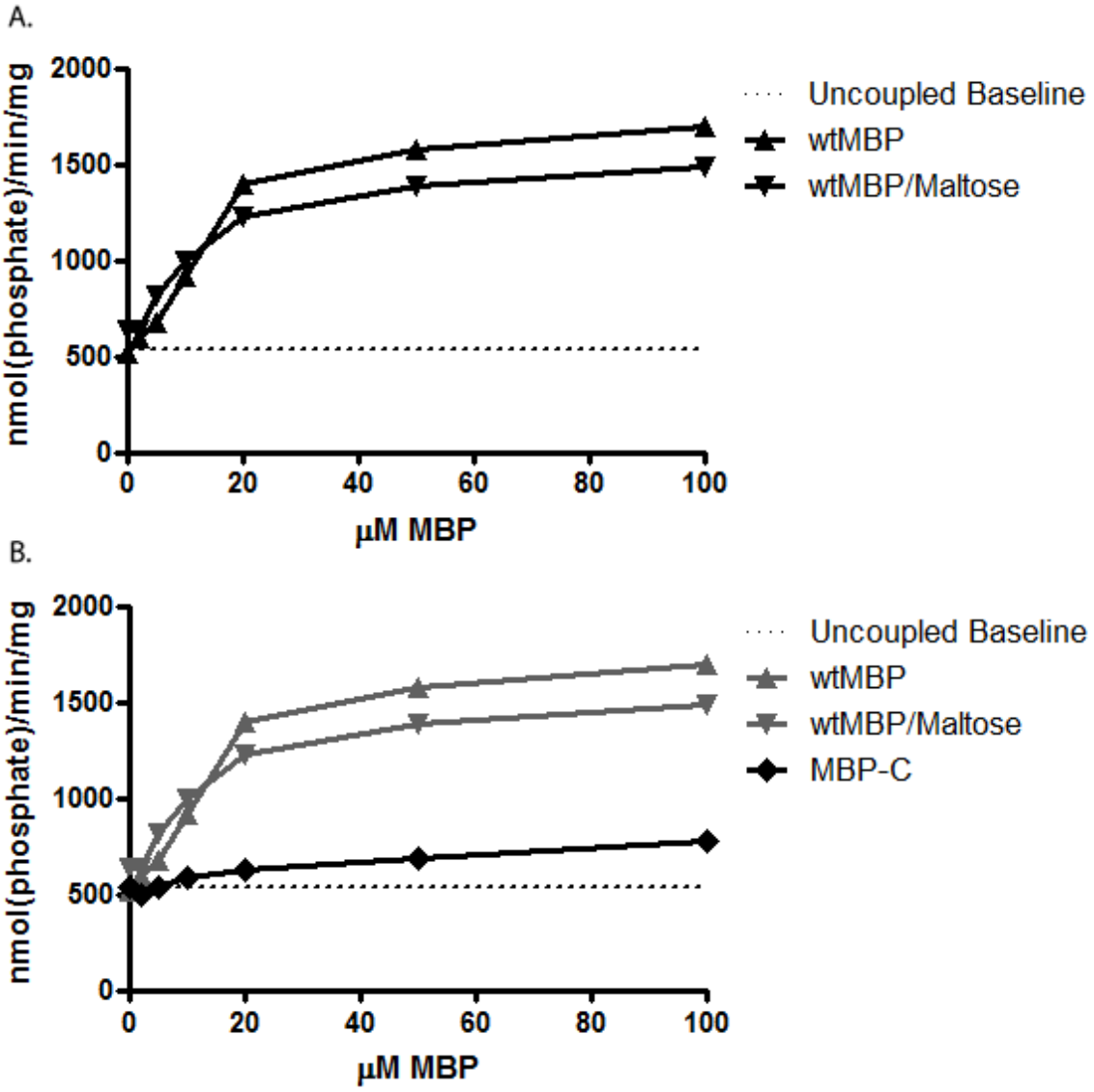
A.
nmol(phosphate)/min/mg
2000
1500
1000
500
0
0
20
40
60
80
100
µM MBP
Uncoupled Baseline
wtMBP
wtMBP/Maltose
B.
nmol(phosphate)/min/mg
2000
1500
1000
500
0
0
20
40
60
80
100
µM MBP
Uncoupled Baseline
wtMBP
wtMBP/Maltose
MBP-C

maltose (Fig. 4.3A). This result may not have been previously reported because activation by apo-wtMBP was not thought to be informative, but shows that detergent solubilization has made the transporter more receptive to the open resting state of wtMBP.

Concerns that these data might be explained by an ability of DDM to mimic maltose proved unfounded as intrinsic tyrosine fluorescence showed no binding of DDM to wtMBP and ATPase experiments demonstrated that DDM did not increase the ability of wtMBP to activate ATPase in PLS (data not shown).

While in liposomes it appears the closed form of MBP, as represented by MBP-C, is more activating than open unliganded wtMBP, in the detergent solubilized system the relationship has reversed and wtMBP activates higher levels of ATPase than MBP-C.

Characterization of MBP-C

With such unexpected results observed in ATPase studies, it was necessary to better characterize how disulfide bond formation has altered the characteristics of MBP-C from the wild type. Due to the similar bond chemistries of amylose and maltodextrins, wtMBP shows substantial affinity for amylose and will bind to immobilized amylose affinity resin [26]. To characterize the effect of the inter-domain disulfide on the activity of MBP-C we performed amylose chromatography. Unlike wtMBP, oxidized MBP-C was not retained by amylose, however binding was restored by reduction with DTT. Further, we measured the intrinsic tryptophan fluorescence of MBP-C as it was titrated with maltose. Unlike wtMBP, MBP-C shows

Fig **4.4 Maltose Binding Measured by Intrinsic Fluorescence Quenching**

Intrinsic Tryptophan Fluorescence quenching by maltose was measured for wtMBP, MBP-C and MBP-O in a Horiba-Jobin-Yvion Fluorolog-3 fluorimeter [18]. Proteins were excited at 280nm, and fluorescence was measured at 347nm. For each protein: (A) The reduction in fluorescence is shown at increasing maltose. (B) The reduction in fluorescence is expressed as a percentage of initial fluorescence, with Michaelis-Menten saturation curve.

A.

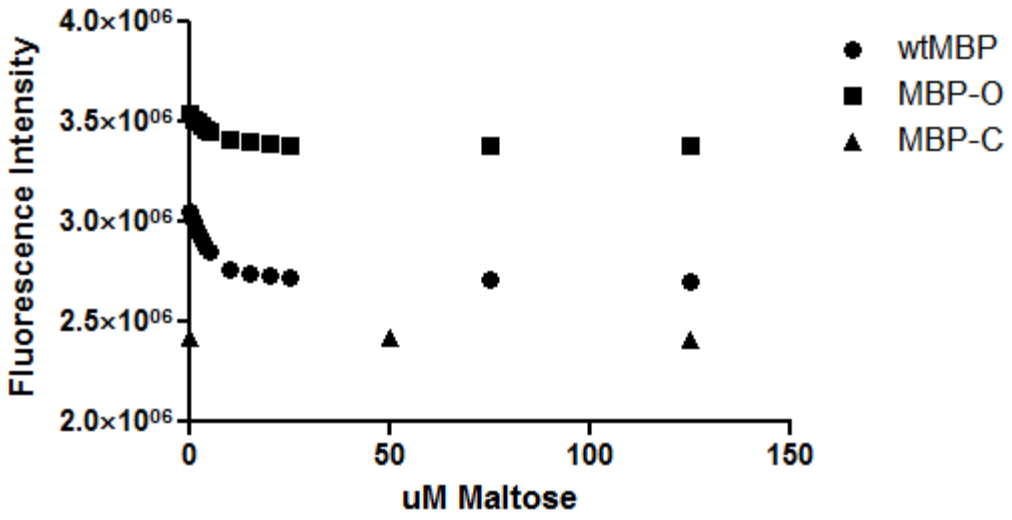
Fluorescence Intensity
4.0×10^06
3.5×10^06
3.0×10^06
2.5×10^06
2.0×10^06
0
50
100
150
uM Maltose
wtMBP
MBP-O
MBP-C

B.

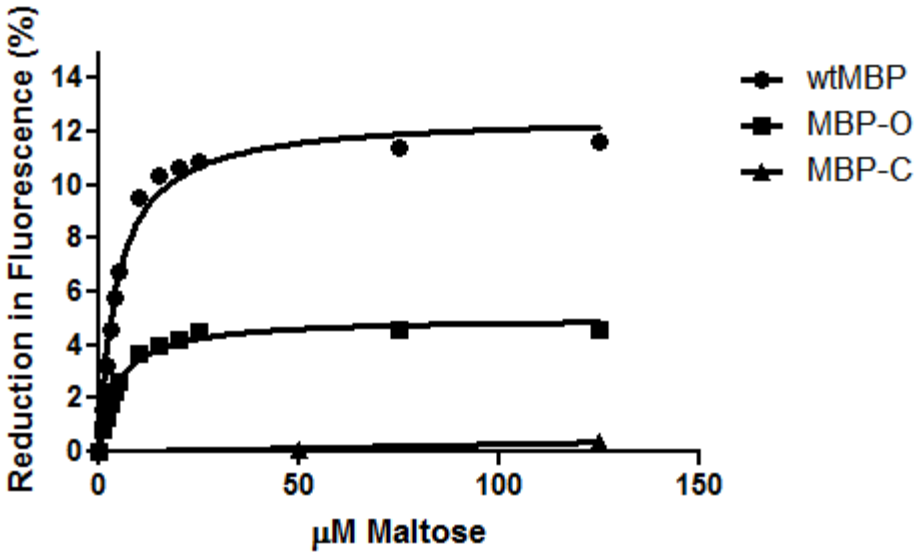
Reduction in Fluorescence (%)
14
12
10
8
6
4
2
0
0
50
100
150
µM Maltose
wtMBP
MBP-O
MBP-C

little change in fluorescence with the addition of maltose (Fig. 4.4). Together these results suggest that MBP-C has no capacity to bind additional substrate.

Samples of oxidized MBP-C were further analyzed by Small Angle X-ray scattering to observe the in-solution conformational changes brought on by the addition of maltose. This analysis showed a radius of gyration in the absence of maltose of 21.8 Å. This is consistent to the measured radius of maltose saturated wtMBP, 21.8 Å, suggesting that MBP-C is in the closed conformation. The addition of saturating maltose (5 mM) resulted in a virtually unchanged radius of gyration of 21.9 Å (Table 4.4). This was consistent with intensity difference curves of the protein's total SAXS spectrum with and without maltose, which demonstrate minimal change in the spectra of MBP-C on the addition of maltose (Fig. 4.5).

These results indicate a significant change in the binding characteristics of MBP-C from wild type and suggest that our reproduction of the disulfide locked MBP mutant of Zhang et al was successful. The protein is perpetually locked in the closed conformation, likely with a permanently resident molecule of maltose occupying its binding site [16]. The increased ATPase stimulated in PLS, as compared to wtMBP is therefore a result of the closed conformation in isolation, while the reduced ATPase observed in DDM likewise results from the inability of MBP-C to open.

Design of a Stabilized-Open Maltose Binding Protein

Having seen that the closed conformation of MBP in isolation displays a markedly different ability to stimulate the transporter from the wild type protein,

Fig 4.5 Changes in SAXS Profile of MBP-C with Maltose

SAXS intensity curves are shown for MBP-wt and MBP-C overlaying the curves of the proteins with and without maltose (above). The difference curves of these profiles are shown, indicating the degree of change on the addition of maltose to wtMBP and MBP-C (below).

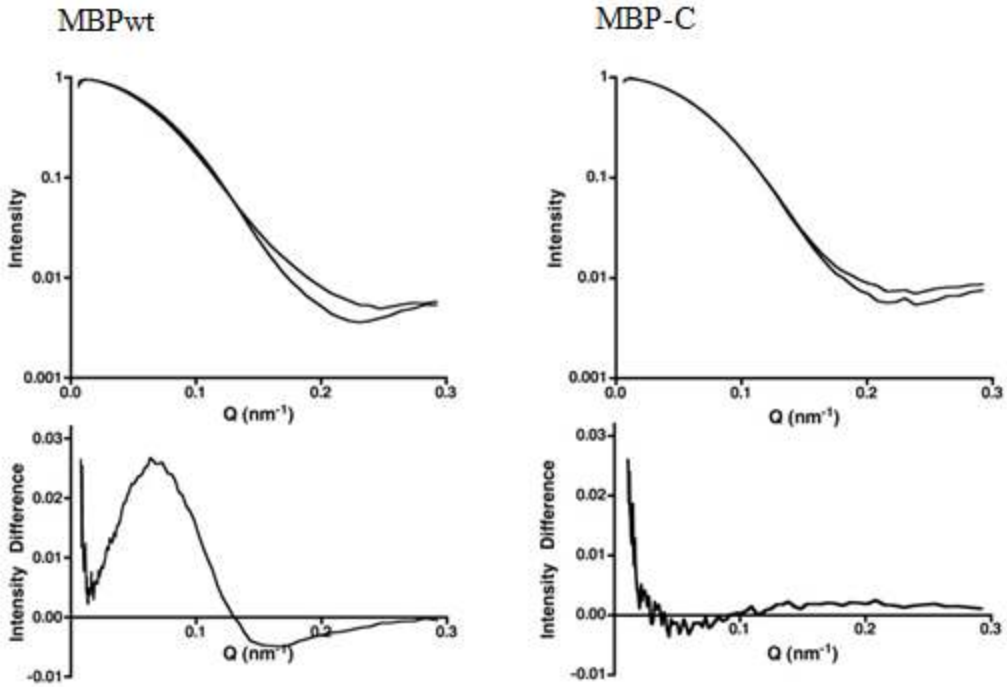
MBPwt
MBP-C
Intensity
Q (nm⁻¹)
Intensity Difference
1
0.1
0.01
0.001
0.0
0.1
0.2
0.3
0.03
0.02
0.00
-0.01

Table 4.2 Radii of Gyration of MBP-C from GNOM Analysis

Protein	Ligand	Radius of Gyration (Å)
wtMBP	-	22.8 ± 0.02
wtMBP	5mM Maltose	21.8 ± 0.03
MBPC	-	21.8 ± 0.04
MBPC	5mM Maltose	21.9 ± 0.03

the investigation was continued by attempting to isolate and stabilize the open form of MBP. The tendency of MBP to adopt a closed conformation is normally resisted, and largely prevented in the absence of maltose, by a region of MBP known as the balancing interface, which comprises a series of hydrophobic contacts between the two domains [11]. When MBP binds maltose these contacts are abolished by domain rotations, such that their formation influences the equilibrium between open and closed MBP (Fig. 4.6A). Disrupting favorable interactions in the balancing interface is known to shift MBP towards a closed conformation [11]. It was theorized that stabilization of the balancing interface would disfavor the closed conformation, potentially holding MBP in the open state. An open stabilized MBP would enable examination of the interactions between the open conformation and the transporter without the complicating influence of a conformational equilibrium between open to closed MBP.

We used the available X-ray crystal structures of MBP [4,5,8] to incorporate a potential disulfide bridge that spans the balancing interface to link the N- and C-terminal domains. Cysteines were introduced at positions G101C and G174C (Fig. 4.6A). Neither position is predicted to make contacts with the transporter. These positions were selected such that a disulfide bond between them would be compatible with the open conformation seen in the transporter ATPase catalytic state but not with the closed conformation. The sulfur atoms of the mutated residues are 4.0 Å apart in the open form of the protein but are separated by 14.8 Å in the closed maltose bound state. A disulfide bond between them should therefore

Fig 4.6 MBP-O Cysteine Mutations

Cysteine mutations (yellow) are shown mapped to X-ray crystal structures of open and closed MBP. The maltose-binding site is shown as a yellow wedge, with bound maltose (green and red). The hydrophobic balancing interface is highlighted in blue. (A.) MBP-O mutations G101C and G174C are shown. (B.) MBP-O95/171 mutations D95C and Y171C are shown. PDB Reference 2R6G [8], 1ANF [4]

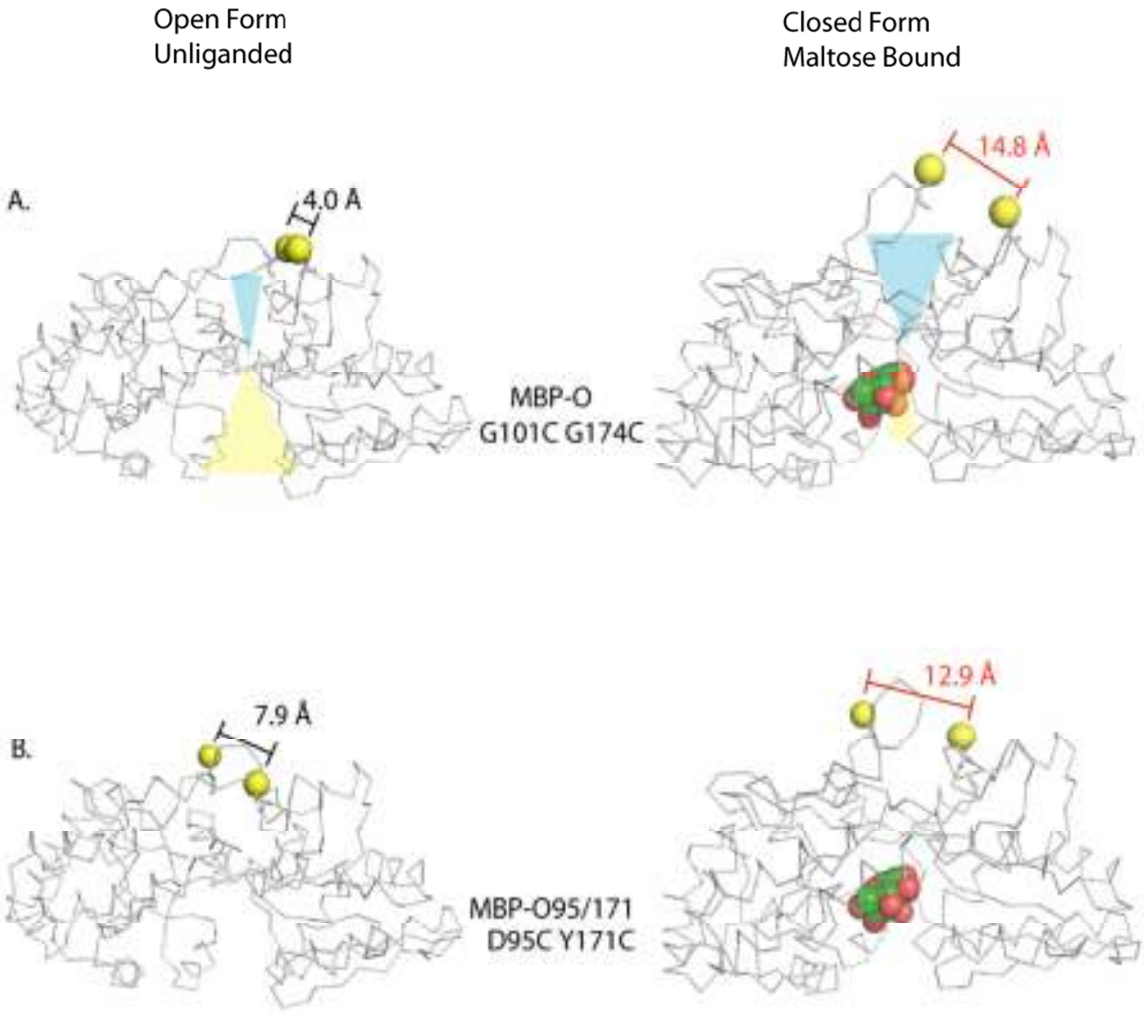
Open Form
Unliganded
Closed Form
Maltose Bound
A.
4.0 Å
14.8 Å
MBP-O
G101C G174C
B.
7.9 Å
12.9 Å
MBP-O95/171
D95C Y171C

prevent the protein from adopting a closed conformation by destabilizing that state through bond length constraints. This mutant binding protein is referred to as MBP-open (MBP-O) in reference to its predicted favoring of the open state.

When MBP-O was purified it proved resistant to direct oxidation by $CuCl_2$. We instead chose to cross-link the mutant by modification with the bi-functional cysteine-reactive linker Bis(maleimido)ethane (BMOE). BMOE has an effective length of 8.0 Å which could allow MBP-O greater conformational flexibility than a direct disulfide bond between residues 101 and 174. We therefore designed and purified an alternative mutant with mutations D95C and Y171C. This mutant, referred to as MBP-O95/171 has more widely spaced cysteines in the open state and should therefore be more constrained by BMOE (Fig. 4.6B). These mutations were also not predicted to contact the transporter.

When purified MBP-O and MBP-O95/171 were reacted with BMOE, samples were taken of the reaction at successive time points and reacted with excess fluorescene maleimide. SDS-PAGE and fluorescence imaging revealed that the reaction reduced the availability of free cysteines to be labeled, with no detectable labeling in the final preparation (Fig. 4.7). This indicated that all cysteine residues were modified by BMOE. The BMOE-modified MBP-O and MBP-O95/171 were next analyzed by Matrix Assisted Time of Flight (MALDI-TOF) mass spectrometry to confirm its modification (Table 4.3). The molecular masses of both proteins indicated the covalent attachment of a single BMOE molecule. Further, examination of the mass spectra of each protein indicated a single homogenous peak, without detectable contamination from unmodified protein species, or protein cross-linked

Fig 4.7 Fluorescene Labeling of BMOE Cross-Linked MBP-O.

BMOE was repeatedly added to reduced MBP-O in a 1:2 molar ratio at 30 minute time intervals. Samples were removed at 30 minute intervals, arrested with excess Fluorescene maleimide (FM) and fluorescence was measured after SDS-PAGE. Lane 1: Reduced MBP-O fully labeled with FM, Lanes 2-10: time course of cross linking reaction (minutes), Lane 11: Over-night incubation of reaction and final product.

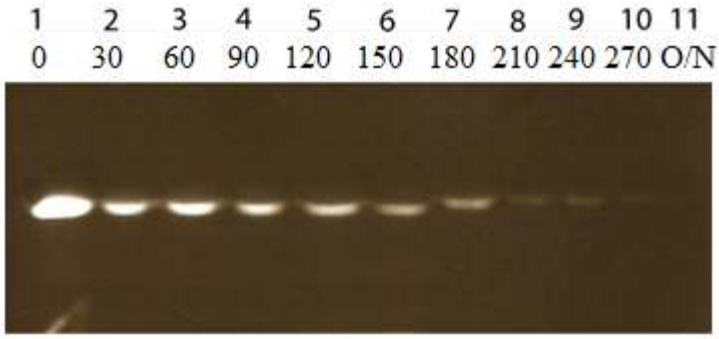
1 2 3 4 5 6 7 8 9 10 11
0 30 60 90 120 150 180 210 240 270 O/N

Table 4.3 MALDI-TOF Analysis of Prepared Binding Proteins

MBP mutant	Modification	Mass(Da)	
		Predicted	Observed
wtMBP	No mod.	40835.4	40810.8
MBP-O	No mod.	40927.6	40927.2
MBP-O	2 BMOE	41368.0	41411.4
MBP-O*	1 BMOE	41147.8	41151.5
MBP-O95/171	No mod.	40763.4	40799.3
MBP-O95/171*	1 BMOE	40983.6	40956.8

*Protein sample used for further studies

Fig 4.8 MALDI-TOF Profile of Cross-Linked MBP-O and MBP-O95/171.

Mass spectra were collected of the purified and crosslinked MBP-O and MBP-O95/171 binding proteins in Linear Mode on a MALDI-TOF mass spectrometer. The dominant peaks are circled for MBP-O and MBP-O95/171.

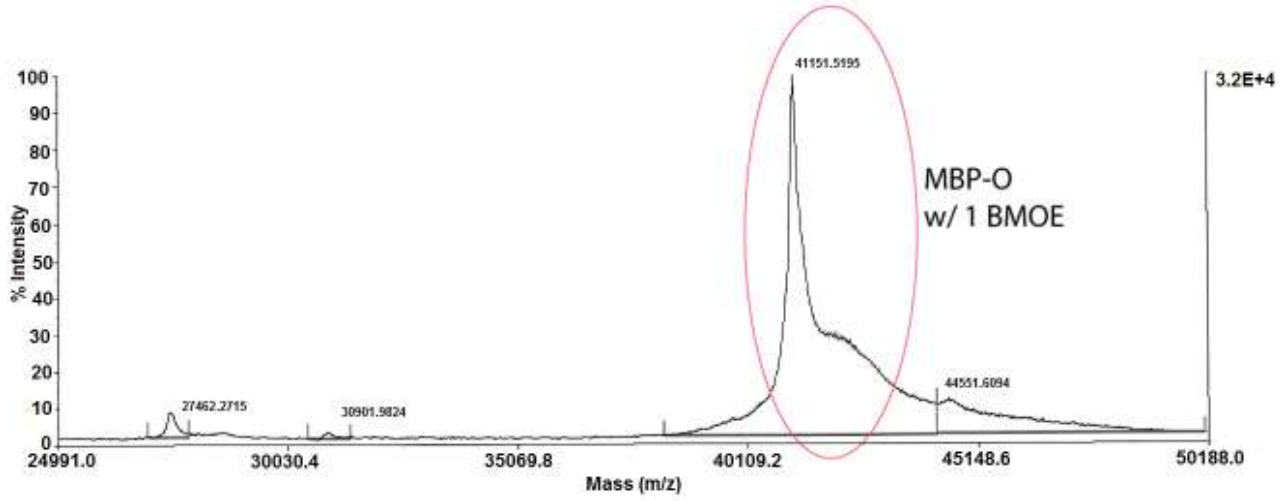
41151.5195
3.2E+4
MBP-O
w/ 1 BMOE
% Intensity
27462.2715
30901.5824
44551.6094
24991.0
30030.4
35069.8
40109.2
45148.6
50188.0
Mass (m/z)

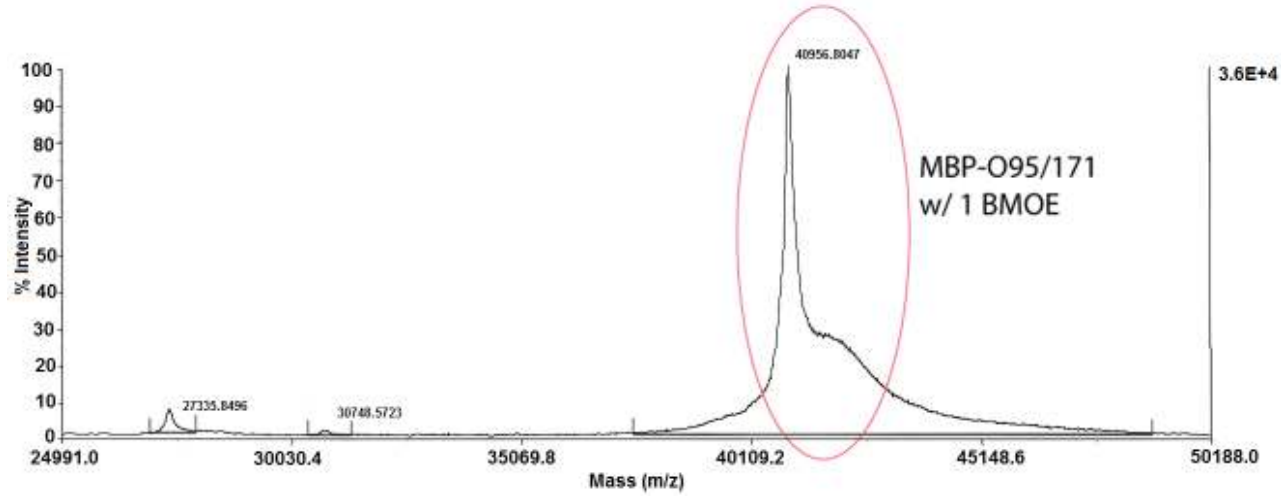
40956.8047
3.6E+4
MBP-O95/171
w/ 1 BMOE
% Intensity
27335.8496
30748.5723
24991.0
30030.4
35069.8
40109.2
45148.6
50188.0
Mass (m/z)

to two BMOE molecules (Fig. 4.8). With both mutants demonstrating the blocking of two cysteines by a single molecule of BMOE it was concluded that the protein had been correctly modified, with a single BMOE molecule spanning two cysteines across the balancing interface.

Stimulus of the wild-type maltose transporter by BMOE modified mutants

Surprisingly, when MBP-O was added to PLS containing $MalFGK_2$ a large degree of ATPase activation was seen, comparable to full activation by MBP-maltose (Fig. 4.9A). The addition of maltose did not significantly change this activation, even at 10 mM . This activity was also seen with MBP-O95/171, indicating that the effect is not a unique feature of the mutations in MBP-O (Fig. 4.9B). This high degree of activation by both MBP-O mutants was highly unexpected, as the conformation of MBP-O is predicted to closely mimic that of wtMBP, which activates very little ATPase in the absence of maltose. In both mutants a BMOE cross-link across the MBP balancing interface has induced a high level of uncoupled ATPase in the absence of maltose, although the mechanism underlying this effect is unclear.

Both MBP-O mutants were also added to detergent solubilized $MalFGK_2$ to test whether the maltose indifferent phenotype would be retained. In the DDM solubilized system the addition of MBP-O and MBP-O95/171 stimulates high rates of ATP hydrolysis, comparable to that of wtMBP and wtMBP-maltose (Fig. 4.10AB). MBP-O activates a high level of ATP hydrolysis that is not affected the presence of maltose (Fig. 4.10A). Whereas MBP-O95/171 stimulates high activity at lower concentrations (2-50μM), activation appears to drop as the transporter becomes

Fig 4.9 ATPase Stimulus by MBP-O in Proteoliposomes.

Purified $MalFGK_2$ was reconstituted into Proteoliposomes and incubated at 37°C with (A.) MBP-O, and MBP-O with maltose and (B.) MBP-O95/171. The rate of ATP hydrolysis was calculated as described in Fig. 4.2.

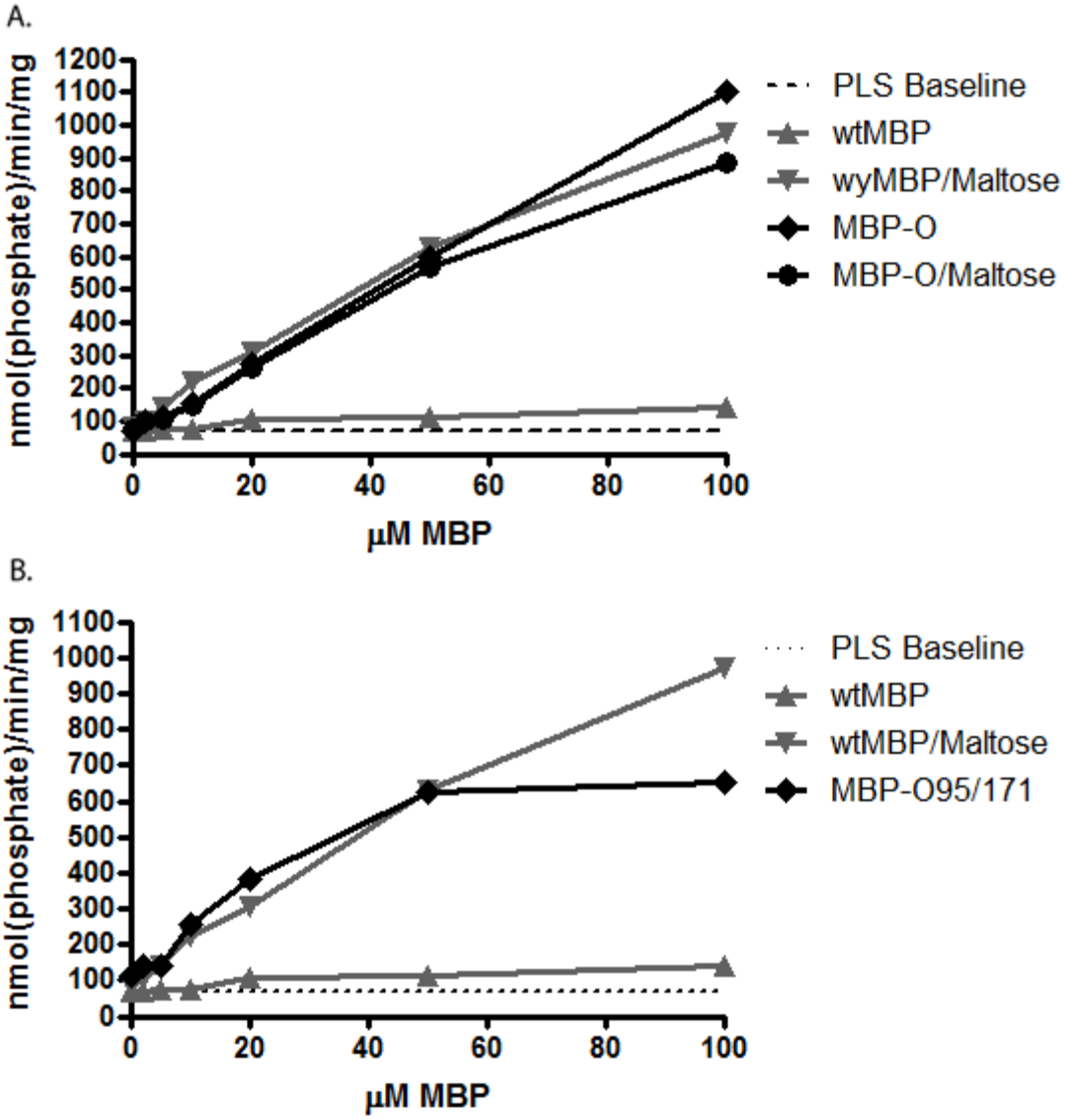
A.
nmol(phosphate)/min/mg
1200
1100
1000
900
800
700
600
500
400
300
200
100
0
0
20
40
60
80
100
µM MBP
PLS Baseline
wtMBP
wyMBP/Maltose
MBP-O
MBP-O/Maltose
B.
nmol(phosphate)/min/mg
1100
1000
900
800
700
600
500
400
300
200
100
0
0
20
40
60
80
100
µM MBP
PLS Baseline
wtMBP
wtMBP/Maltose
MBP-O95/171

Fig 4.10 ATPase Stimulus by MBP-O of Detergent Stabilized MalFGK$_2$.
Purified MalFGK$_2$ was extracted from the cell membrane and solubilized in 50 mM Tris pH7, 4mM MgCl2, 5% glycerol, 0.01% dodecyl-maltoside [15]. The resulting uncoupled transporter was incubated at 37°C with A. wtMBP, wtMBP with maltose(5mM) and B. MBP-O95/171. The resulting rate of ATP hydrolysis was calculated as described in Fig. 4.2.

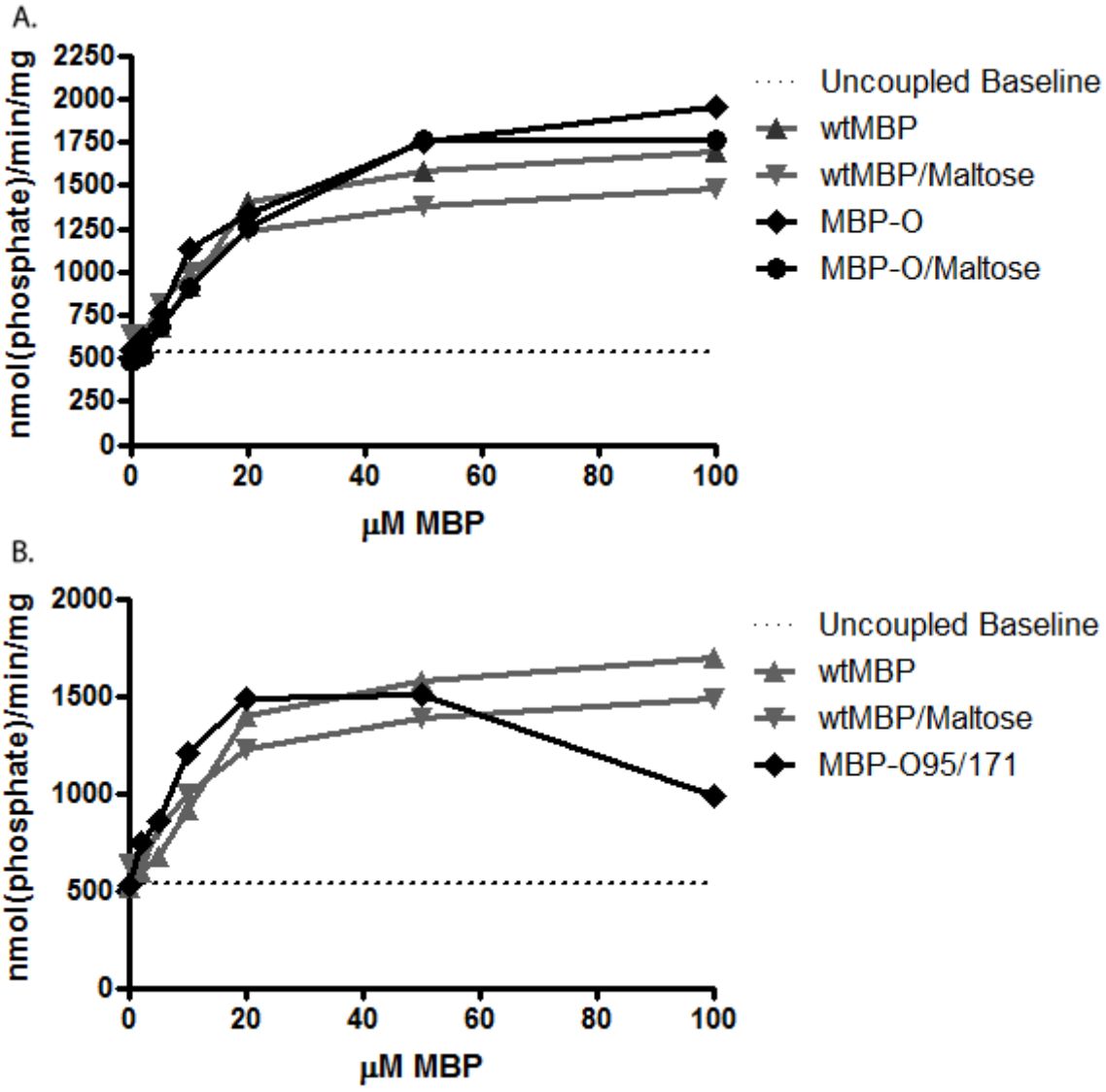
A.
nmol(phosphate)/min/mg
2250
2000
1750
1500
1250
1000
750
500
250
0
0
20
40
60
80
100
µM MBP
Uncoupled Baseline
wtMBP
wtMBP/Maltose
MBP-O
MBP-O/Maltose
B.
nmol(phosphate)/min/mg
2000
1500
1000
500
0
0
20
40
60
80
100
µM MBP
Uncoupled Baseline
wtMBP
wtMBP/Maltose
MBP-O95/171

saturated with binding protein. This difference from wtMBP and MBP-O may be a result of reduced conformational flexibility in MBP-O95/171.

Characterization of MBP-O mutants

The high levels of constitutive ATPase activity seen on the addition of either MBP-O mutant to wild type $MalFGK_2$, were very unusual, so the conformational mechanics of the mutants were investigated to better interpret their phenotype. Modified MBP-O and MBP-O95/171 were both retained on the resin during amylose chromatography, which indicated maltose binding. Analysis of intrinsic tryptophan fluorescence quenching showed that MBP-O has a wild-type affinity for maltose, with a K_D (concentration at half maximal binding) of 4.5 ±0.4 μM, nearly identical to the wild-type K_D of 4.4 ±0.5 μM (Fig. 4.4). These results indicate that BMOE modification was not sufficient to abrogate maltose binding.

SAXS analysis was performed on both mutants to observe conformational changes in the proteins on maltose binding. The program GNOM was used to derive the radius of gyration (Rg) of the proteins. In the relaxed state without maltose, MBP-O displays an Rg of 23.0 Å, similar to the 22.8 Å Rg of wtMBP. MBP-O95/171 adopts a more closed conformation, with an Rg of 22.5 Å (Table 4.4). To test whether this change was a result of the crosslink a sample of MBP-O95/171 was modified with N-ethylmaleimide (NEM) rather than BMOE. NEM covalently blocks each cysteine similar to BMOE modification, but each cysteine is modified by a separate molecule of NEM, so the two sites are not cross-linked in a way that constrains conformational changes. MBP-O95/171 modified in this way

Table 4.4 Radii of Gyration of MBP-O and MBP-O95/171 from GNOM Analysis

Protein	Modification	Ligand	Radius of Gyration (Å)
wtMBP	-	-	22.8 ± 0.02
wtMBP	-	5mM Maltose	21.8 ± 0.03
MBPO	BMOE	-	23.0 *
MBPO	BMOE	5mM Maltose	22.3 **
MBPO95/171	BMOE	-	22.5 ± 0.04
MBPO95/171	BMOE	10mM Maltose	21.9 ± 0.04
MBPO95/171	NEM		23.3 ± 0.05
MBPO95/171	NEM	5mM Maltose	22.1 ± .03

* Average of 4 measurements
** Average of 5 measurements

demonstrated a more open conformation with an Rg of 23.3, indicating that the reduced Rg seen with BMOE modified MBP-O95/171 is a result of the crosslink between mutant cysteines (Table 4.4).

On the addition of maltose both mutant proteins show a reduction in Rg that indicates a conformational change towards a more compact, and likely more closed, structure. Both mutants display a smaller reduction in Rg than wtMBP. However, because MBP-O95/171 is more compact in the relaxed state this change results in a more compact maltose-bound conformation than wtMBP. The NEM modified sample of MBP-O95/171 demonstrated a reduction in Rg similar to wtMBP (Table 4.4).

These data indicate that BMOE modification has not constrained the mutant proteins to an open conformation or prevented maltose binding. These findings are corroborated by a broader analysis of the full SAXS spectra of the mutants. A substantial shift is seen in the scattering spectra of each protein with and without maltose, as indicated by difference curves of those spectra (Figure 4.11). BMOE modified mutants however, display a lesser shift, which suggests some constraint on conformational changes.

This analysis indicates that while both mutant proteins are modified with BMOE, they are still able to bind maltose and are not restricted solely to the open conformation. However, despite the modest observable influence BMOE has on MBP conformational changes, it has resulted in rapid constitutive ATPase activation of $MalFGK_2$.

Fig 4.11 Changes in SAXS Profile of MBP-O and MBP-O95/171 with Maltose

SAXS intensity curves are shown for MBP-wt, MBP-O, MBP-O95/171 and MBP-O95/171 modified instead with NEM. The curves of the proteins with and without maltose are overlaid (above). The difference curves of these profiles are shown, indicating the degree of change on the addition of maltose to each protein (below).

MBPwt

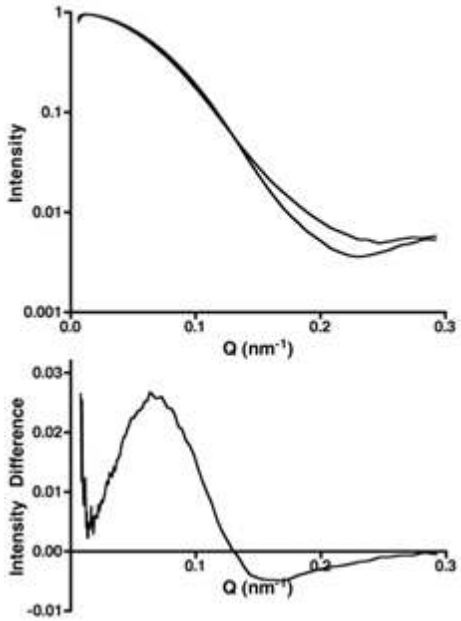

MBP-O
BMOE modified

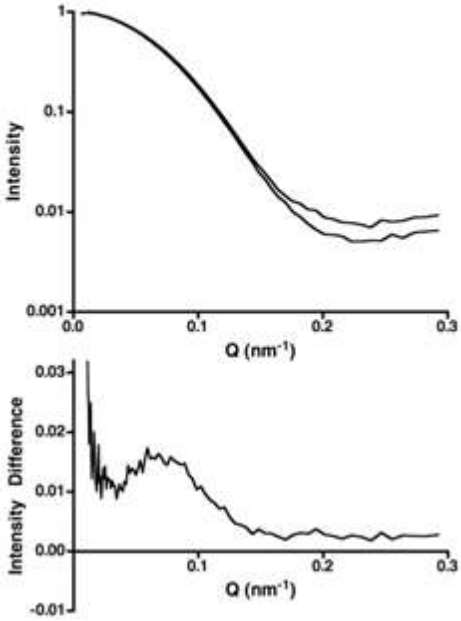

MBP-O95/171
BMOE Modified

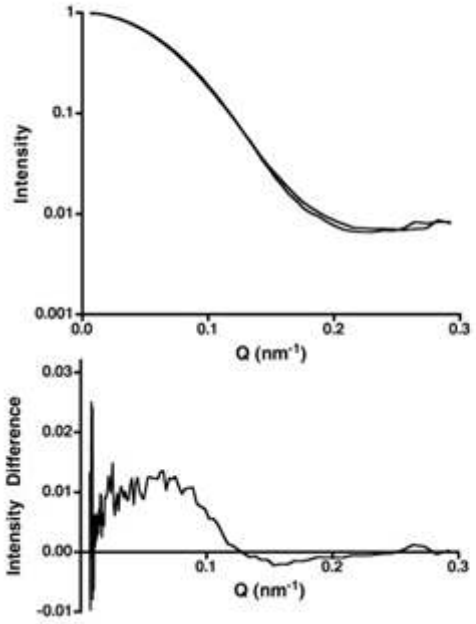

MBO-O95/171
NEM Modified

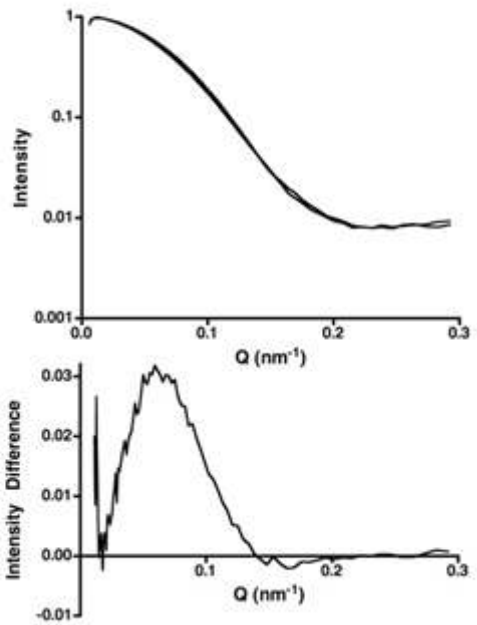

4.4 Discussion

In this study I have observed that each of three conformationally stabilized MBP mutants, MBP-C, MBP-O and MBP-O95/171, are able to activate significant amounts of ATPase activity. Previous studies have demonstrated that both the open and closed forms of MBP interact with different conformations of the transporter [8,9,10,27]. Here it has been shown that both of these interactions promote ATP hydrolysis.

MBP-C adopts the closed conformation, even in a solution lacking maltose. The dominant negative phenotype observed by Zhang *et al* demonstrates that MBP-C does not open sufficiently to release maltose into the transporter, and therefore cannot promote transport [16]. This indicates that the protein is constrained to the closed state even when bound to $MalFGK_2$. Here we show that despite this limitation, the protein is significantly activating for ATPase. Concerns that the observed activation in proteolipsomes might be caused by undetected contamination from reduced MBP-C are refuted by the high level of activation observed. Further, the rate of ATPase is far in excess of the maximal rate stimulated by excess unliganded wtMBP. This activity is also not increased by the addition of maltose, unlike reduced MBP-C or wtMBP, which is not consistent with contamination.

The ability of MBP-C to activate the wild type transporter indicates that the closed form in isolation is sufficient to stimulate some ATPase activity. However activation by MBP-C displays a defect, as the rate of hydrolysis supported by MBP-C is considerably less than the maximal rate activated by wtMBP with maltose.

Previous work in this thesis has shown that the substrate does not play a direct role in ATPase activation, so the defect must arise from the inability of the binding protein to adopt the open conformation [17]. This is consistent with a model of maltose transport in which MBP domain opening is a significant step in the ATPase catalytic cycle. However, the large degree of stimulus by MBP-C, relative to the basal rate, indicates that the closed conformation of MBP is sufficient to partially complement the need for MBP. The closed conformation of the protein must therefore trigger the complex to progress into the catalytic cycle.

Note that these results complement previous findings in chapter 2 of this thesis that transient, or unstable, closed species of MBP do not activate ATPase [12:chapter2]. In that work, MBP was forced towards the closed conformation by mutations or deletions within the balancing interface. These mutations disfavored the open conformation of MBP but did not stabilize the closed state, whereas the closed form of MBP-C is highly stabilized by both a disulfide bond and captive molecule of maltose. The resulting mutants showed reduced ATPase stimulation in the presence of maltose, displaying a defect in activation consistent with our findings for MBP-C. However unlike MBP-C, these mutants did not become more activating for ATPase in the absence of maltose. Further, it was found that the ATPase stimulus observed from unliganded MBP-wt was not consistent with causation by transiently closed species of MBP. Taken together these results indicate that the closed conformation of MBP is only activating for ATPase when it is stabilized and energetically favorable and that these features must play a role in its mechanism of activation.

These results are consistent with a model of activity by which closed MBP selects for an otherwise transient conformation of the transporter by binding and stabilizing a high-energy intermediate. The closed form of MBP could mediate access to the ATPase catalytic state of the transporter by binding and stabilizing the pre-catalytic state; 'flattening' or lowering an unfavorable energetic barrier in the same way that enzyme accelerated reactions lower the activation energy by stabilizing disfavored chemical transition states [28,29]. Indeed, it is the precatalytic state of the transporter, intermediate between the cytoplasmic facing resting state and periplasmic facing catalytic state, which has been observed through X-ray crystallography and paramagnetic resonance imaging to bind closed MBP [9,30].

When $MalFGK_2$ was solubilized by a mild detergent, ATP hydrolysis was activated at a high rate by wtMBP, wtMBP with maltose, MBP-O and MBP-O95/171; all of the binding proteins capable of adopting the open conformation. MBP-C however, being unable to adopt the open state, stimulated significantly less ATPase. This result is particularly striking when contrasted with the behavior of unliganded wtMBP. ATPase activation by the two proteins is differently impacted by detergent solubilization of the transporter. While the ability of MBP-C to activate the transporter is reduced relative to background, wtMBP activates a far greater increase in ATPase in detergent than in proteoliposomes. This is strong evidence that the two proteins are activating the transporter through different mechanisms; targeting distinct conformations of the transporter which are differently disrupted by detergent solubilization.

In previous work it was shown that unliganded wtMBP stimulates ATPase by targeting the small fraction of transporter able to transiently adopt the catalytic state [12]. The crystal structure of the catalytic state transporter shows that the catalytic state is the conformation of $MalFGK_2$ bound by unliganded MBP [8]. That detergent solubilization increases the ATPase stimulus of unliganded wtMBP suggests that the catalytic state of the transporter has become more accessible to MBP. Note that this increased availability of catalytic state $MalFGK_2$ is correlated with a decrease in the ability of MBP-C to activate the transporter above background. These results are consistent with a role for closed MBP in binding and stabilizing the pre-catalytic state to promote the appearance of catalytic state $MalFGK_2$. Detergent solubilization has removed the transporter from its native membrane environment and altered the relative energies and frequencies of its competing conformations. The increase in background ATPase suggests that this alteration has made the catalytic state more accessible. Doing so has made wtMBP, which directly targets the catalytic state, more activating and simultaneously renders the ability of MBP-C to stabilize the pre-catalytic state less significant. Detergent solubilization has already lowered the energy of activation of the catalytic cycle by stabilizing the pre-catalytic state. This likely explains the ability of Oldham and Chen to crystallize the pre-catalytic state transporter in detergent [9].

The behavior of both MBP-O and MBP-O95/171 in liposomes was a great surprise. The mutations and BMOE modification we introduced into MBP-O and MBP-O95/171 had been intended to hold those proteins in the open conformation. Modification proved insufficient to reduce the proteins maltose-binding affinity, but

SAXS analysis indicated that the ability of each mutant to close had been altered. A profound effect on activity was observed however, as both BMOE modified mutants stimulate high levels of ATPase from proteoliposome embedded $MalFGK_2$ without the addition of maltose. This represents a pronounced gain-in-function in the transporter brought on solely by changes in MBP; with constitutive ATPase freed from coupling to maltose transport.

A change in the relative favorability of the open and closed conformations should have revealed itself as a change in the binding affinity of the protein for maltose as has been previously observed in other mutants [12]. However, as both SAXS and intrinsic fluorescence quenching experiments observe the protein at an equilibrium state, it is possible for changes in the kinetics of the protein to go undetected. During the ATPase catalytic cycle the binding protein undergoes significant changes in conformation and dynamically alters its interaction with the transporter. A change in the rate of conformational change would significantly impact the ATPase catalytic cycle even if it did not alter substrate binding behavior at equilibrium. This is likely what has occurred in MBP-O and MBP-O95/171 stimulated ATPase trials.

Despite an ability to bind and close around maltose, MBP-O stimulates a high level of activity in either the presence or absence of substrate. That there is little or no change in the stimulated rate of hydrolysis between liganded and unliganded forms of MBP-O suggests that the closed conformation is not playing a significant role in the uncoupled activity observed. This is an indication that the normal catalytic cycle has been short-circuited. Although comparatively little is known

about the dissociation mechanics of the transporter following ATP hydrolysis, conversion of the catalytic state, which binds open MBP with high affinity, to the resting state which does not, will necessarily involve a loss of affinity for open conformation MBP. Paramagnetic resonance studies of the post-catalytic transporter seem to indicate that it reverts to the resting state via rigid body rotations which are broadly the reverse of changes prior to catalysis [1]. This means that the interface between the catalytic state transporter and open MBP will move towards a conformation that is more consistent with closed conformation MBP, likely causing wtMBP to dissociate as the closed state is energetically disfavored.

In the case of MBP-O and MBP-O95/171, the BMOE modification might delay or resist conformational changes in the binding protein. This could cause the transporter to become arrested in a catalytic-like conformation long enough for ADP in the ABC subunits to be exchanged for ATP, priming the transporter for repeat hydrolysis. This is supported by the high affinity of open MBP for the catalytic state transporter, as observed by its failure to dissociate during size exclusion chromatography [27]. The high affinity of open MBP for the transporter suggests it would have significant binding energy with which to influence the conformation of the complex before being forced to dissociate. This mechanism could be very similar to that by which maltose transport is inhibited by wtMBP in 'MBP-independent' transporter mutants, which have mutationally stabilized catalytic states [25,31,32]. In each case, a change in the conformational dynamics of

competing MBP and transporter conformations disrupts the normal ATPase catalytic cycle and prevents the complex from dissociating.

It is possible that the mutations or BMOE linker incorporated into MBP-O and MBP-O95/171 have disrupted some ATPase relevant interaction between local residues of MBP and the transporter. However this is unlikely, as all mutations are near the MBP balancing interface, which is not on the juxtamembrane facing of MBP. The P2 arm of MalF intrudes into the periplasm to contact portions of MBP that are not on the juxtamembrane surface and this arm has been implicated in conformational coupling between MBP and $MalFGK_2$ [33,34,35]. However, the MBP-O mutants used here were designed with this risk in mind and consequentially the introduced cysteines are not proximal to any sites of contact between MBP and the transporter. Further, as both MBP-O and MBP-O95/171 displayed similar uncoupled ATPase phenotypes, despite their lack of common mutations, it is less likely that the introduced cysteines account for this phenotype directly. In the future, X-ray crystal structures of the BMOE cross-linked mutants will help to interpret what effect the BMOE modification has had on the MBP conformational equilibrium.

Bibliography:

1. Orelle, C., Ayvaz, T., Everly, R.M., Klug, C.S., Davidson, A.L., (2008) Both maltose-binding protein and ATP are required for nucleotide-binding domain closure in the intact maltose ABC transporter. *Proc Natl Acad Sci U S A*. **105**: 12837-42.
2. Davidson, A.L., Shuman, H.A., Nikaido, H., (1992) Mechanism of maltose transport in Escherichia coli: transmembrane signaling by periplasmic binding proteins. *Natl Acad Sci U S A* **89**: 2360-4
3. Hall, J.A., Ganesan, A.K., Chen, J., Nikaido, H., (1997) Two modes of ligand binding in maltose-binding protein of Escherichia coli. Functional significance in active transport. *J Biol Chem*. **272**: 17615-22.
4. Quiocho, F.A., Spurlino, J.C., Rodseth, L.E., (1997) Extensive features of tight oligosaccharide binding revealed in high-resolution structures of the maltodextrin transport/chemosensory receptor. *Structure* **5**: 997-1015.
5. Sharff, A.J., Rodseth, L.E., Spurlino, J.C., Quiocho, F.A., (1992) Crystalographic evidence of a large ligand-induced hinge-twist motion between the two domains of the maltodextrin binding protein involved in active transport and chemotaxis. *Biochemistry* **31**: 10657-63.
6. Hor, L.I., Shuman, H.A., (1993) Genetic analysis of periplasmic binding protein dependent transport in Escherichia coli. Each lobe of maltose-binding protein interacts with a different subunit of the MalFGK2 membrane transport complex. *J Mol Biol*. **233**:659-70.
7. Jardetzky, O., (1966) Simple allosteric model for membrane pumps. *Nature* **211**: 969-970.
8. Oldham, M.L., Khare, D., Quiocho, F.A., Davidson, A.L., Chen, J., (2007) Crystal structure of a catalytic intermediate of the maltose transporter. *Nature* **450**: 515-21.
9. Oldham, M.L., Chen, J., (2011) Crystal structure of the maltose transporter in a pretranslocation intermediate state. *Science* **332**: 1202-5.
10. Bohl, E., Shuman, H.A., Boos, W., (1995) Mathematical Treatment of the Kinetics of Binding Protein Dependent Transport Systems Reveals that Both the Substrate Loaded and Unloaded Binding Proteins Interact with the Membrane Components. *J theor Biol*. **172**: 83-94.
11. Telmer, P.G., Shilton, B.H., (2003) Insights into the conformational equilibria of maltose-binding protein by analysis of high affinity mutants. *J Biol Chem*. **278**: 34555-67.
12. Gould, A.D., Telmer, P.G., Shilton, B.H., (2009) Stimulation of the maltose transporter ATPase by unliganded maltose binding protein. *Biochem* **48**: 8051-61. Appears as chapter 2 of this thesis
13. Tang, C., Schwieters, C.D., Clore, G.M., (2007) Open-to-closed transition in apo maltose-binding protein observed by paramagnetic NMR. *Nature* **449**: 1078-82.
14. Bucher, D. 2011 Accessing a Hidden Conformation of the Maltose Binding Protein Using Accelerated Molecular Dynamics. *PLoS Comput Biol*. **7**: e1002034.

15. Reich-Slotky, R., Panagiotidis, C., Reyes, M., Shuman, H.A., (2000) The Detergent-Soluble Maltose Transporter is Activated by Maltose Binding Protein and Verapamil. *J Bacteriol*. **182**: 993-1000.
16. Zhang, Y., Mannering, D.E., Davidson, A.L., Yao, N., Manson, M.D. (1996) Maltose-binding protein containing an interdomain disulfide bridge confers a dominant-negative phenotype for transport and chemotaxis. *J. Biol. Chem*. **271**: 17881-9.
17. Gould, A.D., Shilton, B.H., (2010) Studies of the maltose transport system reveal a mechanism for coupling ATP hydrolysis to substrate translocation without direct recognition of substrate. *J Biol Chem*. **285**: 11290-6. Appears as chapter 3 of this thesis
18. Szmeleman, S., Schwartz, M., Silhavy, T. Boos, W., (1976) Maltose transport in Escherichia coli K12. A comparison of transport kinetics in wild-type and lambda-resistant mutants as measured by fluorescence quenching. *Eur J Biochem*. **65**: 13-19.
19. Semenyuk, A., and Svergun, D. (1991) GNOM - a program package for small-angle scattering data processing, *J. Appl. Cryst*. **24**: 537-540.
20. Davidson, A.L., Nikaido, H., (1990) Overproduction, Solubilization, and Reconstitution of the Maltose Transport System from Escherichi coli. *J Biol Chem*. **265**: 4254-60.
21. Bangham, A.D., Standish, M.M., Watkins, J.C., (1965) Diffusion of univalent ions across the lamellae of swollen phospholipids. *J Mol Biol*. **13**: 238-52.
22. Marvin, J.S., Hellinga, H.W., (2001) Manipulation of ligand binding affinity by exploitation of conformational coupling. *Nat Struct Biol* **8**: 795-8.
23. Cui, J., Qasim, S., Davidson, A.L., (2010) Uncoupling Substrate Transport from ATP Hydrolysis in the *Escherichia coli* Maltose Transporter. *J Biol Chem* **51**: 39986-93.
24. Sharma, S., Davidson, A.L., (2000) Vanadate-Induced Trapping of Nucleotides by Purified Maltose Transport Complex Requires ATP Hydrolysis. *J Bacteriol* **182**: 6570-6.
25. Dean, D.A., Hor, L.I., Shuman, H.A., Nikaido, H., (1992) Interaction between maltose-binding protein and the membrane-associated maltose transporter complex in *Escherichia coli*. *Mol Microbiol* **6**: 2033-40.
26. Pattenden, L.K., Thomas, W.G., (2008) Amylose affinity chromatography of maltose-binding protein: purification by both native and novel matrix-assisted dialysis refolding methods. In: *Methods Mo. Biol.* **421**: 169-89
27. Chen, J., Sharma, S., Quiocho, F.A., Davidson, A.L., (2001) Trapping the transition state of an ATP-binding cassette transporter: Evidence for a concerted mechanism of maltose transport. *PNAS.* **98**: 1525-30.
28. Klingenberg, M., (2005) Ligand-protein interaction in biomembrane carriers. The induced transition fit of transport catalysis. *Biochemistry* **44**: 8563-8570.
29. Schramm, V., (1998) Enzymatic transition states and transition state analog design. *Ann. Rev. Biochem.* **67**:693-720
30. Orelle, C., Alvarez, F.J., Oldham, M.L., Orelle, A., Wiley, T.E., Chen, J., Davidson, A.L., (2010) Dynamics of alpha-helical subdomain rotation in the

intact maltose ATP-binding cassette transporter. *Proc Natl Acad Sci U S A* **107**: 20293-8.
31. Covitz, K.M., Panagiotidis, C.H., Hor, L.I., Reyes, M., Treptow, N.A., Shuman, H.A., (1994) Mutations that alter the transmembrane signaling pathway in an ATP binding cassette (ABC) transporter. *EMBO* **13**: 1752-9.
32. Merino, G., Shuman, H.A., (1997) Unliganded maltose-binding protein triggers lactose transport in an Escherichia coli mutant with an alteration in the maltose transport system. *J Bacteriol*. **179**: 7687-94.
33. Daus, M.L., Grote, M., Schneider, E., (2009) The MalF P2 Loop of the ATP-Binding Cassett Transporter $MalFGK_2$ from *Escherichia coli* and *Salmonella enterica* Serovar Typhimurium Interacts with Maltose Binding Protein (MalE) throughout the Catalytic Cycle. J Bacteriol. **191**:754-61.
34. Daus, M.L., Berendt, S., Wuttge, S., Schneider, E., (2007) Maltose binding protein (MalE) interacts with periplasmic loops P2 and P1 respectively of the MalFG subunits of the maltose ATP binding cassette transporter (MalFGK2) from *Escherichia coli/Salmonella* during the transport cycle. Mol Microbiol. **66**:1107-22.
35. Daus, M.L., Landmesser, H., Schlosser, A., Müller, P., Herrmann, A., Schneider, E., (2006) ATP Induces Conformational Changes of Periplasmic Loop Regions of the Maltose ATP-binding Cassette Transporter. *J Biol Chem*. **281**:3856-65.

Chapter 5 Discussion and Conclusions

At the commencement of this thesis it was believed that only the closed conformation of MBP played a significant role in ATP hydrolysis by the maltose transporter. This was largely due to the ability of maltose to induce MBP domain closure [1,2,3,4,5]. During the work of this thesis a ground breaking $MalFGK_2$ crystal structure was resolved by another group, showing the interaction of open MBP with the ATPase catalytic conformation of the transporter, which faces the periplasm [6]. Later, a resting-state structure was resolved which showed the transporter in a cytoplasmic facing, and without a binding site for MBP [7]. Finally, a pre-catalytic state structure illustrated the interaction of closed form MBP with a transporter conformation intermediate between the resting and catalytic states [8]. These structures are tremendous contributions to the understanding of $MalFGK_2$ function and agree with the results of previous in-solution studies of transporter conformation [9,10,11,12]. These findings helped to define the conformational changes undertaken during maltose transport and the interactions between the binding protein and transporter. However the functional significance of these interactions was not understood. Further the mechanism by which these interactions reverse the autoinhibition of ATPase and instead activate the transporter was not understood, as indicated by the lock-and-key hypothesis, which rested on a tacit assumption that unliganded closed MBP would activate the transporter through simple surface complementarity [13,3].

The purpose of the research presented in this thesis was to identify the mechanism by which ATP hydrolysis in the maltose transporter is regulated and coupled to substrate transport; how the transmembrane (TM) subunits of the complex can inhibit ATP

hydrolysis in the resting state, but activate ATPase in response to maltose bound MBP. This mechanism has implications for our understanding of transporters across the whole ABC family. Based on the findings presented here, a model of transporter regulation has been developed to explain the observed behavior (Fig 1.4). In this model, uncoupled ATP hydrolysis is inhibited by energetically disfavoring conformations of the transporter that are competent for ATPase. While in isolation the MalK dimer can freely close and hydrolyze ATP, when incorporated into the full $MalFGK_2$ complex this motion becomes coupled to highly unfavorable conformational changes within the MalFG TM regions. The resting state conformation therefore represents a valley in the energetic landscape of the complex which is bounded by disfavored, high-energy, alternative conformations. This forms the 'first energetic barrier' by which the transporter is effectively restricted to conformations near its cytoplasm-facing resting state, which is inactive with respect to ATP hydrolysis (Fig 1.4).

However, when the closed maltose-bound form of MBP targets and binds the pre-catalytic state of the transporter it lends some of its considerable conformational stability to the complex. This has the effect of selecting, and favoring, the pre-catalytic state out of an equilibrium that is normally biased overwhelmingly towards the resting state. The high energetic barrier represented by the pre-catalytic state is therefore lowered and the energetic landscape flattened, which increases the tendency of the transporter to reside in conformations other than the resting state. In this way the catalytic state of the transporter is made more accessible by reducing the activation energy necessary to exit the resting state.

The work presented here agrees with and supports this model, suggesting that the role of closed MBP is to mediate the conversion of the resting state transporter to the ATPase catalytic state by stabilizing the pre-catalytic state. This can be seen in the capacity of MBP-C and sMBP with sucrose to activate hydrolysis, while unliganded closed-wtMBP, MBP-DM, and MBPA96W/I329W are all incapable of stimulating high levels of activity. All these binding proteins are capable of adopting the closed conformation, however only the proteins which are energetically stable in that state are capable of activating the transporter. Of particular note is the contrast of MBPA96W/I329W with MBP-C. Neither of these proteins adopts the open conformation, and both are held near to the closed state. However MBP-C, which is stabilized by a disulfide bond, is significantly activating for ATPase while MBPA96W/I329W, which has an average conformation very near the closed state but is not energetically favored in the fully closed conformation, is wholly incapable of activating hydrolysis without being stabilized by maltose. When MBPA96W/I329W is stabilized in the closed state by maltose, but still incapable of adopting a fully open state, it appears to stimulate ~20% of the maximal activity of wtMBP-maltose (Fig 2.8 and 4.3). This is a rate of hydrolysis similar to that seen with MBP-C, brought on by stabilization of the closed form of MBPA96W/I329W. Additionally, in chapter 2 it was found that unliganded closed-MBP, as opposed to unliganded open-MBP, was not capable activating the transporter, despite evidence that such a species exists in solution [14]. These results demonstrate that the ability of closed MBP to activate the transporter is a function of its conformational stability, or persistence, as those binding proteins

which adopt only a transiently closed conformation have no 'energy budget' in binding to the pre-catalytic state transporter with which to contribute to the complexes stability.

However, this interaction is not sufficient for full transporter activity. The MalK ABC dimer is only partially closed in the pre-catalytic state, making it unlikely that this conformation can hydrolyze ATP at a significant rate [8]. Further, at this point in the catalytic cycle maltose is still enclosed within MBP on the periplasmic membrane face. To fulfill its physiological role the transporter must ensure that maltose enters the translocation pathway before the complex reverts to its resting state. To this end, it is likely that the energy of ATP binding is realized at this stage, by an energetic closure of the MalK subunits around their bound ATP molecules. Dimer closure becomes favorable when the transporter enters the pre-catalytic state. This could be a result of MBP lowering the entropy of the resting state transporter and so reducing the entropy cost of dimer closure. ABC dimer closure will move the transporter towards the ATPase catalytic conformation (Fig 1.4)[6].

The motion of MalK dimer closure is communicated across the membrane through rigid body rotations of the TM subunits and forces MBP to open [7]. With MBP bound in the open state, maltose is exposed to the translocation pathway, and its affinity for MBP has been reduced, owing to the opening of the MBP maltose binding site. However, to efficiently couple ATP hydrolysis to transport, ATPase must be delayed until the substrate has been recognized as leaving MBP and entered the TM regions. This is likely accomplished by the MalG P3 'scoop loop' [6]. The scoop loop invades the MBP maltose-binding site once maltose has entered the TM regions. It is therefore a sensor which can determine the position of maltose without directly interacting with the

substrate. The loop is structurally linked to the C-terminal tail of MalG, which is part of an extensive hydrogen bond network in the center of the MalK dimer. This structure forms a likely transmission mechanism to link ATP hydrolysis to the absence of maltose within the MBP maltose binding site.

While it was previously recognized that open MBP binds with high affinity to the catalytic state complex there was no functional evidence that this interaction promotes ATP hydrolysis. This thesis has shown that the open conformation of MBP is capable of activating considerable ATP hydrolysis distinct and separate from activation by closed MBP. In chapter 2 it was found that open MBP, rather than closed, was responsible for the ATPase activation stimulated by unliganded MBP. In chapter 4 this was developed further in experiments with the detergent solubilized transporter which showed that both MBP-C and unliganded wtMBP stimulated ATPase activity, but do so by mechanisms which are differently impacted by detergent solubilization. This differential effect is a strong indication that the open and closed forms of MBP stimulate the transporter by targeting different conformations of $MalFGK_2$. A previous study using a mutant $MalFGK_2$ complex is also consistent with this finding, as it was found that a mutant, which was presumably able to adopt the catalytic conformation due to a lowered first energetic barrier, was activated by open wtMBP to transport a substrate that does not induce MBP domain closure [15]. Finally the high rates of ATP hydrolysis seen from BMOE modified MBP-O and MBP-O95/171, which were indifferent to the presence or absence of maltose, are strong evidence that the binding of open MBP to the catalytic state is a functional interaction by which MBP promotes ATP hydrolysis. The functional significance of the MalG scoop loop was recognized in chapter 3. The equivalent rates of

ATP hydrolysis stimulated by sMBP with maltose or sucrose showed that ATP hydrolysis is not influenced by direct interactions between the substrate and the TM domains. The reduced rate of hydrolysis stimulated by the mutant, as compared to wtMBP, indicated that interactions between the maltose binding site and scoop loop promote ATPase (Fig. 3.2). This reduced activity was seen even when sMBP was stabilized in the closed state by maltose or sucrose. These results indicate that the open form of MBP plays a major functional role by allowing the catalytic state transporter to overcome a second energetic barrier by which ATP hydrolysis is otherwise prevented (Fig. 1.4).

It should be noted that while unliganded open wtMBP was seen to activate ATPase in proteoliposomes [13], and while this is highly revealing, this activity is not likely significant *in vivo*. The catalytic transporter conformation targeted by open MBP is effectively down-stream of activation by closed MBP, limiting the rate of uncoupled hydrolysis in the absence of maltose. However, as detergent solubilization studies have shown, removing the transporter from its native environment relaxes its autoinhibition of ATPase by lowering the first energetic barrier and making the catalytic state more accessible to open MBP. It is therefore likely that the artificial membranes of proteoliposomes form an intermediate environment between the loose ATPase regulation observed in detergent and tighter regulation in the native cell membrane.

Once maltose has entered the TM translocation pathway, the vacant maltose-binding site of MBP is recognized as a signal to initiate ATP hydrolysis and motions of the MalG scoop loop and MalG C-terminus bring the transporter into a conformation in which ATP can be hydrolyzed. From the perspective of conformational dynamics, this

state likely reflects an end point of extreme energetic stability. Although entropic movements are likely to be minimal, enthalpic considerations have now stabilized the transporter in a very tight complex. This is reflected in the high affinity of open conformation MBP for this transporter state, as the complex will not dissociate if ATP hydrolysis is inhibited [16]. In practice however, the complex has significant potential energy in the phosphoanhydride bonds of each bound ATP molecule. In this conformation, hydrolysis of one or both ATP molecules is both spontaneous and rapid. ATP hydrolysis will disrupt the MalK dimer, promoting its separation, destabilize the catalytic conformation such that it can revert to the resting state.

The sequence of conformational changes which return the transporter complex to its cytoplasmic facing resting state are not as well understood, perhaps owing to the instability of each discreet stage as the complex progresses to conformations of increasing entropy. Paramagnetic resonance measurement of the separation of spin-labeled MalK subunits has suggested that the dissociation of inorganic phosphate causes the MalK dimer to partially open [10]. Given the rigid body domain rotations seen in the TM domains between existing $MalFGK_2$ crystal structures, it is likely that MalK dimer separation causes the complex to adopt a conformation more like the pre-catalytic than the catalytic state, broadly mirroring changes seen prior to hydrolysis [7,8,6]. This will cause the interface with MBP, which supports high-affinity binding to open MBP in the catalytic state, to revert to a position that is instead complementary to closed MBP. Bound MBP will be under strain from the transporter and driven towards the unliganded closed conformation. Because the closed form of MBP is no longer stabilized by

maltose, this represents a disfavored conformation, and will result in dissociation of MBP from the complex when the strain exceeds the energy of binding.

Observations in chapter 4 with MBP-O and MBP-O95/171 are consistent with this model of dissociation. If the BMOE crosslink of these proteins causes them to resist domain closure by $MalFGK_2$, then the modified mutants would resist conversion of the transporter to the resting state to a greater degree than wtMBP. This could trap the complex in a conformation near to the catalytic state sufficiently long for ADP to dissociate and be replaced by ATP. The substitution of ADP for ATP would short-circuit the catalytic cycle and stabilize the transporter for repeated ATP hydrolysis. These findings are very preliminary, requiring a great deal of further investigation, but do hint that the reversion of the transporter to the resting state involves conformational changes in MBP, providing a tiny window into that as yet little-understood stage of transport where maltose passes the membrane and is released into the cytoplasm. Observations of the activities of the BMOE cross-linked mutants have formed an intriguing coda to this thesis although more study is needed to better characterize the effect of modification on MBP conformational dynamics.

The findings of this thesis definitively explain the role of maltose in regulating transporter activity. With respect to ATPase activation, the substrate is not functionally recognized by the TM regions of the transporter. In the third chapter it was observed that the rate of ATP hydrolysis by sMBP was not altered by the substitution of maltose for sucrose. This was observed in spite of the inability of the TM substrate binding site to accommodate sucrose. Further, in the fourth chapter we observed very high rates of ATPase activation from MBP-O and MBP-O95/171 in the absence of maltose. These

data all indicate that the presence of maltose is not an absolute requirement for transporter activation and can be complemented by mutations in MBP. The recognition of maltose can be considered 'upstream' of MBP conformational changes. The role of maltose in activating $MalFGK_2$ ATP hydrolysis is therefore exclusively to stabilize conformational changes in MBP. It is important to note that this does not mean that interactions between maltose and the transporter are irrelevant to transporter function, but rather that they do not contribute to the decision to hydrolyze ATP. Indeed, the presence of a specific maltose-binding site within the TM regions of $MalFGK_2$ testifies to the importance of contacts between substrate and transporter [6,15]. It is likely that contacts at this site play a role in ensuring that ATP hydrolysis results in substrate transport rather than in initiating ATP hydrolysis in response to the availability of substrate. Consistent with this theory, a recent study has found that mutations which prevent the passage of substrate into the translocation pathway prevent transport without preventing ATP hydrolysis [17]. It therefore appears that ATP binding and hydrolysis is influenced by interactions between maltose and MBP and between MBP and the TM regions, while the energy released from that hydrolysis is directed towards substrate transport by interactions between maltose and the TM regions of the transporter.

More studies are needed to fully develop and test this model of activity. During the work of this thesis, work was begun on a course of experiments intended to observe the effects of altering the relative stabilities of competing $MalFGK_2$ conformations. Time constraints have unfortunately prevented this work from being completed. Prior to the suspension of this work, nine mutant forms of the transporter were cloned with mutations in MalF and MalG known to cause a MBP independent phenotype (appendix 3)[18].

MBP independent $MalFGK_2$ mutants are able to transport maltose without being stimulated by MBP, as indicated by their ability to complement growth on maltose in MBP deficient *E. coli* [19]. In this respect they resemble ABC export complexes, which act directly on substrate. Intriguingly, these mutants exhibit a level of constitutive ATP hydrolysis that is in proportion to their rate of MBP independent maltose transport [18]. This is reminiscent of the phenotype brought on by detergent solubilisation. The nine mutants selected and cloned display a varying degree of constitutive ATPase activity across a wide range.

In the future, these mutant transporters can be tested in liposomes and detergent as the wild-type transporter has been tested. The presented model indicates that, like $wtMalFGK_2$ in the detergent solubilized phase, independent transporters have catalytic states that are more readily accessible to open MBP. That these transporters can act directly on maltose is an indication that they can adopt the periplasmic facing ATPase catalytic conformation without MBP, which indicates that mutation has lowered at least the first energetic barrier. Transporters that demonstrate loosened regulation by an increase in uncoupled ATPase activity should have stabilized ATPase catalytic states, as indicated by greater ATPase stimulus by open MBP without maltose. A correlation should exist between the rate of constitutive uncoupled ATP hydrolysis and the degree of further ATPase stimulation by the open unliganded form of MBP. Such a finding would support the proposed model by indicating that dis-regulation of the mutant transporters, and the accompanying independence from MBP, is carried out by a stabilization of transporter conformations that are normally disfavoured in the absence of binding protein. Further testing using conformational mutants such as MBP-C could further

distinguish the impact of MBP independent mutations on each stage of the catalytic cycle.

The findings of this work emphasize the complexity of the interaction between binding protein and cognate ABC transporter. Coupled ATP hydrolysis and substrate transport are not simply triggered by the association of a complementary binding surface, but arise from a multistage shepherding of the transporter through the catalytic cycle. $MalFGK_2$ exists in an ensemble of competing conformations which regulate ATP hydrolysis by their relative stability. Both conformations of the maltose binding protein serve to promote ATP hydrolysis by modulating the relative stability of these conformations. Using a series of mutant binding proteins it has been demonstrated that both open and closed binding protein conformations promote ATP hydrolysis through their interactions with the transporter. It has also been determined that the transported substrate does not initiate ATP hydrolysis by interactions with the transporter, but instead acts to stabilize the closed conformation of MBP to enable it to activate the transporter.

Bibliography

1. Hall, J.A., Gehring, K., Nikaido, H., (1997) Two modes of ligand binding in maltose-binding protein of Escherichia coli. Correlation with the structure of ligands and the structure of binding protein. *J Biol Chem*. **272**:17605-9
2. Hall, J.A., Thorgeirson, T.E., Liu, J., Shin, Y.E., Nikaido, H., (1997) Two modes of ligand binding in maltose-binding protein of Escherichia coli. Electron paramagnetic resonance study of ligand-induced global conformational changes by site-directed spin labeling. *J Biol Chem* **272**:17610-14.
3. Hall, J.A., Ganesan, A.K., Chen, J., Nikaido, H., (1997) Two modes of ligand binding in maltose-binding protein of Escherichia coli. Functional significance in active transport. *J Biol Chem*. **272**:17615-22.
4. Wolf, A., Shaw, E.W., Nikaido, K., Ames, G.F., (1994) The histidine-binding protein undergoes conformational changes in the absence of ligand as analyzed with conformation-specific monoclonal antibodies. *J Biol Chem*. **269**:23051-8
5. Walmsley, A.R., Shaw, J.G., Kelley, D.J., (1992) Perturbation of the equilibrium between open and closed conformations of the periplasmic C4-dicarboxylate binding protein from Rhodobacter capsulatus. *Biochem*. **31**:11175-81.
6. Oldham, M.L., Khare, D., Quiocho, F.A., Davidson, A.L., Chen, J., (2007) Crystal structure of a catalytic intermediate of the maltose transporter. *Nature* **450**:515-21
7. Khare D., Oldham, M.L., Orelle, C., Davidson, A.L., Chen, J., (2009) Alternating access in maltose transporter mediated by rigid-body rotations. *Mol Cell*. **33**:528-36
8. Oldham, M.L., Chen, J., (2011) Crystal stucture of the maltose transporter in a pretranslocation intermediate state. *Science*. **332**:1202-5
9. Bohl, E., Shuman, H., and Boos, W. (1995) Mathematical Treatment of the Kinetics of Binding Protein Dependent Transport Systems Reveals that Both the Substrate Loaded and Unloaded Binding Proteins Interact with the Membrane Components, *J. Theor. Biol*. **172**: 83-94.
10. Orelle, C., Ayvaz, T., Everly, R.M., Klug, C.S., Davidson, A.L., (2008) Both maltose-binding protein and ATP are required for nucleotide-binding domain closure in the intact maltose ABC transporter. *Proc Natl Acad Sci U S A*. **105**:12837-42.
11. Austermuhle, M.I., Hall, J.A., Klug, C.S., Davidson, A.L., (2004) Maltose-binding protein is open in the catalytic transition state for ATP hydrolysis during maltose transport. *J Biol Chem.* **279**:28243-50.
12. Reyes, M., Treptow, N.A., Shuman, H.A., (1986) Transport of p-nitrophenyl-alpha-maltoside by the maltose transport system of Escherichia coli and its subsequent hydrolysis by a cytoplasmic alpha-maltosidase *J. Bacteriol.* 165:918-22.
13. Davidson, A.L., Shuman, H.A., Nikaido, H., (1992) Mechanism of maltose transport in *Escherichia coli*: transmembrane signalling by periplasmic binding proteins. *Proc Natl Acad Sci U S A*. **89**:2360-4.

14. Bucher, D., Grant, B.J., Markwick, P.R., McCammon, J.A., (2011) Accessing a Hidden Conformation of the Maltose Binding Protein Using Accelerated Molecular Dynamics. *PLoS Comput Biol*. **7**:e1002034.
15. Merino, G., Shuman, H.A., (1997) Unliganded maltose-binding protein triggers lactose transport in an Escherichia coli mutant with an alteration in the maltose transport system. *J Bacteriol*. **179**: 7687-94.
16. Chen, J., Sharma, S., Quiocho, F.A., Davidson, A.L., (2001) Trapping the transition state of an ATP-binding cassette transporter: Evidence for a concerted mechanism of maltose transport. *PNAS.* **98**: 1525-30.
17. Cui, J., Qasim, S,. Davidson, A.L., (2010) Uncoupling substrate transport from ATP hydrolysis in the Escherichia coli maltose transporter. *J Biol Chem*. **285**:39986-93.
18. Covitz, K.M., Panagiotidis, C.H., Hor, L., Reyes, M., Treptow, N.A., Shuman, H.A., (1944) Mutations that alter the transmembrane signaling pathway in an ATP binding cassette (ABC) transporter. *EMBO J*. **13**:1752
19. Treptow, N.A., Shuman, H.A., (1985) Genetic evidence for substrate and periplasmic-binding-protein recognition by the MalF and MalG proteins, cytoplasmic membrane components of the Escherichia coli maltose transport system. *J. Bacteriol.* 163:654-60

Appendix 1 Coomassie Stained 15% SDS-PAGE gel of Prepared Binding Proteins

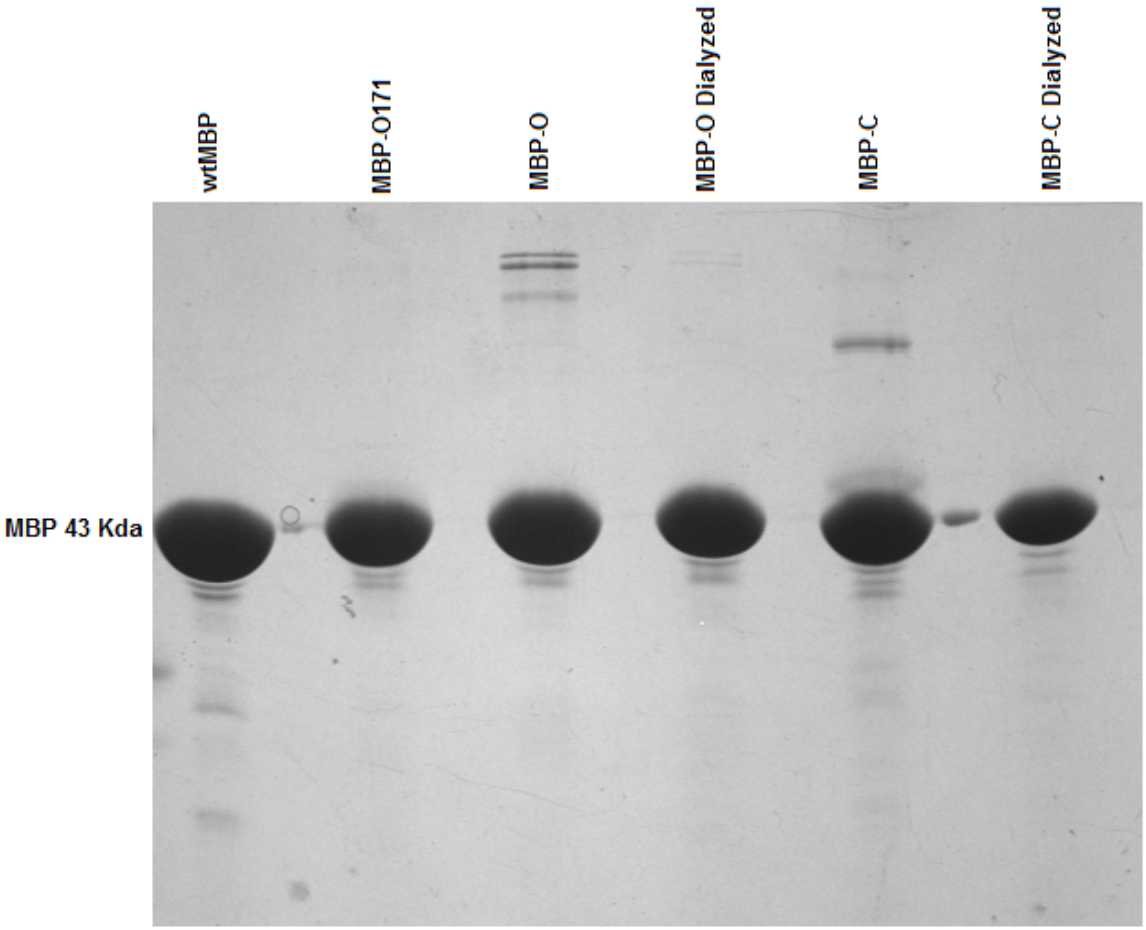

Appendix 2 Coomassie Stained 12% SDS-PAGE gel of prepared transporter

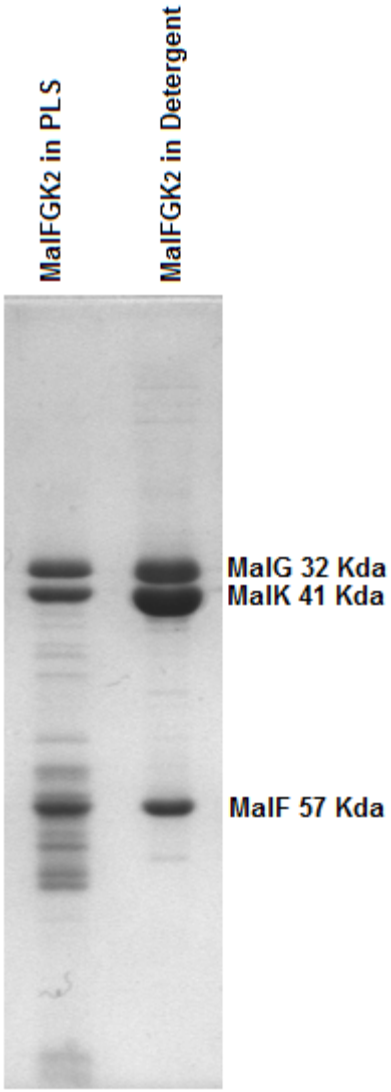

Appendix 3 Cloned MBP Independent Transporter Mutants

MBP Independent mutant [18]	Incorporated Mutations	Constitutive ATPase (nmol/min/mg) [18]
malF500	MalF: G338R/N505I	287
malF525	MalF: G338R/N505S	93
malF502	MalF: G338R/A502V	82
malF506	MalF: G338R/W378C	46
malF526	MalF: L334W/N505I	237
malF534	MalF: L334W/N505S	68
malF533	MalF: L334W/A502V	59
malF531	MalF: L334W/378C	104
malG510	MalG: L135H	59

Appendix 3 Mutagenic Primers used in Independent Transporter Cloning

Mutation	Mutagenic Primer Sequence (5'>3')
MalF: G338R	GATTTTCAAACGGTTGTTTAACCAGAGCTTCGG
MalF: L334W	CATTTCAATCTGGATTTTCAAAGGGTTGTTTAACC
MalF: N505I	GGCGATAGTGATCCTGAAAGCCACGCG
MalF: N505S	GGCGATAGTGTCCCTGAAAGCCACGCG
MalF: A502V	GGGTGCGCTGGTGATAGTGAACCTG
MalF: W378C	CGTCAATACCTGCCTGGGTTATCCG
MalG: L135H	CCCGGCAGTACATTCACTGGTCGC

Alister Douglas Gould

Curriculum Vitae

Education

2009-2011 University of Western Ontario-Shilton Lab London, Ont.
- Doctorate program.
- Continuing Thesis with emphasis on mutagenic transporters measuring interactions with cell membrane

2007-2009 University of Western Ontario-Shilton Lab London, Ont.
- Master's program in Biochemistry. Transferred into PhD program before completion
- Thesis on Membrane bound transporters, combining enzymatic assays with crystallographic data

2002-2006 University of Western Ontario London, Ont.
- Bachelor of Medical Science with Honors in Biochemistry
- Undergraduate Senior Thesis on ATP synthase in Lab of Dr. Stan Dunn

1998-2002 Kincardine District Secondary School Kincardine, Ont.
- High School Diploma with Honors and Ontario Scholar Distinction

Published Articles

Alister Gould, Brian Shilton (2010) Studies of the maltose transport system reveal a mechanism for coupling ATP hydrolysis to substrate translocation without direct recognition of substrate. Journal of Biological Chemistry. 11290-6.

Alister Gould†, Patrick Telmer†, Brian Shilton. (2009) Stimulation of the maltose transporter ATPase by unliganded maltose binding protein. Biochemistry 48 8051-61.
†These authors contributed equally to this work.

Conference Contributions

*Presenting Author

Alister D. Gould*, Patrick G. Telmer, and Brian H. Shilton (2007). Conformationally Engineered Periplasmic Binding Proteins and Substrate specificity in the E. coli ABC Maltose Transporter. 65th Annual Pittsburgh Diffraction Conference. Hauptman-Woodward MRI, Buffalo New York; Poster Presentation

Alister D. Gould*, Patrick G. Telmer, and Brian H. Shilton (2008). Activation of the maltose transporter by unliganded maltose binding protein.
2008 Infection and Immunity Research Forum, University of Western Ontario, London Ontario; Poster Presentation

Alister D. Gould*, Patrick G. Telmer, and Brian H. Shilton (2009). Insight into ABC Transporter Mechanism by Analysis of an Engineered Sucrose Binding Mutant of MBP. Gordon Research Conference 'Mechanisms of Membrane Transport', Colby College, Maine; Poster Presentation.

Alister D. Gould*, and Brian H. Shilton (2009). A Sucrose Binding Mutant of MBP Provides Insights into the Mechanism of the Escherichia coli Maltose Transporter. 2009 American Crystalographic Association Annual Meeting, Toronto Ontario; Poster Presentation

Brian H. Shilton*, Alister D. Gould, and Patrick G. Telmer (2010) The Open conformation of Maltose Binding Protein has a Critical Role in Energetic Coupling. ABC2010 – 3rd FEBS Special Meeting on ABC Proteins, Innsbruck Austria; Oral presentation

Alister D. Gould*. And Brian H. Shilton (2010) The ABC Maltose Transporter of E. coli: tight regulation and poly-specific activation. 53rd Annual Meeting of the Canadian Society of Biochemistry, Molecular & Cellular Biology: Membrane Proteins in Health and Disease, Banff Alberta.

Awards

CSBMCB Travel Award $500
Canadian Society of Biochemistry, Molecular & Cell Biology
53rd Annual Meeting, 2010, Banff Alberta

ACA Travel Award $300
American Crystalographic Association
2009 Annual Meeting, 2009, Toronto Ontario

Graduate Enhancement $5,000
University of Western Ontario
2007, London Ontario

In-course Scholarship $300
University of Western Ontario
2003, London Ontario

In-course Scholarship $200
Bruce County
2002, Kincardine Ontario

Scholarship of Distinction $1,000
University of Western Ontario
2002, London Ontario

Professional Affiliations

Industrial Microbiologist Sept 2011 - Present
Omnizyme Bioproducts
Brampton Ontario

Member 2009-Present
Canadian Light Source
Saskatoon, Saskatchewan

Member 2010-Present
Canadian Society of Biochemistry, Molecular & Cell Biology